Paleoceanography and Paleoclimatology

RESEARCH ARTICLE
10.1029/2018PA003508

Special Section:
Atlantic Meridional Overturning Circulation: Reviews of Observational and Modeling Advances

Variability in the Northern North Atlantic and Arctic Oceans Across the Last Two Millennia: A Review

P. Moffa-Sánchez[1,2], E. Moreno-Chamarro[3], D. J. Reynolds[1,4], P. Ortega[3], L. Cunningham[5], D. Swingedouw[6], D. E. Amrhein[7], J. Halfar[8], L. Jonkers[9], J. H. Jungclaus[10], K. Perner[11], A. Wanamaker[12], and S. Yeager[13]

[1]School of Earth and Ocean Sciences, Cardiff University, Cardiff, UK, [2]Department of Geography, Durham University, Durham, UK, [3]Barcelona Supercomputing Center (BSC), Barcelona, Spain, [4]Laboratory of Tree Ring Research, University of Arizona, Tucson, AZ, USA, [5]Department of Geography, University of Portsmouth, Portsmouth, UK, [6]Environnements et Paléoenvironnements Océaniques et Continentaux (EPOC), CNRS-Université de Bordeaux, Pessac, France, [7]School of Oceanography and Department of Atmospheric Sciences, University of Washington, Seattle, WA, USA, [8]Department of Earth Sciences, University of Toronto, Toronto, Ontario, Canada, [9]MARUM Center for Marine Environmental Sciences, University of Bremen, Bremen, Germany, [10]Max Planck Institute for Meteorology, Hamburg, Germany, [11]Leibniz Institute for Baltic Sea Research, Warnemünde, Germany, [12]Department of Geological and Atmospheric Science, Iowa State University, Ames, IA, USA, [13]National Center for Atmospheric Research, Boulder, CO, USA

Abstract The climate of the last two millennia was characterized by decadal to multicentennial variations, which were recorded in terrestrial records and had important societal impacts. The cause of these climatic events is still under debate, but changes in the North Atlantic circulation have often been proposed to play an important role. In this review we compile available high-resolution paleoceanographic data sets from the northern North Atlantic and Nordic Seas. The records are grouped into regions related to modern ocean conditions, and their variability is discussed. We additionally discuss our current knowledge from modeling studies, with a specific focus on the dynamical changes that are not well inferred from the proxy records. An illustration is provided through the analysis of two climate model ensembles and an individual simulation of the last millennium. This review thereby provides an up-to-date paleoperspective on the North Atlantic multidecadal to multicentennial ocean variability across the last two millennia.

Key Points:
- Review of the progress made to date on the study of variability in the northern North Atlantic and Arctic Oceans in the last two millennia
- Synthesis of the advancements in high-resolution marine proxies and climate models and compare them both

Supporting Information:
- Supporting Information S1

Correspondence to:
P. Moffa-Sánchez,
paola.l.moffa-sanchez@durham.ac.uk

Citation:
Moffa-Sánchez, P., Moreno-Chamarro, E., Reynolds, D. J., Ortega, P., Cunningham, L., Swingedouw, D., et al. (2019). Variability in the northern North Atlantic and Arctic Oceans across the last two millennia: A review. *Paleoceanography and Paleoclimatology*, *34*, 1399–1436. https://doi.org/10.1029/2018PA003508

Received 29 OCT 2018
Accepted 25 APR 2019
Accepted article online 18 JUN 2019
Published online 24 AUG 2019

1. Introduction

The short temporal span of ocean observations precludes the development of a full understanding of how our climate has naturally varied on timescales from decades to centuries. This clearly undermines our understanding of the role of natural variability in the recent changes, most notably at the regional scale (Hawkins & Sutton, 2009). To this end, proxy reconstructions facilitate the extension of ocean measurements back in time. The combined analyses of proxy data and climate models complement and strengthen the interpretation of past ocean changes and processes and at the same time set the framework for the validation of the climate models that are also used for future climate projections.

Historical, documentary, and climatic records across the last two millennia reveal relatively small changes in the climate concomitant with certain historical events (e.g., Denton & Karlen, 1973; Lamb, 1965; Lamb, 1977). Societal impacts were mostly recorded in Europe and include mild climate periods during Roman and Medieval times (often known as Roman Warm Period and the Medieval Climatic Anomaly; RWP and MCA, respectively) and the colder periods of the Dark Ages and the Little Ice Age (LIA; Lamb, 1977). Even if these events coincided with important changes in the solar and volcanic radiative forcings (e.g., Sigl et al., 2015; Steinhilber et al., 2009), the fact that these were mostly recorded around the North Atlantic (e.g., Denton & Karlen, 1973) suggests that changes in the North Atlantic circulation, specifically in the strength of the overturning circulation (known as the Atlantic Meridional Overturning Circulation, AMOC) may have modulated the northward heat transport to Europe (Bond et al., 1997; Broecker, 2005; Lamb, 1979). The involvement of AMOC was initially proposed to explain centennial-scale changes in the Holocene through parallelisms with abrupt centennial climate changes in the Last Glacial known as Dansgaard-Oeschger events (Bond et al., 1997). For this reason, the study of the North Atlantic

paleoceanography of the last millennia has largely focused on finding evidence that would demonstrate the involvement of changes in the AMOC in these multicentennial climate events. In particular, a large part of this research focused on understanding the prominent cooling during the LIA (ca. 1450–1850 years CE), recorded in terrestrial proxies such as tree rings, ice core, and glacier extent records (Dahl-Jensen et al., 1998; Denton & Karlen, 1973; Esper et al., 2002).

The North Atlantic and Nordic Seas are key climatological regions as they host deep water formation processes that ventilate 50% of the world's ocean abyss (Kuhlbrodt et al., 2007). In today's North Atlantic, warm and saline tropical waters deriving from the Gulf Stream are transported northeastward as different branches of the North Atlantic Current (NAC), crossing the North Atlantic basin (e.g., Daniault et al., 2016). These warm surface and subsurface waters reach the northern latitudes, progressively losing heat to the atmosphere and becoming denser. Colder surface waters become even denser from the salt rejection during the formation of sea ice. Eventually, these waters are denser than those underneath, an imbalance that favors the formation of deep ocean mixing in the Nordic Seas. These dense waters form intermediate and deep waters that accumulate in the Nordic Seas basins and flow over the Greenland-Scotland Ridge, a shallow submarine ridge that limits the flow of dense waters into the Atlantic Basin. These dense waters flow through deep channels including the Denmark Strait and through the Faroe Bank Channel and are respectively known as the Denmark Strait Overflow Water and the Iceland-Scotland Overflow Waters (e.g., Hansen & Østerhus, 2000). As these waters cascade down, they first entrain intermediate waters previously formed through open ocean convection in the subpolar North Atlantic and then follow the bathymetry until they reach the southern tip of Greenland. This flow continues around the deep Labrador Basin anticlockwise and south along the NE American continental margin and through intermediate pathways as part of Deep Western Boundary Current (DWBC; Bower et al., 2009). The combination of these processes forms the overturning circulation in the North Atlantic, with North Atlantic Deep Waters being the end-product flowing into the Southern Hemisphere (e.g., Dickson et al., 2008; Dickson & Brown, 1994). The collective of the surface-to-deep water mass transformation in the North Atlantic is often characterized through the AMOC. Although this rather simplified description of water mass transformation has prevailed for years, recent observations and modeling studies suggest a more complicated picture: for example, changes in deep convection regions do not always appear to result in changes in net sinking rates (Katsman et al., 2018), and the buoyancy-driven overturning processes described earlier may be more important on longer timescales than the wind-driven overturning shown over the observational timescales (Buckley & Marshall, 2015; Lozier, 2012; Srokosz & Bryden, 2015).

Due to its complexity, attempts to reconstruct the AMOC in the past have focused on the retrieval of independent time series from key water masses. Initial paleoceanographic reconstructions suggested that the LIA was as an extension or muted version of the abrupt climate changes experienced during the last glacial period (Bond et al., 1997, 1999). Around the early 2000s, new data sets from the North Atlantic started to shed some light on the involvement of the ocean on centennial-scale climate variability, particularly during the LIA (Bianchi & McCave, 1999; Bond et al., 2001; Broecker, 2000; Chapman & Shackleton, 2000; Keigwin & Boyle, 2000; Oppo et al., 2003). Yet, these records from a few marine locations were not able to resolve the last couple of millennia with enough resolution to study centennial-scale variability, leaving a myriad of unknowns.

Twenty years later, the number and quality of high-resolution marine proxy reconstructions across the last two millennia have dramatically increased. This is largely a result of the birth of new marine proxies and the discovery of high temporal resolution archives offering a more detailed and perhaps more complex picture to this old paradigm. In addition, the important computational advances combined with the availability of refined estimates of past changes in radiative forcings have allowed the generation of the first coupled climate simulations with general circulation models covering the last millennium. These have proven extremely useful to test and refine some of the hypotheses, in particular about the role of external forcings and internal processes in climate variability. For this reason, the rapid advancement of this field in the past two decades forms the basis of this review paper.

This review aims to collate existing high-resolution paleoceanographic records, enabling the past variability of key ocean currents and hydrographic conditions in the North Atlantic and Nordic Seas to be examined and, further, to synthesize our current understanding of climate model outputs, with a particular

focus on the dynamical changes. This paper is structured as follows: First, the tools used to study past ocean variability including proxy archives and networks and climate models will be introduced (section 2). The description of the methodology (section 3) will outline the selection approach for the available proxy records and the definition of the model indices used in this study. Section 4 will discuss the proxy records within each region. Model results will be presented in section 5, which will describe the simulated changes in a selection of ocean circulation and current indices (section 5.1) and their concomitant changes in sea surface temperature as a fingerprint tool (section 5.2). Section 6 will present a joint discussion of proxies and models through the data-model comparison of the surface temperatures across different time slices of the last millennium, and section 7 will conclude by summarizing the major findings of this study.

2. Studying Past Ocean Changes

2.1. Proxy Archives

2.1.1. Sediment Cores

Layers of sediment accumulated on the seafloor create an excellent archive that can be used to investigate past ocean conditions. These deposits contain calcareous (foraminifera and ostracods), siliceous (diatoms), and organic (dinocysts), as well as organic molecules produced by organisms that lived in and on the sediments or at the oceanic surface and sunk to the bottom o after their death and were subsequently preserved within the sediments. As different species of these organisms have varying ecological preferences, changes in the species composition of communities preserved within the sediments, also called assemblages, can reveal changes in environment. Given the large number of species within some taxa, multivariate analyses and transfer functions are typically used in order to quantify the environmental changes (Table 1). In addition, the remains of these organisms provide a wealth of geochemical data that can be used to reconstruct past changes in the ocean. This includes oxygen isotopes and the elemental composition of the preserved parts, particularly in the calcareous foraminifera, and also the chemistry of various organic compounds (e.g., pigments, fatty acids, and lipids; Table 1). Marine sediments also contain nonbiogenic particles, which can be transported at the surface by drift ice, and fine-grained terrigenous particles transported and deposited by near-bottom ocean currents, mainly boundary currents.

Marine sediment cores are frequently dated using radiogenic isotopes, typically of carbon and lead. Radiocarbon is incorporated into the calcareous shells of organisms living in the surface ocean, which are preserved in the sediment (Hughen, 2007). The age errors of this method between measurement and calibration can be ~80–200 years. Larger uncertainties may be introduced by the ocean setting, as some water masses can contain older radiocarbon compared to the atmosphere, often referred to as the reservoir effect, which could increase the dating error (Hughen, 2007). Furthermore, the bomb-radiocarbon spike from nuclear testing in the 1960s complicates the radiocarbon calibration for dating recent sediments. For this reason, more recent sediments are dated using other methodologies such as Lead-210-dating (Appleby & Oldfield, 1978), the presence of Cesium-137 released from atomic bomb testing, Spheroidal Carbonaceous Particles (e.g., Rose, 2015), or the detection of the Suess effect in the carbon isotopes (Suess, 1955). Lastly, tephra (small, often microscopic ash fragments from volcanic eruptions) can also be incorporated into sediment records and represents an important chronological tool within the North Atlantic region. The geochemical composition of tephra can be compared to that of known eruption events enabling some tephras to be dated with a precision of 1–2 years and hence facilitating the development of accurate chronologies. However, this technique cannot be easily applied at all sites, particularly if they contain lateral sediment transport of volcanic debris, similar geochemistry from other eruptions, or chemical alteration of the tephra (e.g., Lowe, 2011).

2.1.2. Biological Banded Archives

Many marine organisms living on the seabed in coastal/shelf settings, including bivalve mollusks and coralline algae, produce bands within their carbonate shell or skeletal structure, which represent discrete periods of growth. A subset of these, including some mollusks and coralline algae, form annual or subannual growth bands, akin to rings in a tree. Multiple parameters can be analyzed from these archives, including the width of the growth bands and their isotopic and elemental composition. This can reveal information about water temperatures, water mass variability, and productivity (Table 1; e.g., Butler et al., 2010; Halfar et al., 2013; Reynolds et al., 2013; Chan et al., 2017; Moore et al., 2017; Reynolds et al., 2017). Through layer counting

Table 1
Summary of Proxies Used to Reconstruct Ocean Parameters and Which Are Presented and Discussed in Section 4

Ocean parameter	Archive	Proxy	Description
Sea surface temperature	Core	Alkenones	Organic compounds synthesized by haptophyte algae, which mostly bloom in spring/summer at high latitudes. The alkenone unsaturation index is dependent on temperature[2] but ambiguity remains with regard to the vertical and temporal origin of the signal, with the timing of maximum alkenone production/fluxes showing marked regional differences[12,22]. The alkenone unsaturation index is not affected by salinity[25], but alkenones can be advected over long distances and hence may not always reflect conditions at the site and time of deposition[10].
	Core	Dinocyst assemblages	The relative abundance of taxa of resistant organic-walled dinoflagellate cysts varies in relation to sea surface temperatures during their summer bloom[10,20]. Dinoflagellates are largely found in continental margins and present relatively high diversity, which makes them useful to study the past ocean in the high latitudes. Microfossil assemblages are often shaped by multiple environmental variables, which can affect the reconstructed temperature[11].
	Core	Diatom assemblages	Diatoms are algae that have siliceous cell walls; thus, they are restricted to regions where silicic acid is not limiting (e.g., polar regions). Some species have very narrow ecological preferences including temperature and ice cover (light availability); hence, species abundances (single, ratio or statistically grouped) reflect temperatures and sea ice coverage, with transfer functions enabling quantitative reconstructions[3,30]. Caveats remain as salinity, water depth, nutrient availability, and other environmental variables may also influence the community composition[9].
Temperature (0–200 m)	Core	Foraminiferal $\delta^{18}O$*	The $\delta^{18}O$ in biogenic carbonates reflects temperature and $\delta^{18}O$ of seawater ($\delta^{18}O_{sw}$), which is related to salinity and to a lesser degree carbonate ion[1,7]. Foraminifera are calcareous zooplankton, and their $\delta^{18}O$ is often used to estimate past temperature. However, unless applied in regions where the variability of $\delta^{18}O_{sw}$ is relatively low this poses several complications due to influence of $\delta^{18}O_{sw}$ on the foraminifera $\delta^{18}O$. Foraminifera habitat preferences are spatially and temporally variable[26,33] adding uncertainty to the origin of the proxy signal.
	Bivalve	$\delta^{18}O_{shell}$/Growth increment widths	$\delta^{18}O$ composition in mollusc shells is a function of temperature and $\delta^{18}O_{sw}$. The subannually resolved and absolutely dated $\delta^{18}O_{shell}$ records allow calibration with modern observations in order to quantify its relationship with water temperatures and disentangle the $\delta^{18}O_{sw}$ component, which is then assumed to remain constant back in time. Growth in marine bivalves can also be driven by factors other than temperature, including food availability, river discharge[17], and age-related growth trends, which remove the low-frequency variability through detrending[4].
	Coralline Algae	Mg/Ca/Growth increment widths	Magnesium incorporation into the calcite skeleton of coralline algae and growth increment width depend on temperature and light (the deconvolution of the two factors leads to uncertainties in paleotemperature interpretations)[37]. Encustration[38] and bioerosional processes may introduce temperature estimate and dating errors[22], respectively.
	Core	Mg/Ca planktonic foraminifera	The incorporation of magnesium into the calcite of foraminiferal shells is largely temperature dependent[8], with salinity and pH having a minor effect[36]. Calibrations are used to estimate surface to thermocline ocean

Table 1 *(continued)*

Ocean parameter	Archive	Proxy	Description
			temperatures according to the species calcifying depth. Foraminifera habitat preferences are spatially and temporally variable[26,33] adding uncertainty to the origin of the proxy signal. Note that similarly Mg/Ca paleothermometry can also be applied to osctracods[20].
	Core	Planktonic foraminifera assemblages	Planktonic foraminifera species are distributed around the world in global belts related to surface water temperatures[13]. Faunal counts are used to reconstruct relative/quantitative surface temperatures (approximately 0–200 m) with the use of transfer functions. The exact living season and depth are uncertain and may vary in space and time[21].
Bottom Temperature	Core	Benthic foraminifera assemblages	Foraminifera that live on or within the sediment have environmental preferences and some benthic species particularly on the Greenland shelf have proven useful to study past hydrographic seafloor conditions[18]. These assemblages, however, can also be modified by other environmental parameters and also food availability[6].
	Core	Mg/Ca benthic foraminifera	Similar to planktonic foraminifera the amount of Mg incorporated into the benthic foraminiferal shell is an indicator of the calcifying temperatures with secondary effects from carbonate ion changes[11,35]. In this case the organism lives on or in the top layer of the sediment and hence records the temperature at the water depth of the sediment core.
Salinity	Core	Dinocyst assemblages	Dinocysts are found in freshwater to hypersaline environments; in some environments their assemblages can be used as a qualitative indicator of sea surface salinities. As with temperature, reconstructions of salinity can be quantified through the use of transfer functions[3,30]. Similar caveats as to the influence of other environmental variables with sea surface temperatures potentially a confounding factor[24].
	Core	Paired Mg/Ca-$\delta^{18}O$ in foraminifera	Combing $\delta^{18}O$ and the Mg/Ca proxy enables reconstruction of $\delta^{18}O_{sw}$, which is in turn related to salinity. Salinity estimates, however, assume that regional $\delta^{18}O_{sw}$-salinity relationships remained constant in the past introducing large uncertainties in the salinity reconstructions that are difficult to quantify. Foraminifera habitat preferences are spatially and temporally variable[26,33] adding uncertainty to the origin of the proxy signal.
Sea/Drift ice	Core	Organic biomarkers (IP_{25})	Organic molecule produced by certain Arctic sea ice diatoms. Abundance change of IP_{25} in the sediment is indicative of past spring/summer sea ice conditions[17].
	Core	Ice Rafted Debris (IRD) particles	Lithogenic and terrigenous particles carried within the drift ice are released and deposited on the seafloor when the ice melts. Counts and composition of IRD are used to reconstruct the amount of drift ice transported to the core site and the source of the particles and hence the pathway of the ice to the core site[5],
	Core	Chemical composition of the sediment	The sediment composition can be informative as some minerals such as quartz will be indicative of debris transported by drift ice. Changes in composition may also derive from regional changes in the bottom transported sediment[16,19].
	Coralline Algae	Growth increment widths	The light dependency of the growth rates of coralline algae has been used as a sea ice proxy, but this signal may be confounded by temperature[23,32].
	Core	Diatom/Dinocyst assemblages	Some taxa of diatoms and dinoflagellates have high affinity to sea ice cover making them useful indicators.

Table 1 *(continued)*

Ocean parameter	Archive	Proxy	Description
			Some diatom species live within, or under, sea ice. Other diatom species are adapted for low light conditions so also prefer sea ice cover. Finally, the melting of sea ice often triggers diatom blooms, which follow the edge of the melting ice. As such, diatoms are good indicators of sea ice cover and its retreat. As with temperature, reconstructions of sea ice cover can be quantified through the use of transfer functions[10,9,30]. And contain similar caveats as to the influence of other environmental variables as a potential confounding factor.
Circulation	Core	Sortable Silt Mean Grain Size	The nonbiogenic fraction of the sediment between 10–63 μm is transported and deposited by bottom currents, which sort the deposited particles grain sizes and can be used to infer the relative speed of the depositing bottom current. This flow speed proxy has to be applied in current controlled depositional settings (with no downslope sediment transport), areas/times where the bottom current did not vertically migrate and with no interfering signals from ice rafted debris[15].
	Core/Bivalve	Radiocarbon reservoir ages (ΔR)	Radiocarbon in the surface ocean is in semiequilibrium with the atmosphere, but when the waters sink and are isolated from the atmosphere, the radiocarbon in the water starts decaying. Diverging ages in absolutely dated archives or cores with good age constraint are used to study past changes in the water masses present at the site[20].

Note. The star in the oxygen isotopes as a proxy for temperature denotes the complication of the application of this proxy to reconstruct temperature. References: [1]Urey (1948), [2]Prahl et al. (1988), [3]Koc and Schrader (1990), [4]Cook et al. (1995), [5]Bond et al. (1997), [6]Schmiedl et al. (1997), [7]Spero et al. (1997), [8]Elderfield and Ganssen (2000), [9]Jiang et al. (2001), [10]Vernal et al. (2001), [11]Lear et al. (2002), [12]Ohkouchi et al. (2002), [13]Morey et al. (2005), [14]Prahl et al. (2005), [15]McCave and Hall (2006), [16]Moros et al. (2006), [17]Belt et al. (2007), [18]Perner et al. (2011), [19]Kissel et al. (2009), [20]Hillaire-Marcel and De Vernal (2007), and references herein), [21]Telford and Birks (2011), [22]Adey et al. (2013), [23]Halfar et al. (2013), [24]Juggins (2013), [25]Rosell-Melé and Prahl (2013), [26]Jonkers and Kučera (2015), [27]Featherstone et al. (2017), [28]Freitas et al. (2017), [29]Jonkers and Kučera (2017), [30]Krawczyk et al. (2017), [31]Li et al. (2017), [32]Moore et al. (2017), [33]Rebotim et al. (2017), [34]Reynolds et al. (2017), [35]Barrientos et al. (2018), [36]Gray et al. (2018), [37]Williams, Adey, et al. (2018), [38]Williams, Halfar, et al. (2018).

and the application of dendrochronological cross-dating techniques, these annual bands can facilitate the construction of absolutely dated chronologies (referred as sclerochronologies). Cross-dating techniques can extend these chronologies from the life span of an individual to over 1,000 years (Butler et al., 2013; Reynolds et al., 2013), thus providing a temporal framework for paleoenvironmental reconstruction at annual and subannual resolutions.

2.2. Proxy Compilations and Networks

The generation of proxy compilations, or spatial proxy networks, enhances our ability to reconstruct broad-scale climate variability. The statistical approaches used to isolate the coherent variability across the proxy records are essentially averaging out signals that are only present in individual records, that is, noise (Cunningham et al., 2013; Jansen et al., 2007; Wilson et al., 2010). Reconstructions of North Atlantic (Ocean) climate that span the last two millennia, or part thereof, are predominantly based on terrestrial archives, most frequently tree rings and speleothems (Gray et al., 2004; Mann et al., 2008; Mann et al., 2009; Rahmstorf et al., 2015). Such reconstructions assume that teleconnections between the atmosphere and ocean have remained constant over time. Recently, North Atlantic composite reconstructions based on proxies solely from the marine realm have been produced (Cunningham et al., 2013; Reynolds et al., 2017; Reynolds et al., 2018). Yet, one of the remaining challenges in proxy compilations is the integration of high-resolution annually resolved proxy records with longer but lower temporal resolution

(sedimentary) time series and larger dating uncertainties. This dichotomy often results in either annually resolved short temporal networks (Reynolds et al., 2017; Reynolds et al., 2018) or longer lower temporal resolution binned records (McGregor et al., 2015).

2.3. Climate Models and Simulations for the Last Millennium

Climate models are complementary to climate proxies as a source of information for understanding the climate of the last two millennia. They provide a versatile and powerful framework for hypothesis testing, allowing us to investigate different aspects of past climate variability and the underlying physical mechanisms (e.g., Ottera et al., 2010; Swingedouw et al., 2011). Models are thus useful to perform sensitivity experiments to investigate the role of the external forcings and internal climate variability during particular events of the past climate (Coats et al., 2014; Coats et al., 2016; Swingedouw et al., 2015) and to relate local proxy-based observations to the larger-scale circulation and/or variability modes (Jungclaus et al., 2014; Lohmann et al., 2015). Climate models can further be used as a surrogate reality to validate the use of different reconstruction techniques and approaches (Gagen et al., 2016; Lehner et al., 2012; Moreno-Chamarro, Ortega, et al., 2017), the interpretation and suitability of different climate proxies (Bakker et al., 2015; Dee et al., 2016; Thornalley et al., 2018), and to guide future paleoceanographic efforts to new regions and variables with relevant information for reconstructing different indices of climate variability (e.g., North Atlantic Oscillation and Atlantic Multidecadal Variability, AMOC). The identification of regions sensitive to those indices can be addressed by determining their model-derived ocean fingerprints (Zhang, 2008) and testing their stationarity through time (Zanchettin et al., 2015). Covariances between different model variables and regions provide the basis for data assimilation techniques that relate paleoclimate proxies to quantities like AMOC structure and strength that are not directly observed (Hakim et al., 2016; Singh et al., 2018).

As imperfect representations of the real world and its variability, however, climate models present certain limitations to bear in mind. While the incorporation of the Paleo Model Intercomparison Project phase 4 (PMIP4) into the Coupled Model Intercomparison Project phase 6 (CMIP6; Kageyama et al., 2018) ensured that the same models are used for past, present, and future simulations, long-term transient simulations pose limits to model resolution and cannot be carried out with the most advanced models. This comes at the expense of resolving less accurately several potentially key oceanic processes, which play a significant role in the climate of the North Atlantic, such as turbulent mixing and deep convection, or overflow exchanges between the Nordic Seas and the subpolar North Atlantic. Particularly, relevant for the study of this region is the presence of mean state model biases affecting the Gulf Stream extension (Eden et al., 2004; Schoonover et al., 2016) and the upper ocean temperatures of the subpolar gyre (SPG) region (Keeley et al., 2012; Menary et al., 2015; Sgubin et al., 2017). Such biases can, in turn, influence the representation of Atlantic multidecadal variability in the North Atlantic (Drews & Greatbatch, 2016) and its main driver, the AMOC, and thus contribute to the diversity in the underlying model mechanisms (Buckley & Marshall, 2015). Last millennium simulations are also subject to uncertainties in external forcings, such as the timing and magnitude of the major volcanic eruptions (Sigl et al., 2015; Swingedouw et al., 2017) or the amplitude of the changes in solar irradiance (Jungclaus et al., 2017). There is also evidence that internal climate variability contributed substantially to North Atlantic regional climate changes in the past millennia (Goosse et al., 2005; Moreno-Chamarro, Zanchettin, Lohmann, & Jungclaus, 2017), which hampers any direct model-data comparisons. Furthermore, model-based inferences about the climate response to external forcings are subject to considerable uncertainty given that the ensemble size required to isolate forced variability is not known a priori and is probably larger than recent experiments have afforded (Deser et al., 2012).

Due to their high computational cost, simulations with coupled general circulation models only cover the last millennium, a period for which the forcings are also better known. In the following, to illustrate the state-of-the-art knowledge of North Atlantic variability from climate models, we will use three sets of simulations currently at our disposal: a single experiment with IPSL-CM5A-LR (Swingedouw et al., 2015), a three-member ensemble with MPI-ESM (Jungclaus et al., 2014), and the 13 full-forcing members of the Last Millennium Ensemble with CESM1 (CESM-LME; Otto-Bliesner et al., 2016). Results from other last millennium simulations will also be described in the model discussion section.

3. Methodology

3.1. Proxy Record Selection Criteria

In order to study and discuss the hydrographic properties and ocean processes of different currents over the last 2,000 years, we followed a set of strict selection criteria of available paleoceanographic reconstructions. Records selected for our discussion needed to have a minimum of four dating constraints in the last 2,000 years or over the length of the record. These dating points could include radiocarbon dates, a set of Lead-210 dating, presence of tephras from precisely dated eruptions, and/or SCPs, or be based on layer counting. In addition, the resolution had to be 100 years per sample, on average over the last 2,000 years, and time series were only included if they were longer than 100 years.

3.2. Model Analysis

The selected models represent a small sample of all last millennium simulations performed within the CMIP5/PMIP3 initiatives. Since they all follow the protocol suggested by PMIP3 (Schmidt et al., 2011), we regard them to some extent comparable, even though the combination of external forcings they use is not exactly the same (see details in Table S1 in the supporting information). These simulations only cover the period from 850 year CE onward, because it is the period for which the most accurate estimates of the external forcings were available. Climate model simulations extending over longer periods do indeed exist, such as the TraCE-21ka simulation covering the last 21,000 years; however, they are performed with models of intermediate complexity (like the LOVECLIM climate model) with a too simplistic ocean or do not include key external forcings (like volcanic eruptions; e.g., Ahmed et al., 2013) that can be required to reproducing major climate excursions in the past millennium like the LIA. For such reasons, we decided not to include them in this study. During the process of writing this review, the first results of a transient simulation for the past 2,000 years within PMIP4 were published with the CESM model (Zhong et al., 2018).

We will use these three models to illustrate the simulated changes in large-scale ocean dynamical variables that cannot be easily captured by proxies (section 5.1) and their associated fingerprints on surface temperature (section 5.2). In particular, we will focus on the AMOC strength at subpolar latitudes (computed as the average of the zonal mean overturning stream function between 35°N–50°N and 500–1,500-m depth), the SPG strength (computed as the maximum absolute value of the barotropic stream function between 50°N–65°N and 20°W–60°W), and the Denmark Strait Overflow (DSO; computed as the source water transport from an overflow parameterization in CESM, the southward mass transport across the sill between 500 m and the ocean bottom in the IPSL model, and the southward transport for waters denser than 27.8 kg/m^3 in the MPI-ESM; these different definitions account for differences in model characteristics, configurations, and parameterizations).

For this exploration of the climate models, we will use decadally smoothed data (with 10-year running means) to filter out interannual variability and thus focus on the decadal to multidecadal timescales, which are more relevant for the interpretation of proxy records. Model ensembles will be described by their ensemble mean and spread (represented by the ensemble maximum and minimum).

4. North Atlantic Variability Over the Last 2,000 Years: A Proxy Perspective

4.1. Surface Hydrography Changes of the Northward Flowing Warm Atlantic Waters

The northward transport of heat and salt via the surface ocean across the North Atlantic is not only a key process for the modulation of European climate but is also essential for the densification of the surface waters and hence the formation of deep waters as part of the AMOC. In this section we will review the available surface hydrographic reconstructions in the region where the relatively warm and saline waters of the Gulf Stream (section 4.1.1) flow northwestward across the North Atlantic basin as the NAC (section 4.1.2) into the Nordic Seas (section 4.1.3 and Figure 1).

4.1.1. Gulf Stream Region

Most paleoceanographic records in the region of the Gulf Stream that meet our criteria (see section 3.1) are located along the eastern North American coast, more enclosed locations such as Chesapeake Bay/Gulf of Maine, and open ocean records from the Sargasso Sea (Figure 1). Farther north, ocean reconstructions can be found mainly on or nearby the Scotian Shelf. However, the Scotian Shelf region is not exclusively bathed by the warm and saline Gulf Stream waters detaching from the continental slope around Cape

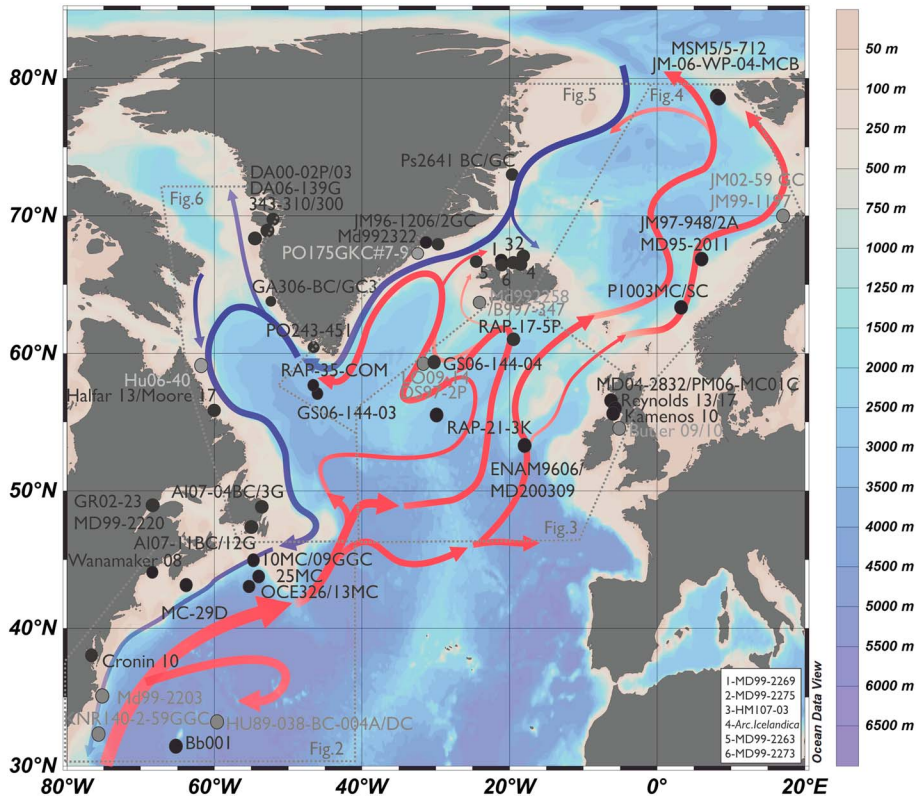

Figure 1. Regional schematic map of the surface ocean currents. Based on Orvik and Niiler (2002), Daniault et al. (2016), and Bosse et al. (2018). Red arrows indicate the pathway of relatively warm and saline waters and blue arrows the pathway of cold southward polar waters. The locations of the proxy records that are plotted in Figures 2–6 and discussed in this section are indicated by the black (plotted and discussed) and gray (only discussed) circles, respectively. The subregions covered in Figures 2–6 are enclosed by the grey dotted lines and labeled accordingly (base bathymetric map made using Ocean Data View; ODV; Schlitzer, 2015).

Hatteras but is also strongly influenced by the slope waters and the southward extension of the Labrador Current. Therefore, this region likely contains multiple water mass signatures through time.

Most southern records (~35°N) show a mix of hydrographic signals at multicentennial timescales and millennial timescales. For example, a long-term warming (0.5°C) is evident off the coast of South Carolina (Saenger et al., 2011; KNR140-2-59GGC; Figure 1), whereas a 2°C cooling and freshening (200–1400 years CE) is found in the surface waters with a warming of the upper thermocline off Cape Hatteras (Cléroux et al., 2012; MD99-2203; Figure 1). The transition to higher $\delta^{18}O$ planktonic foraminifera at the onset of the LIA from a location farther offshore in the Sargasso Sea can be interpreted as a transition to colder surface conditions (Keigwin, 1996). Yet, this could also be related to the increased salinity (and hence higher $\delta^{18}O_{sw}$ values) recorded in the Florida Current record (Lund & Curry, 2006). A higher-resolution surface temperature record developed from ostracod Mg/Ca values from a more coastal setting in Chesapeake Bay (Figure 1) shows clear centennial variability, with warmer conditions during Medieval times (600 to 1,000 CE) followed by a relatively colder interval (1100 to 1800 CE) and a pronounced warming after 1800 CE (Figure 2f; Cronin et al., 2010). The recent warming trend is similar to the warming recorded from 1850 to present in annually resolved coral-based records from Bermuda (Goodkin et al., 2008; Figure 2g) and also records farther north (Figures 2a, 2b, and 6i–6k). These data sets reveal different regional hydrographic trends adjacent to the Gulf Stream waters; however, they do not constrain heat/salt fluxes. To this end, geostrophic calculations based on temperature and salinity reconstructions in the Florida Strait have suggested a decrease in the transport of the Gulf Stream during the LIA of about 10% (Lund et al., 2006), which may explain some of the variability found in the more removed Chesapeake Bay record (Cronin et al., 2010).

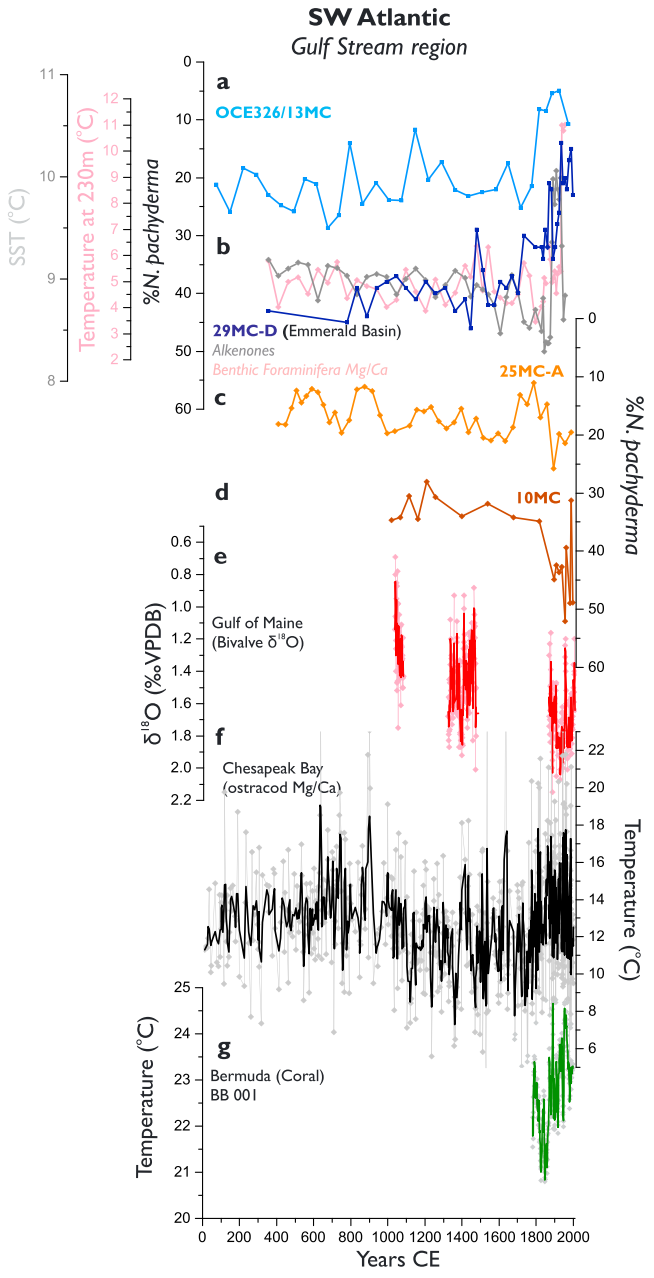

Figure 2. Surface ocean records from the southwest and northwest Atlantic. Percentages of the polar foraminiferal species *N. pachyderma* from (a) Laurentian Fan (Keigwin & Pickart, 1999) (b) Nova Scotia (Emerald Basin; blue; note that superimposed are two records from the same core: Mg/Ca-based temperatures based on benthic foraminifera *C. lobatus*, in pink, and sea surface temperature (SST) record from alkenones, in gray (Keigwin et al., 2003); (c, d) % *N. pachyderma*from Laurentian Fan (25MC-A and 10MC, respectively; Thornalley et al., 2018); (e) δ^{18}O from the bivalve *Arctica islandica* from the Gulf of Maine (Wanamaker et al., 2008); (f) Ostracod Mg/Ca-based temperature reconstructions based on three spliced sediment cores from Chesapeake Bay (Cronin et al., 2010); (g) temperature reconstructions based on Sr/Ca in brain coral from Bermuda (Goodkin et al., 2008). Bold lines are weighted three-point smoothing.

Farther north, three snapshots of annually resolved δ^{18}O values from the bivalve Arctica islandica collected from the Gulf of Maine suggest a long-term cooling and/or increase in salinity across the last millennium (Figure 2e). If the shell-based δ^{18}O record was primarily controlled by temperature, this record would be consistent with the cooling found in alkenone records from the NW Atlantic slope waters (Virginia Slope, Laurentian Fan, and Scotian Margin; Sachs, 2007). In both studies, the inferred cooling was interpreted as an increase in Labrador Current influence or transport to the region and/or more offshore positioned Gulf Stream compared to modern conditions (Sachs, 2007; Wanamaker et al., 2008). However, records from the Scotian Shelf interpreted as lying in the direct path of the inner branch of the Labrador Current reveal different results. Different temperature indicators between 0 and 250 m from Emerald Basin off Nova Scotia broadly show little variability with the exception of the recent warming/decrease of polar waters (~1850–1950 years CE: Figures 2a and 2b; Keigwin et al., 2003). Yet, other nearby sites show cooling at the same time (Figures 2c and 2d; Keigwin & Pickart, 1999; Keigwin et al., 2003). These different surface temperature trends between the preindustrial and industrial period can be clearly seen in Figure 10b. Recently, Thornalley et al. (2018) refined the age models for the published foraminiferal assemblages, specifically the polar planktonic %N. pachyderma time series reflecting the surface conditions (0–70 m) in this region (Keigwin & Pickart, 1999; Keigwin et al., 2003; Figures 2a–2d). Data-model comparisons revealed surface temperature records showing diverging trends in the northwest Atlantic, which matched the sea surface temperature model fingerprints for a slowdown in AMOC across the last 150 years (Thornalley et al., 2018).

In summary, surface ocean reconstructions in this region show large variability in their pattern across records with perhaps the most common signal being the anomalous (either cooling or warming) conditions starting ~1850 years CE (Figure 2). This diverging pattern possibly arises from the complex regional interactions between the Gulf Stream and the Labrador Current (including changes in the Gulf Stream detachment) and/or larger basin-scale circulation changes.

4.1.2. Subpolar NAC Waters

Open ocean records along the NAC pathways are entirely based on marine sediment cores found in high-deposition sediment environments, which allow for high temporal (subdecadal to decadal) resolution proxy reconstructions (Figure 1). On the Reykjanes Ridge, foraminiferal assemblage reconstructions record gradual cooling over the Common Era potentially involving increased freshwater and decreased subpolar frontal influence at the site (Perner et al., 2018). This is in line with previous low-resolution reconstructions farther north (Thornalley et al., 2009). Farther to the NE (North Iceland and Reykjanes), diatom-based sea surface temperature (SST) reconstructions show a gradual warming over the last 2,000 years (Berner et al., 2008; Justwan et al., 2008; Miettinen et al., 2012; Figure 3a), whereas the alkenones in the Reykjanes Ridge show centennial variability but no long-term trends (Sicre et al., 2011; Figure 3b). South of Iceland, however, Mg/Ca-based temperature reconstructions from a deeper-dwelling foraminiferal species (below the summer thermocline and hence likely recording annual conditions) present marked (~3.5°C) centennial variability (periodicity of ~200 years) with a gradual cooling trend over the last millennium (Moffa-Sanchez et al., 2014;

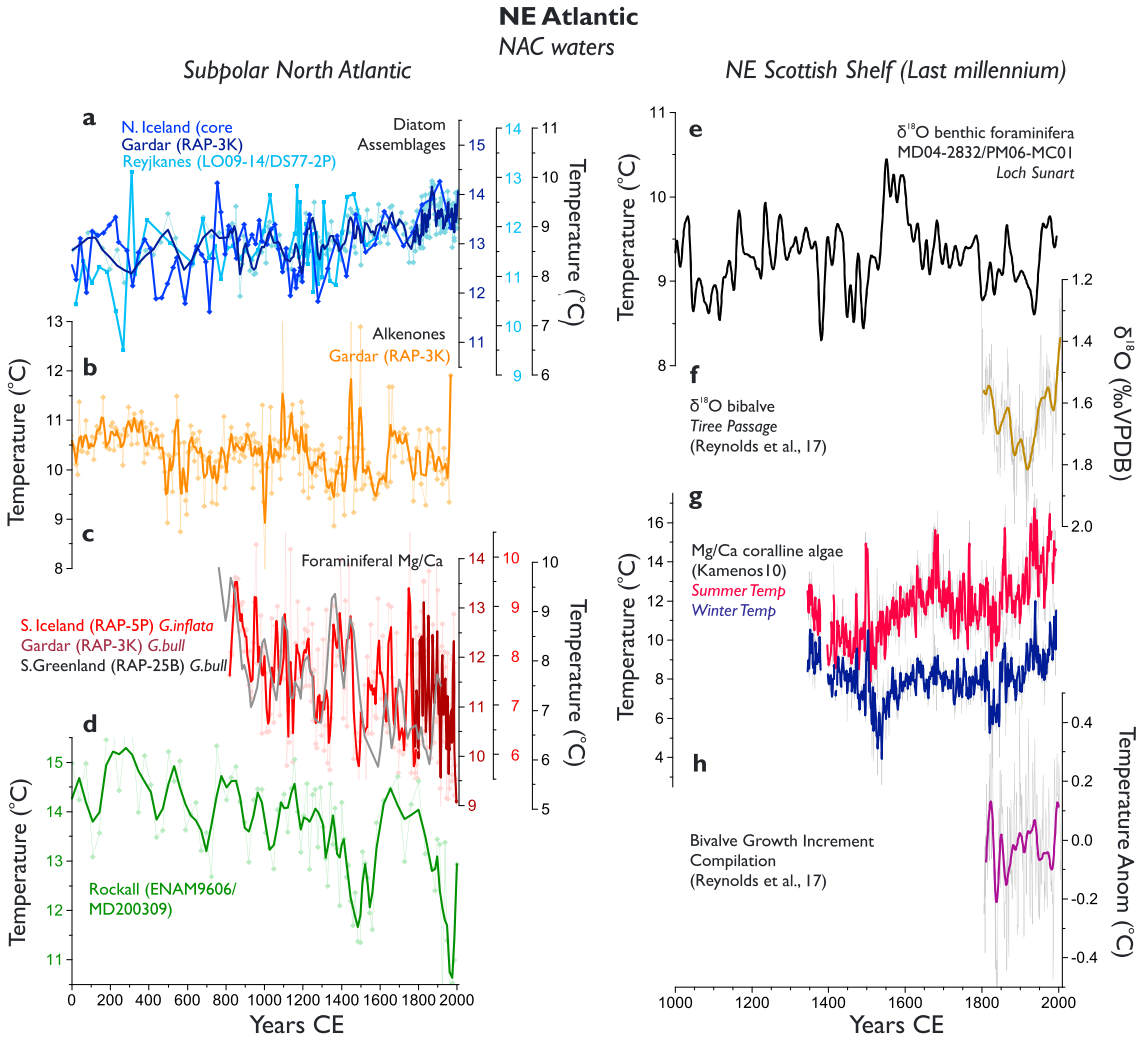

Figure 3. NE Subpolar Atlantic surface reconstructions lying in NAC waters. Left panel: upper water column reconstructions in the Subpolar North Atlantic. Diatom reconstructions from (a) North Iceland MD99-2269 (Justwan et al., 2008), Gardar Drift (RAPiD-21-3K; Miettinen et al., 2012), Reyjkanes Ridge LO09-14/DS77-2P (Berner et al., 2008); (b) alkenone records from RAPiD-21-3K (Sicre et al., 2011); foraminiferal Mg/Ca-based temperature reconstructions from (c) RAPiD-17-5P south of Iceland based on the near-thermocline dweller *G. inflata* (Moffa-Sanchez et al., 2014), and the 230-year record from the surface dweller *G. bulloides* RAPiD-21-12B Gardar Drift (Hall et al., 2010), RAPiD-35-25B (same location as RAPiD-35-COM, Figure 1) South Greenland (Moffa-Sanchez et al., 2014); and (d) Rockal Trough ENAM9606/M2003209 (Richter et al., 2009). Right panel: upper water column temperature reconstructions from the Scottish Shelf (e) Loch Sunart temperature calculated based on the $\delta^{18}O_{foram}$ assuming no salinity changes (Cage & Austin, 2010), (f) Tiree Passage $\delta^{18}O_{shell}$ (Reynolds et al., 2017), (g) Coralline algae Mg/Ca-based winter and summer temperatures (Kamenos, 2010), and (h) proxy network temperature anomalies with respect to the series mean based on bivalve growth increments (Reynolds et al., 2017). Bold lines on raw data are weighted three-point smoothing.

Figure 3c). The amplitude and patterns are similar to SST and sea surface salinity records farther south on the Reykjanes Ridge (Hall et al., 2010; Figure 3c) and on the Rockall Trough (Richter et al., 2009; Figure 3 d) and also to foraminifera-based hydrographic reconstructions of North Atlantic Central Waters off Morocco (Morley et al., 2011). These diverging results within the surface subpolar North Atlantic temperature proxies, especially considering that some of them are from the same sediment core, highlight the differences between the used proxies (Table 1). They likely reflect previously highlighted seasonal biases recorded by the proxy carriers due to blooming and production times and also diverging habitat depths (Leduc et al., 2010; Lohmann et al., 2013).

NAC waters are transported northward to the southern tip of Greenland by the Irminger Current and to the North Icelandic Shelf by the North Icelandic Irminger Current (e.g., Daniault et al., 2016). In the Denmark Strait, proxy records show that the influence of the relatively warm NAC waters transported by the Irminger

Current and the North Icelandic Irminger Current has diminished over the last 2,000 years with respect to the influence of polar East Greenland Current (EGC) waters (Jennings et al., 2011; Ólafsdóttir et al., 2010). Additionally, temperature records from the NAC-derived waters South Greenland are coherent in magnitude and pattern with the records from the south of Iceland (Moffa-Sanchez et al., 2014; Figure 3c).

Farther to the east, observational studies have shown that the waters on the northwest European shelf consist of modified NAC waters that get onto the shelf as a result of tidal internal mixing and other shelf processes (Inall et al., 2009; Marsh et al., 2017). A number of molluskan growth increment width and stable oxygen isotope sclerochronological records exist from this region (Figure 1). The interpretation of the growth increment width series is inherently complex due to the influence of multiple parameters that are likely driving growth (e.g., seawater temperature, quantity, and quality of food; Butler et al., 2010; Reynolds et al., 2013; Reynolds et al., 2017). The 200-year-long Tiree Passage $\delta^{18}O_{shell}$ record shows multidecadal variability with a warming over the twentieth century (Reynolds et al., 2017; Figure 3g) broadly coherent with variability contained in the Loch Sunart $\delta^{18}O_{foram}$ record (Cage & Austin, 2010; Figure 3e). Longer-term temperature records from northwest Scotland, the calcareous algal record (Kamenos, 2010; Figure 3g) and the Loch Sunart $\delta^{18}O_{foram}$ record (Cage & Austin, 2010; Figure 3e), exhibit contrasting pictures with regard to long-term trends. While the Loch Sunart $\delta^{18}O_{foram}$ record contains no persistent trend over the last millennium, except for a light $\delta^{18}O_{foram}$ (hence warmer and/or fresher) period between 1550 and 1600 CE (Cage & Austin, 2010), the calcareous algal record exhibits a gradual increase in temperatures punctuated by multicentennial variability with increased seasonality since 1353 CE (Kamenos, 2010; Figures 3e and 3g). Nevertheless, all records show pronounced multidecadal-scale variability and a consistent notable warming over the industrial period of the European Shelf Current waters (Cage & Austin, 2010; Kamenos, 2010; Reynolds et al., 2017; Figure 3 and 12b).

To summarize, reconstructions from the NAC (and its branches) in the subpolar North Atlantic over the last 2,000 years reveal diverging millennial trends. Diatom surface temperature records show warming (Figure 3a), the alkenone-based temperatures show no discernible changes, whereas the foraminifera consistently show cooling with large-amplitude changes at the centennial scale. These differences likely reflect previously highlighted recording biases and/or postdepositional alterations of the proxy signals (Table 3). The records from the slope waters across the Scottish shelf are shorter and mostly reveal a common warming trend from 1800 CE to present (Figures 3f, 3g, and 10b), which is not clearly recorded in the sediment cores of the subpolar North Atlantic (Figures 3a–3d and 10b). This may reflect a more pronounced recent warming of coastal waters compared to the center of the subpolar gyre (e.g., Rahmstorf et al., 2015).

4.1.3. Atlantic Inflow Into the Nordic Seas: The Norwegian Atlantic Front and Slope Current

The northward transport of Atlantic waters in the Nordic Seas predominantly occurs as two different branches, largely deriving from the east and west branches of the NAC, respectively. These two branches separate and surround the Voring Plateau from either side, one taking a more western versus an eastern pathway and eventually merging close to the Fram Strait (Figure 1; e.g., Wekerle et al., 2017). Paleoceanographic reconstructions from the southern region of the Nordic Seas (~67 N) indicate that sea surface temperature variability across the last 2,000 years was small in the alkenone- and diatom-based reconstructions (~1°C; Calvo et al., 2002; Berner et al., 2011; Figure 4d). The only record that continues into the twentieth century indicates that the warmest conditions occurred just before the year 1000 CE and coolest around 1500 CE, thus coinciding with the LIA. This cooling is attributed to a slowdown in oceanic deep convection in the Nordic Seas in response to negative summer solar anomalies (Berner et al., 2011). Similar patterns are found in the foraminiferal Mg/Ca temperatures at the same site, albeit with a larger magnitude (Nyland et al., 2006; Figure 4d). Planktonic foraminifera oxygen isotope records at this site display a long-term increase, indicating colder/saltier conditions toward the LIA (this trend is less pronounced in the time series from a species that reflects a deeper/colder season signal; Risebrobakken et al., 2003; Figure 4e). The cooling trend is also found in the planktonic foraminiferal assemblage reconstructions from this same site (Andersson et al., 2003; Figure 4d) and in a $\delta^{18}O_{foram}$ record farther south (~64°N), where it is argued to largely reflect changes in SSTs (Sejrup et al., 2011; Figure 4f). The coherent regional cooling across the MCA-LIA transition can be seen in Figure 10a.

Farther north, in the Fram Strait, three independent SST time series exist (Figures 4a and 4b; Bonnet et al., 2010; Spielhagen et al., 2011). Those based on planktonic foraminifera show relative stability for most of the

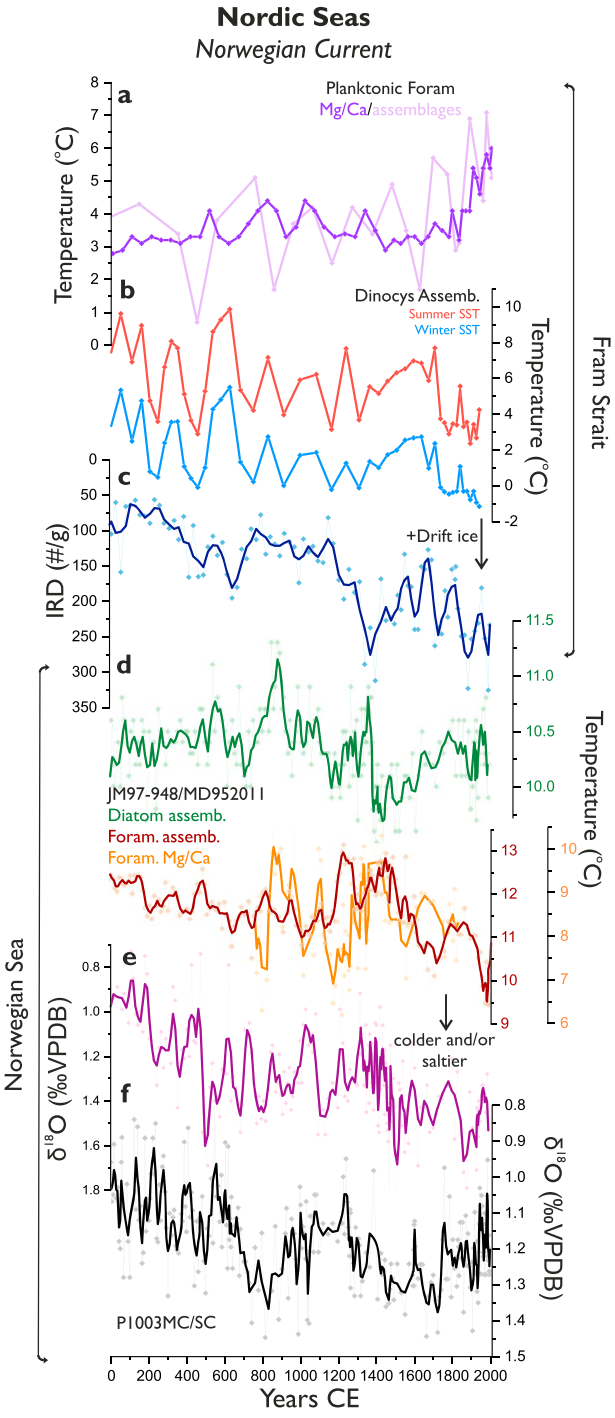

Figure 4. Properties of Atlantic Inflow waters in the Nordic Seas. Fram Strait (a) MSM05/5_712-1: Planktonic foraminifera assemblages and Mg/Ca temperature indicators (Spielhagen et al., 2011); (b) JM06-WP-04-MCB: Dinocyst assemblages (Bonnet et al., 2010); (c) ice-rafted debris counts per gram (MSM5/5-712-1; Werner, Spielhagen, et al., 2011); Voring Plateau core JM97-948/MD952011 surface ocean reconstructions; (d) temperatures based on diatom assemblages (green; Berner et al., 2011), Mg/Ca composition of planktonic foraminifera (orange; Nyland et al., 2006) and planktonic foraminifera assemblages (burgundy; Andersson et al., 2003); (e) $\delta^{18}O_{foram}$ (Risebrobakken et al., 2003); and (f) $\delta^{18}O_{foram}$ from P1003MC/SC (Sejrup et al., 2011). Bold lines on raw data are weighted three-point smoothing.

Common Era and only a rapid increase since the industrial era (Spielhagen et al., 2011; Figure 4a), which is argued to reflect enhanced advection of Atlantic waters into the Arctic. On the other hand, SST estimates from the same site based on dinocyst assemblages show a long-term cooling trend, accompanied by a reduction in salinity, over the last 2,000 years (Bonnet et al., 2010; Figure 4b). This recent diverging trend in the Fram Strait, also shown in Figure 10b, may be real or potentially reflect habitat bias in the different proxies or postdepositional calcium carbonate preservation changes (Zamelczyk et al., 2013). Over the same period, the influence of drift ice increased at the Fram Strait (Werner, Spielhagen, et al., 2011; Figure 4c). So, apart from the planktonic foraminifera proxies in the Fram Strait, all surface parameters appear to show a coherent millennial cooling that culminated in the LIA or in some cases continued until the twentieth century (Figure 4). This is consistent with the previously observed global SST trend, possibly as a result of accumulated volcanic forcing (McGregor et al., 2015) or a Neoglaciation decrease in Northern Hemisphere summer insolation.

In summary, surface reconstructions of the Atlantic inflow in the Nordic Seas largely reveal a millennial-scale cooling and increased drift ice (Figure 4). Additionally, the higher-resolution records reveal centennial changes, with the most noticeable being the surface cooling and increased drift ice at ~1300–1450 years CE around the MCA-LIA transition (Figures 4c–4f and 10a).

4.2. Changes in the Southward Flowing Surface and Subsurface Polar Waters: From Fram Strait to the Labrador Current

Polar waters originating from the Arctic Ocean reach the subpolar North Atlantic via two pathways: the EGC and the Labrador Current (LC). The EGC flows through the Fram Strait southward along the East Greenland shelf and finally through the Denmark Strait into the Subpolar North Atlantic. This current acts as an important route for the southward transport of freshwater and sea/drift ice between the Arctic and the Subpolar North Atlantic. Once it reaches the subpolar North Atlantic, it flows alongside NAC-derived currents such as the North Icelandic Irminger Current (North Iceland) and the Irminger Current (along Southeast Greenland south of the Denmark Strait) forming a clear front, often referred to as the polar front (Figure 1). At Cape Farewell, the EGC mixes with the Irminger Current forming the northward flowing West Greenland Current (WGC). As the WGC circles around Baffin Bay, it merges with other outflows from the Canadian Arctic Archipelago and Hudson Strait eventually flowing south as the Labrador Current. This section will discuss the reconstruction of the ocean conditions in regions bathed by the EGC during its transit from NE Greenland to the most southern tip of Greenland (section 4.2.1) and the WGC and LC (section 4.2.2).

4.2.1. Polar Waters and Ice Along East Greenland and North Iceland

There are only a few high-resolution sediment records in the direct pathway of the EGC due to the low phytoplankton productivity and carbonate dissolution, which limits our understanding of Arctic Ocean freshwater and sea/drift ice outflow at centennial timescales. For this reason, the available paleoceanographic reconstructions mostly rely on (i) records close to the Greenland continental margin or near fjords in which

signals could be overprinted by local processes or (ii) locations within the polar front, in which shifts can be recorded by studying the relative influence of cold versus warm waters at that site over time.

At Foster Bugt (73°N), in the northeastern part of the Easter Greenland shelf (Figure 1), the surface reconstructions (including planktonic foraminiferal assemblage, biomarkers, and mineral composition) suggest increased and more variable contributions of meltwaters from the Greenland margin to the EGC from ~800 CE to present (e.g., Figure 5a; Perner et al., 2015; Andrews et al., 2016; Kolling et al., 2017). Deeper waters at this site contain Recirculating Atlantic Wasters (Figure 1), and reconstructions of ocean conditions at 469 m show overall cooling (Perner et al., 2015; Figure 5h) in agreement with increased presence of cold polar waters and ice at Fram Strait (Bonnet et al., 2010; Werner, Spielhagen, et al., 2011; Müller et al., 2012; Figures 4b and 4c) implying a reduced northward heat advection and/or cooling of the Atlantic inflow waters.

Farther south, the North Icelandic shelf is a region of great oceanic interest due to its proximity to the polar front. This region marks the boundary between the relatively warm and saline Atlantic waters advected via the Irminger Current through the Denmark Strait clockwise around the north coast of Iceland and the colder and fresher Arctic-derived polar waters transported within the East Greenland and East Iceland currents (e.g., Logemann et al., 2013). Relative shifts in the proportion of these two distinct waters entrained onto the North Icelandic shelf have been demonstrated to cause significant shifts in water temperature, salinity, sea ice extent, biological productivity, and the geochemical composition of the water column, hence allowing the reconstruction of this oceanic front back in time. Paleoceanographic variability on the North Icelandic shelf has been investigated extensively over the past decades using a multitude of proxy archives such as sediment cores (e.g., diatoms, foraminifera, and biomarkers) and bivalves ($\delta\,^{18}O_{shell}$, ΔR; Figure 1).

The analysis of diatom assemblages from sediment core MD99-2269 suggests that there was a gradual increase in summer/August SSTs over the past 2,000 years (Justwan et al., 2008; Figure 3a). Contrastingly, a higher-resolution diatom assemblage temperature from core record (MD99-2275) suggests a gradual cooling with a likely step change in surface temperatures between a relatively warm interval from 800 to 1300 CE to a relatively cooler interval ~1350 CE to present, interpreted as the MCA-LIA transition (Jiang et al., 2005; Ran et al., 2011; Jiang et al., 2015; Figure 5j). Similar surface cooling trends are contained in alkenone reconstructions (Sicre et al., 2008; Sicre et al., 2011; Figure 5i) and an annually resolved $\delta\,^{18}O_{shell}$ (Reynolds et al., 2016; Figure 5k). Furthermore, reservoir ages based on mollusks and bivalves show an increase from ca. 1000 CE to 1850 CE, suggesting a gradual increase in the proportion of (older) polar waters entrained onto the North Icelandic shelf (Figure 5k; Eiríksson et al., 2004; Eiríksson et al., 2011; Wanamaker et al., 2012). These results are consistent with the SSTs (Figures 5i–5k) and sea ice (Figures 5c–5e), suggesting an increase in polar water influence and likely a southward migration of the polar front across the last millennium, which culminates in the LIA. Also, similar to the SST records, the drift ice records from this region show a step change between ~1150 and 1350 CE into colder conditions (Figures 5c–5e) probably associated with the onset of the LIA (Cabedo-Sanz et al., 2016; Massé et al., 2008; Moros et al., 2006; Sha et al., 2015). Some of the records also suggest evidence for an increased presence of warmer Atlantic waters on the North Icelandic Shelf over the industrial era captured in the in the $\delta\,^{18}O_{shell}$ and a reduction of ΔR (Figure 5k; Eiríksson et al., 2004, 2011; Wanamaker et al., 2012).

Farther south in the Denmark Strait, few paleoceanographic records exist. Records from northern Denmark Strait at Nansen Trough show a millennial reduction of subsurface warm Recirculating Atlantic waters (Perner et al., 2016; Figure 5l), consistent with lower resolution time series from the same site (Jennings & Weiner, 1996). Both pieces of evidence either indicate a weaker transport or cooler subsurface/bottom Atlantic waters of the IC. These results are also consistent with the trends seen in diatom-based April sea ice cover in the southern Denmark Strait (Figure 5f; Miettinen et al., 2015). Another record from the eastern side of the Denmark Strait shows a step increase in quartz content (indicator of drift ice) at ~1,600–2,000 compared to the earlier half of the last millennium (Andrews & Jennings, 2014). Yet, other records from the cores in SE Greenland Fjords indicate variable source for the recorded drift ice through the last 2,000 years (Andrews et al., 2014). These discrepancies are potentially a result of the complexities interpreting drift/ice indicators in enclosed dynamic areas on the shelf where the provenance of the grains can be local or more regional as highlighted by the short record spanning 1850 to present (Alonso-García et al., 2013).

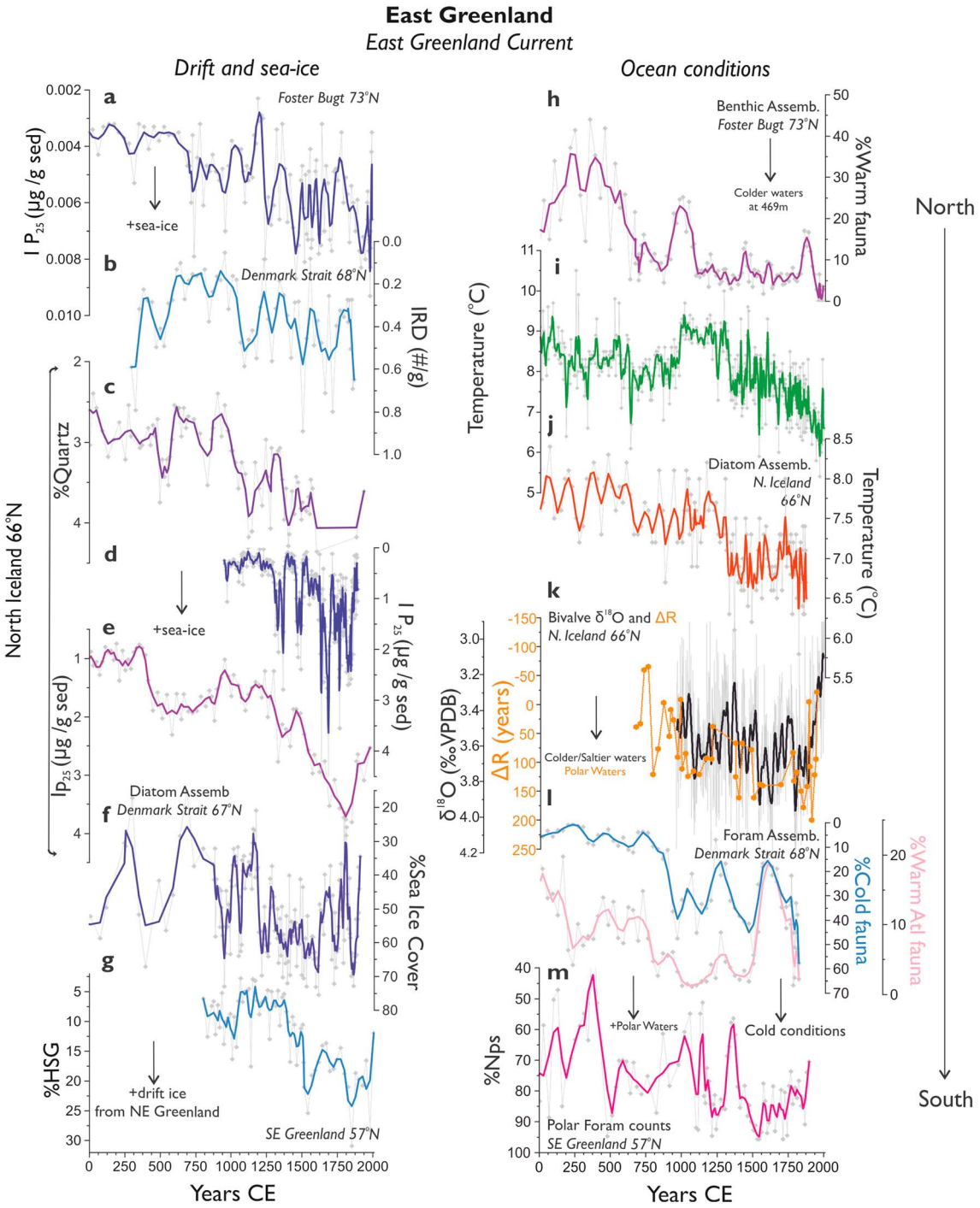

Figure 5. Ice and oceanographic conditions along Eastern Greenland and North Iceland. Left panel shows sea/drift ice conditions (a) sea ice conditions in PS2641 BC/GC at Foster Bugt (Kolling et al., 2017); (b) drift ice recorded in the Denmark Strait JM96-1206/2GC (Perner et al., 2016) North Iceland; (c) %Quartz from MD99-2269 (Moros et al., 2006); sea ice biomarker (d) MD99-2275 (Massé et al., 2008) and (e) MD99-2269 (Cabedo-Sanz et al., 2016); (f) April sea ice cover from diatom assemblages in the West Denmark Strait (MD99-2322; Miettinen et al., 2015);and (g) Haematite Stained Grains (HSG) transported from northwest Greenland to South Greenland (GS06-144-03; Alonso-Garcia et al., 2017). Right panel shows oceanographic conditions (h) benthic foraminiferal assemblages at ~430 m, which are indicator of Atlantic Intermediate Waters (PS2641 BC/GC; (Perner et al., 2015), North Iceland upper water column conditions; (i) sea surface temperatures from alkenones (MD99–2275; Sicre et al., 2008; Sicre et al., 2011); (j) summer sea surface temperatures from diatom assemblages (Jiang et al., 2015; MD99–2275); (k) $\delta^{18}O_{shell}$ (black; Reynolds et al., 2016) and ΔR (orange; Wanamaker et al., 2012) from Arctica islandica from the North Iceland shelf; (l) benthic assemblage from ~400-m deep in the Northern Denmark Strait (JM96-1206/2GC; Perner et al., 2016); (m) % planktonic foraminifera species *N. pachyderma* from the Eastern Labrador Sea (South Greenland; RAPiD-35-COM; Moffa-Sánchez & Hall, 2017). Bold lines on raw data are weighted three-point smoothing.

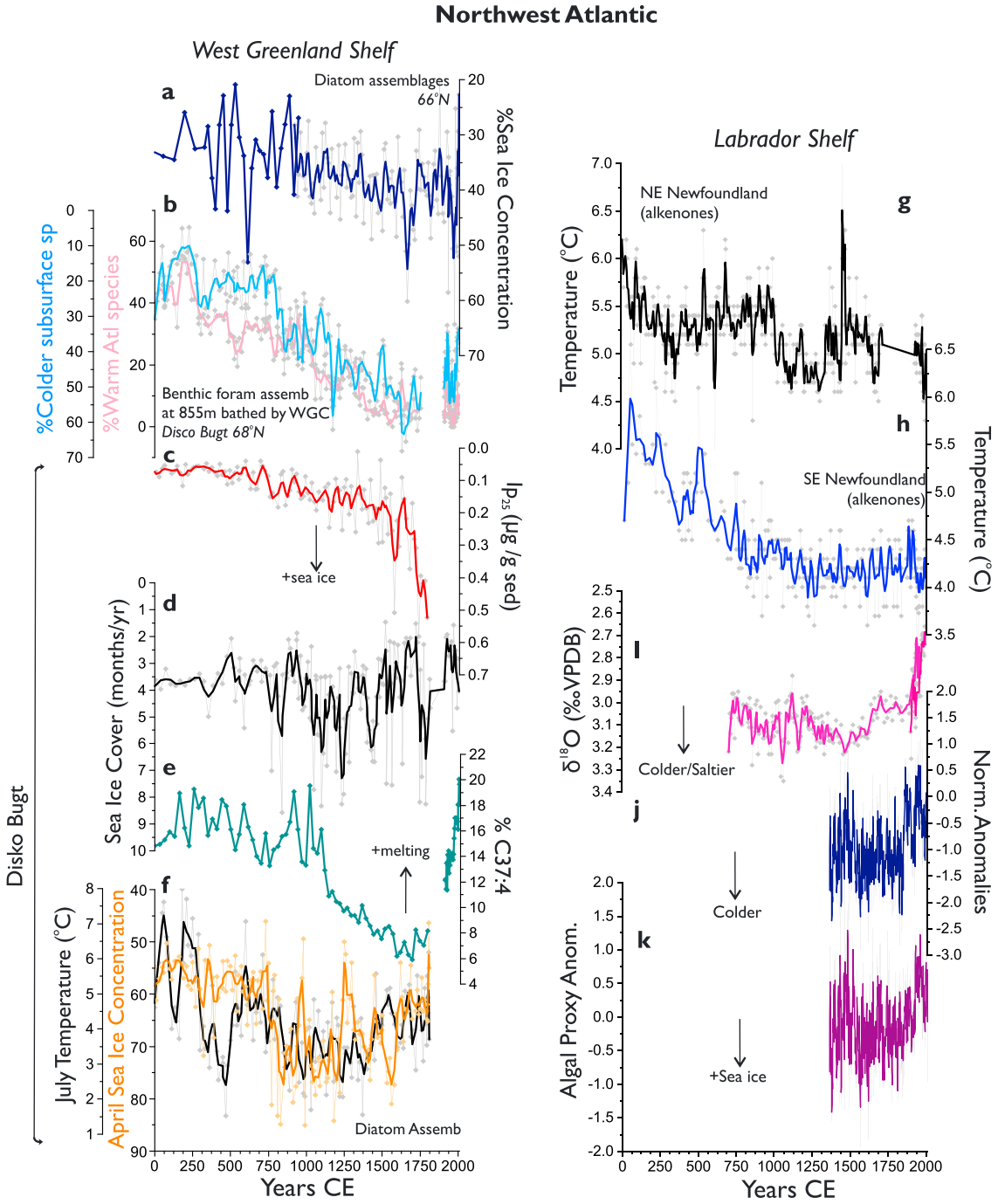

Figure 6. Ocean conditions around West Greenland and the Labrador Shelf. (a) Sea ice concentration from central west Greenland shelf (GA306-BC/GC4 spliced with lower res GA306-GC3; Sha et al., 2016; Sha et al., 2017), (b) benthic foraminifera assemblages at 855 m on the West Greenland Shelf bathed by WGC (343310-MC/GC; Perner et al., 2011), Disco Bugt surface ocean reconstructions; (c) biomarker sea ice reconstructions (343310GC; Kolling et al., 2018); (d) sea ice cover reconstructed from dinocysts (343310-MC/GC; Allan et al., 2018); (e) organic biomarkers as indicators of melting (343310; Moros et al., 2016), (f) diatom assemblages July sea surface temperature reconstructions (black) and April sea ice cover (343310; (Krawczyk et al., 2017); (g) alkenone-based sea surface temperatures from NE Newfounland (AI07-04BC/3G) and (h) (AI07-11BC/12G; Sicre et al., 2014). (i) Benthic $\delta^{18}O_{foram}$ record at 300 m within the Laurentian Channel GR02-23 and MD99-2220 (Thibodeau et al., 2018). (j) Multispecimen record of coralline algae from Labrador and Baffin Island generated by averaging the normalized and annually averaged Mg/Ca (Moore et al., 2017) and (k) annual growth rates (Halfar et al., 2013) giving equal weight to each of the time series. Bold lines on raw data are weighted three-point smoothing.

Farther downstream, in a more open ocean setting off the southern tip of Greenland, colder surface (~25–150 m) conditions are suggested from planktonic foraminiferal Mg/Ca and assemblages suggesting an increase in polar EGC waters reaching the Eastern Labrador Sea (Figures 3c and 5m; Moffa-Sánchez et al., 2014; Moffa-Sánchez & Hall, 2017). It is worth noting that a temperature and salinity record from the same sediment core based on the polar species N. pachyderma reveals very small to no changes for the last millennium (Moffa-Sánchez et al., 2014) perhaps due to their changing habitat preference or, more likely, its insensitivity to temperature (Jonkers et al., 2013). Superimposed on the long-term surface cooling in SE Greenland, clear centennial-scale SST (0–150 m) variability has also been recorded, some coincident with well-known climatic events such as the cold LIA and the Roman Warm Period (Justwan et al., 2008; Moffa-Sanchez et al., 2014; Moffa-Sánchez & Hall, 2017; Figure 5m). Furthermore, drift ice reconstructions from a nearby core show an increase in hematite stained grains, which originate from northwest Greenland at ~1450 CE (Figure 5g; Alonso-Garcia et al., 2017). This record confirms an increase in drift ice transported southward along the East Greenland to the southern tip of Greenland (Alonso-Garcia et al., 2017) and is in line with other more northern records (Figure 5), thus verifying the increase in polar ice-laden waters reaching the subpolar North Atlantic via the EGC.

This section highlights the difficulties in reconstructing the polar waters carried by the EGC from the Fram Strait to the southern tip of Greenland in the past. However, most records consistently show a millennial cooling around the east and south of the Greenland margin. Paleoceanographic records proximal to the location of the polar front, such as North Iceland and South Greenland, suggest a southward shift and an increase in the influence of polar waters versus Atlantic warm waters. Furthermore, sea/drift ice time series also record a gradual increase in the export of drift ice from Northwest Greenland to the subpolar North Atlantic likely within the EGC. Even if most records present the coldest and more ice-laden conditions during the LIA, some records show a more step-like cooling close to the MCA-LIA transition (~1100–1500 CE).

4.2.2. West Greenland and the Labrador-Baffin Bay Region

Regional oceanic conditions on the West Greenland shelf, including both surface (temperature, salinity, and sea ice concentration) and subsurface (temperature, salinity, and flow speed) parameters, vary in response to (i) changes in the WGC's source currents (EGC, Arctic-sourced cold, low-salinity water and the IC, relatively warm, saline Atlantic sourced water; Buch, 1981; Tang et al., 2004) and (ii) the local surface meltwater discharge from the Greenland Ice Sheet (Holland et al., 2008; Rignot et al., 2010). Sea ice reconstructions from central Western Greenland reveal an increase in sea ice culminating around 1650 years CE (Sha et al., 2016; Sha et al., 2017; Figure 6a). This corresponds with the cooling and increased drift/sea ice found in East Greenland (Figure 5; section 4.2.1) but contrasts with records from Igaluku Fjord (Jensen et al., 2004; Lassen et al., 2004).

Most west high-resolution paleoceanographic reconstructions from Greenland are located farther north in Disko Bugt (Figure 1). Proxy records from the shelf (550–800 m) consistently show a warm WGC during the Roman Warm Period (0–600 CE) followed by a long-term cooling culminating at the onset of the LIA (~1300 CE; Perner et al., 2011; Erbs-Hansen et al., 2013; Perner et al., 2013; Figure 6b). This cooling is explained by an increased contribution of polar EGC waters to the WGC as also found in Eastern Greenland (Figure 5). Trends recorded by surface water proxies, however, document the surface ocean response to meltwater discharge from the Greenland Ice Sheet and the duration of sea ice cover (e.g., Moros et al., 2016). For instance, between 0 and 600 years CE (Figure 6b; Perner et al., 2011) a relatively strong and warm WGC-induced melting of marine-based outlet glaciers causing surface freshening and warming (Andresen et al., 2011; Krawczyk et al., 2013; Ouellet-Bernier et al., 2014; Sha et al., 2014; Moros et al., 2016; Krawczyk et al., 2017; Allan et al., 2018; Kolling et al., 2018; Figure 6). From ~800 CE the WGC cooled (Perner et al., 2011; Figure 6b) in parallel to atmospheric cooling and favored a readvance of the ice sheet margin and major outlet glaciers extended again into the fjords (Moros et al., 2016). This led to an overall surface cooling and increased sea ice (Krawczyk et al., 2013; Ouellet-Bernier et al., 2014; Sha et al., 2014; Moros et al., 2016; Krawczyk et al., 2017; Allan et al., 2018; Kolling et al., 2018; Figures 6c–6e). However, around 1300 CE, despite the clear cooling in the WGC (Figure 6b; Perner et al., 2011), the surface records at Disco Bugt show diverging trends in the temperatures and sea ice cover (Krawczyk et al., 2013; Moros et al., 2016; Ribeiro et al., 2012; Seidenkrantz et al., 2008). This decoupling between the WGC and the surface conditions at Disko Bugt at the onset of the LIA highlights the complexities of the ocean-ice dynamics and the regional responses at this location (e.g., Krawczyk et al., 2013; Moros

et al., 2016). Furthermore, the recent, twentieth century subsurface ocean warming increased melting and decrease sea ice have been linked to increase ice retreat and meltwater at Disko Bugt (Krawczyk et al., 2013; Lloyd et al., 2011; Moros et al., 2016).

Unfortunately, no records with suitable resolutions were identified from the Canadian Arctic north of Baffin Bay. High-resolution records derived from sediment cores in the subarctic and Arctic northwest Atlantic are largely concentrated on bays and fjord systems off eastern and southern Newfoundland, which are perhaps not representative of open ocean conditions (Sheldon et al., 2015; Sicre et al., 2014; Thibodeau et al., 2018). In addition, a single record is available off northern Labrador within a midshelf trough in a small basin protected in the north from iceberg scouring (Rashid et al., 2017). The two subdecadal alkenone-based sea surface temperature records from NE and SE Newfoundland show different patterns during the last two millennia (Sicre et al., 2014; Figures 6g and 6h). The diverging features are explained by changes in the influence of the NAC to the southern site versus the Labrador Current to the more northern site (Sicre et al., 2014). Grain size variability and benthic oxygen isotopes and land-derived Ti/Ca ratios are interpreted as an overall Holocene cooling trend (Rashid et al., 2017). This cooling trend is proposed to lead to an increase in sea ice duration in the Labrador Sea that diminishes freshwater supply and results in weakening of the Labrador Current (Rashid et al., 2017). This is an opposing view from the Newfoundland sea surface temperature record (Sicre et al., 2014).

In addition to sediment cores, annually resolved coralline algal time series show warming since the nineteenth century (Moore et al., 2017; Figure 6j). This is interpreted as a regional climate reorganization involving an amplification of the Atlantic Multidecadal Oscillation that coincided with the onset of the industrial era warming (Moore et al., 2017). A combination of Labrador and Baffin Island algal time series indicates increased sea ice throughout the LIA and a steep long-term ice decline in the industrial period (Halfar et al., 2013; Figure 6k). A recent benthic $\delta^{18}O$ record from the Laurentian Channel within the Gulf of St Lawrence reveals a recent (~1900 years CE) step shift to lighter $\delta^{18}O$ interpreted as an increase in subsurface temperatures in the NW Atlantic (Thibodeau et al., 2018) similar to the patterns found in the coralline algae records (Figures 6i, 6j, and 6k). This shift is interpreted as a fingerprint for a recent AMOC weakening, and it is argued that albeit less abruptly, the AMOC weakening started at around the onset of the LIA (~1600 years CE; Thibodeau et al., 2018).

The differences in surface conditions indicated by the proxy records from Western Greenland probably reflect the complex ice-ocean interactions that take place in this region, particularly within enclosed bays. The coastal setting, the limited number of proxy records in the pathway of the LC, and the conflicting interpretations thereof currently limit the interpretation of past ocean conditions in this region. Deeper ocean reconstructions (more representative of the WGC, at 855-m depth) reveal a millennial decrease in Atlantic waters and a concomitant increase in polar waters (Figure 6b) culminating around the LIA. These results are in agreement with an increase in polar waters carried by the EGC around Greenland as concluded in section 4.2.1.

4.3. Deep Circulation in the Subpolar North Atlantic

Several bottom flow speed reconstructions (Table 1) exist across the pathway of the deep overflow waters that cross the Iceland-Scotland Ridge. The subdecadal sortable silt records closer to the sill (2,300–2,080-m depth) reveal broad similarities on multicentennial scales with an increase in flow speed from 0 years CE until 600–800 CE followed by a gradual decline of ISOW flow vigor toward the modern (Mjell et al., 2015; Moffa-Sanchez et al., 2015; Mjell et al., 2016; Figures 7a and 7b). Farther downstream, and at similar depths, the SSrecords also coincide with the slow ISOW between 0 and 600 CE but the rest of the records diverge from the upstream records by showing a steady increase toward the present with several step changes including an increase in the flow at ~1400 CE (Moffa-Sánchez & Hall, 2017; Figure 7c). The subcentennial variability is coherent with a nearby magnetic susceptibility record that, however, this record does not extend beyond 1400 years CE (Kissel et al., 2013; Figure 7c). Farther downstream by the CGFZ (3,100–3,700-m depth), two short magnetic susceptibility records (0–1300 CE) also suggest an increase of overflow vigor peaking around 600 CE and a steady decline until 1,400 m (Kissel et al., 2013; Figure 7d), which is more consistent with the upstream records. The divergence of records from southern Gardar drift can be explained by the relationship found across the last 230 years in which the vigor of the ISOW in the region responded to the overlying Labrador Sea Water and/or atmospheric conditions (Boessenkool et al., 2007) variability along

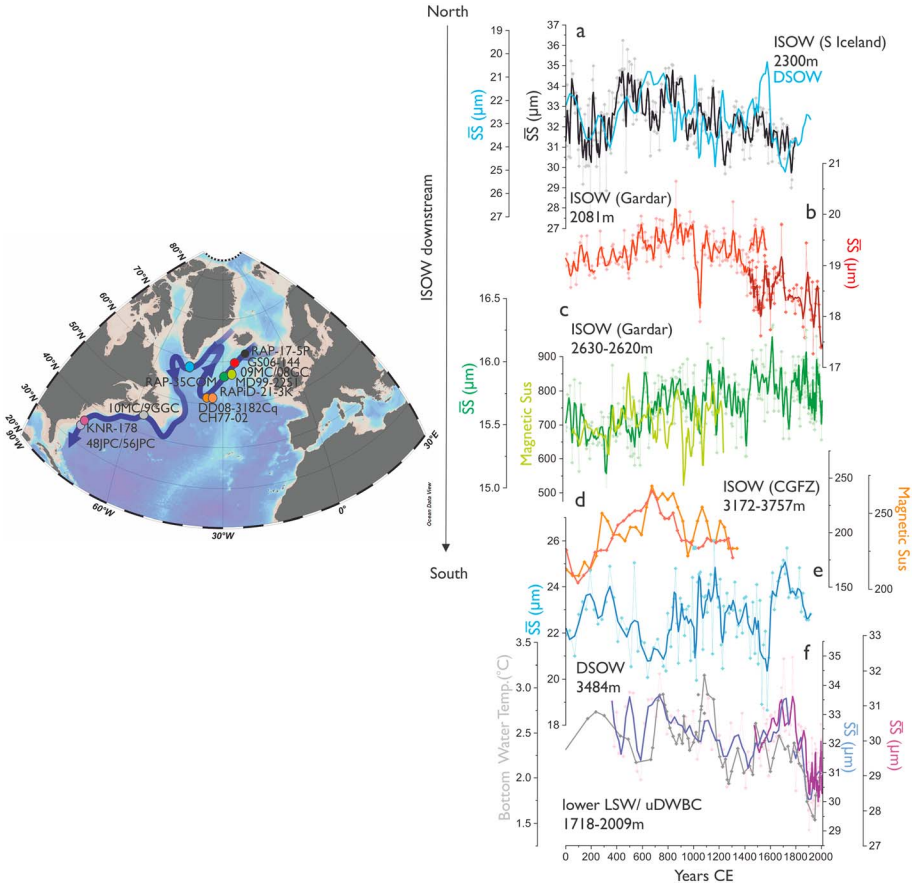

Figure 7. Deep (>1,700 m) ocean records from the subpolar North Atlantic. Inset map outlining the deep circulation boundary currents in the Subpolar North Atlantic including the Nordic Overflows (ISOW and DSOW) and the Deep Western Boundary Current (DWBC), with the proxy record locations indicated by circles color coded to the data in the graph. Bathymetric base map is made using Ocean Data View (ODV; (Schlitzer, 2015). The graph is ordered from the ISOW from north to south including (a) RAPiD-17-5P, which is south of Iceland and close to the Greenland-Scotland Ridge (Moffa-Sanchez et al., 2015; note that the SS from the DSOW, also shown in (e) has been plotted in blue in reverse to show the antiphasing); (b) GS06-144-09MC (dark red; (Mjell et al., 2016) and GS06-144-08GC (red; Mjell et al., 2015; note the discrepancy when splicing); (c) Southern Gardar drift SS from RAPiD-21-3K (Moffa-Sánchez & Hall, 2017) and magnetic susceptibility from MD99-2251 (Kissel et al., 2013); (d) magnetic susceptibility from the deep Charles Gibbs Fracture Zone (CGFZ) CH77-02 and DD08-3182C1 (Kissel et al., 2013); (e) SS record from the from RAPiD-35-COM in the Eirik Drift off the southern tip of Greenland in the path of the DSOW (Moffa-Sanchez et al., 2015); and (e) sortable silt record from KNR-178-48JPC/56JPC in the pathway of lower LSW/upper DWBC (uDWBC; Thornalley et al., 2018). The record in grey denotes three-point smoothed benthic foraminiferal Mg/Ca temperatures at 1,845 m on the Scotian Shelf interpreted as deep LSW (Marchitto & de Menocal, 2003; note that the data from the top 23.5 cm of this record were plotted on the updated age model for KNR-158-10MC from Thornalley et al., 2018). Bold lines on raw data are weighted three-point smoothing.

other pieces of evidence has suggested to be related to changes in the deepwater formation in the Labrador Sea coincident with several of the well-known historical climate periods (Moffa-Sánchez & Hall, 2017). Single-site studies using sortable silt grain size measurements are susceptible to past changes in the vertical position of the deep current (Thornalley et al., 2013). Yet, the overall agreement across proximal sites (Figure 7) lends support to the regional changes arising from downstream changes in the physical mixing/entrainment processes.

In contrast to the Iceland-Scotland Overflow path, there is a scarcity of records from the overflow waters that cross the ridge through the Denmark Strait. There is only one sortable silt record from the southern tip of Greenland at 3,200-m depth (Figure 7e), which shows 400-year oscillations, which are in antiphase with the upstream records of ISOW (Figure 7a; Moffa-Sanchez et al., 2015). The opposite trend in vigor

of the two overflows during this time interval (Figure 7a) implies some diversion mechanism likely implicating atmospheric circulation changes steering the overflow waters east or west of Iceland and potentially compensating (Biastoch et al., 2003; Kohl, 2010). Farther downstream, a bottom temperature record (1,854-m depth) from the Laurentian Slope reveals multicentennial temperature changes related to colder and fresher conditions in the Labrador Sea and glacier expansion on Baffin Island, which influenced the production of Labrador Sea Water (Marchitto & de Menocal, 2003; Figure 7f). In contrast, flow speed records from the DWBC off Cape Hateras at 1,718 and 2,009 m indicate multicentennial variability similar to the ISOW records (Figure 7f; Thornalley et al., 2018). The most noticeable feature in these records is a sudden drop at around 1850 CE interpreted as a decrease in ocean deep convection (1,000–2,500-m depth) in the Labrador Sea contributing to a weakening of the AMOC (Thornalley et al., 2018).

5. Last Millennium Insights From Climate Models

This section provides a model perspective to the major changes that the North Atlantic experienced in the past millennium. Since models cannot resolve the intricacy of signals governing the proxy records, our goal is to highlight model results that provide new insights about physical variables and processes not easily inferred from proxies but that are important for their interpretation. In particular, large-scale dynamical variables such as the AMOC and SPG, and DSO strength, play an important role in the distribution of water masses bathing the North Atlantic. In section 5.1, we illustrate time variability of these variables across multimodel ensembles and describe the results in the context of previous literature. In section 5.2, we give information about the associated fingerprints (regression patterns linking dynamical variables to surface quantities most readily constrained by proxies), which can also help to guide future proxy campaigns. Finally, section 6 juxtaposes proxies and models by comparing long-term anthropogenic changes (industrial, 1850–2005 CE, versus preindustrial, 850–1849 CE) and naturally forced changes (MCA, 850–1250 CE, versus LIA, 1450–1850 CE) in the simulated and proxy-derived surface temperatures.

5.1. Simulated Changes in Ocean Dynamics

To guide and illustrate different aspects of current knowledge from model data, we will use last millennium simulations from three selected climate models (see section 2.3): a 13-member ensemble of CESM, a three-member ensemble of MPI-ESM, and a single realization of IPSL-CM5A-LR. While using ensembles gives insights into the roles of forced and internal variability, care must be taken in comparing model properties. For example, due its larger ensemble size, the CESM ensemble mean is expected to approximate the forced response better than the MPI ensemble, because the average of the internal variability component approaches zero as ensemble size increases (Deser et al., 2012). This comparison between ensemble means is intended to highlight major, long-term forced variability in the North Atlantic, which might be common across models (for example, due to increased greenhouse gas concentration; Cheng et al., 2013). However, we warn the reader that this set of simulations is not adequate to assess the potential interactions between internal variability and particular radiative forcings. These include the potential modulations by the forcing of some modes of internal climate variability such as the Atlantic Multidecadal Variability and also the potential role of background climate conditions in the final forced responses. To address these kinds of questions, the planned efforts within VolMIP (Zanchettin et al., 2016) or through single-forcing simulations in PMIP4 (Jungclaus et al., 2017) should provide a more reliable setup. Similarly, caution should be taken when comparing model simulations and observations. As discussed below, the large role of internal climate variability over the past millennium and the fact that forced variability might be relatively small and hence difficult to detect in both model and real world hamper any direct comparison between the two.

For the different simulations, we have computed key indices for the North Atlantic circulation and overflows. These indices concern the AMOC strength calculated as an average of the overturning stream function in the subpolar region, the SPG strength, and the overflow through the Denmark Strait (see section 2.3 for details). The AMOC strength in Figure 8 shows substantial multidecadal variations in all models, although agreement between the three models is poor (none of the AMOC indices are significantly correlated with each other). Various reasons could explain such disagreement.

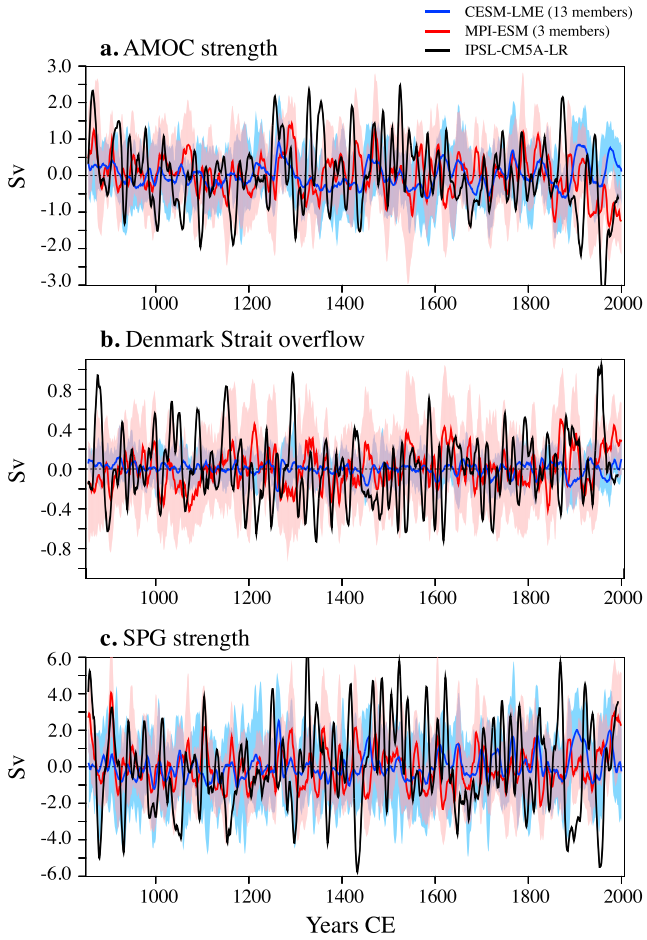

Figure 8. Simulated evolution over the last millennium for the three selected models of three key ocean circulation variables, expressed in Sv (1 Sv = 10^6 m^3/s): (a) the AMOC strength (defined as the average of the overturning stream function between 35°N–50°N and 500–1,500 m), (b) the Denmark Strait overflow (computed as the southward mass transport of dense waters across the Denmark Scotland Ridge; for the exact definition see section 3.2), and (c) the SPG strength (estimated as the maximum absolute value of the barotropic stream function between 50°N–65°N and 20°W–60°W). All values are shown as anomalies with respect to the complete simulated period. The red and blue envelopes respectively represent the total MPI and CESM ensemble spreads (i.e., from the minimum to the maximum values across all members).

First, there might be intermodel differences in the oceanic response to the forcing, including the possibility of a weak response that has no major, direct impact on the North Atlantic circulation. This could be due to the fact that different climate models exhibit internal variability with different characteristics and processes (Ortega et al., 2015; Yan et al., 2018) that can in turn explain different responses to external forcing. Second, model disagreement can reflect that the different ensemble means include different ratios of internal and externally driven variability, depending on their ensemble sizes. A major question to which climate models produce conflicting answers is whether the AMOC strength has been weakening since the onset of the industrial era, as some climate reconstructions suggest (Rahmstorf et al., 2015; Thornalley et al., 2018). Both the MPI (Jungclaus et al., 2014) and the IPSL-CM5A-LR simulations show a decreasing trend over the industrial era that is also seen in other last millennium simulations using the CNRM-CM3.3 and the ECHO-G models (Ortega et al., 2012; Swingedouw et al., 2011). In contrast, the CESM ensemble, for which a larger ensemble size yields a more robust forced signal, has a rather stable AMOC during that period (and lack of sensitivity to the forcing of greenhouse gases, also seen in other transient simulations with the CCSM3 model; Hofer et al., 2011).

Poor agreement between the models throughout the last millennium is also found for the DSO indices (Figure 8). The spread of DSO in CESM is particularly narrow compared to other models, and its ensemble mean shows little variability on most time scales. This model, which includes parameterized overflow physics, is known to exhibit a weak connection between DSO and AMOC variability (Danabasoglu et al., 2012). While overflows have received less attention than other large-scale features of the North Atlantic circulation in the simulations of the past millennium, the ability to constrain overflow rates from proxy information, including sortable silt and magnetic particles (see section 4.3), makes this a useful model diagnostic. In the BCM model, Langehaug et al. (2016) linked velocity changes along the Gardar Drift to the Faroe Shetland Channel overflow, thus supporting the use of ISOW reconstructions from the Gardar Drift as proxies for overflow properties. They also found, however, that velocity changes downstream are not a reliable metric for the strength of the overflow and that, instead, the density of overflow waters can be a better proxy. Lohmann et al. (2014) performed a model-based comparison highlighting the importance of the Nordic Seas overflows and subpolar deep water formation to understand their links with the Atlantic Multidecadal Oscillation and AMOC in last millennium simulations with the MPI-ESM (which is one of the simulations also used here), the IPSLCM4_v2, and the BCM models. They found that the connection between Atlantic Multidecadal Variability and the overflow results from local surface influences in the Nordic Seas and is not mediated by changes in the AMOC.

Similarly as for the AMOC, large intermodel disagreement is found for SPG strength across the three models (Figure 8). The most coherent result is a SPG strengthening in the twentieth century both in the MPI and IPSL simulations, occurring simultaneously to the AMOC weakening. In the MPI model, the AMOC weakening was explained by a substantial reduction in reduced Labrador Sea deep water formation. Following the AMOC decline, the northward heat transport into the subpolar latitudes was reduced, leading eventually to a colder and denser eastern SPG, which responded with a baroclinic strengthening. A similar chain of events had been observed in several CMIP5 historical experiments (Drijfhout et al., 2012), featuring a *warming hole* region in the subpolar North Atlantic. Other periods show a wider diversity of results. For instance, during the LIA the IPSL-CM5A-LR simulation shows again a strengthened SPG state, but the

SPG is anomalously weak in the MPI ensemble (Moreno-Chamarro, Zanchettin, Lohmann, & Jungclaus, 2017) and remains rather stable in the CESM ensemble. Other modeling studies also show conflicting results, supporting either a weaker (Lehner et al., 2013, in CCSM3, and; Zhong et al., 2018, in CESM) or stronger SPG (Schleussner et al., 2015, in CLIMBER-3α) during the LIA. These different responses can be partly due to the different model complexities and experimental setups involved in each study.

As previously indicated, a potential reason behind the low agreement between the indices in the MPI-ESM and the CESM models is their different ensemble sizes and associated ratios of internal to externally forced variability. Figure S4 illustrates how the ensemble size impacts the characterization of the forced signal in the CESM ensemble. The 13-member mean is regarded as the *true forced signal*, and a bootstrapped distribution of correlation scores is generated by randomly subsampling (with replacement) the individual members to generate different N-member ensemble means that are correlated with the *truth*. The analysis thus suggests that a mean anomaly correlation coefficient (ACC) of around 0.6 is needed to conclude (with 95% confidence) that a three-member CESM ensemble contains the same forced signal as the truth. Since the correlation between the three-member ensemble mean of the MPI-ESM and the 13-member ensemble mean of CESM-LME is below 0.15 for all the indices, the analysis implies that the low agreement between them is not due to the different sampling of internal variability by the different ensemble sizes, and it probably reflects incoherences between their respective simulated forced signals. Also, ACC values of about 0.3–0.6 when one member is selected suggest that the forced signal in a single experiment from the CESM-LME explains about 10–35% of its total variance. This analysis highlights that relatively large ensembles are necessary to constrain robustly and analyze the simulated forced signals during the past millennium (i.e., about 10 members would be needed to capture with the ensemble mean half of the variance in the true forced signal).

Another aspect that hampers comparison across models is the uncertainty in the forcing reconstructions used in each simulation. In this case, the PMIP3 protocol proposed different volcanic and solar forcings for *past1000* experiments (Braconnot et al., 2012; Schmidt et al., 2011). The two alternative volcanic forcing data sets differ in the timing and intensity of major eruptions. The differences between the six solar forcing available reconstructions are also large, each differently calibrating the magnitude of the change in the total solar irradiance between present and the Maunder Minimum. The relatively arbitrary decision of using one forcing or another could therefore produce a different representation, for example, in the simulated magnitude, extent, and onset of the LIA cooling (Schurer et al., 2014). Nonetheless, structural uncertainties between different climate models have been found dominating over forcing uncertainty for quantities such as the hemispheric mean temperature (Lehner et al., 2015), although the impact of such uncertainties on past North Atlantic climate variability in particular has not yet been explored.

Despite the uncertainties in the forcing, there is an increasing amount of model evidence (including in the *past1000* PMIP3 simulations shown here) suggesting that strong volcanic eruptions can strengthen the AMOC (Swingedouw et al., 2017), either by triggering a fast atmospheric response that enhances deep convection (Mignot et al., 2011; Zanchettin et al., 2012) or by inducing slow ocean thermodynamic adjustments (Stenchikov et al., 2009). Models further suggest that midsized eruptions (similar to those of mounts Agung and Pinatubo) can synchronize internal North Atlantic ocean variability (Swingedouw et al., 2015) and can thus explain part of the recent decadal basin-wide changes. The potential climatic impacts of volcanic eruptions as a pacemaker of the Atlantic Multidecadal Variability were also highlighted in Ottera et al. (2010). Last millennium simulations have also been used to explore the role that both external forcings and internal ocean dynamics played in the LIA (e.g., Lehner et al., 2013; Miller et al., 2012; Moreno-Chamarro, Zanchettin, Lohmann, & Jungclaus, 2017; Schleussner & Feulner, 2013; Slawinska & Robock, 2018). Most of these studies support the necessity of strong volcanic eruptions for the inception of the LIA but disagree about the causes of its duration. For example, while Slawinska and Robock (2018) explain it by the effect of several minima in solar activity, Miller et al. (2012) suggest the presence of internal sea ice/ocean feedbacks to maintain the initial volcanic-driven cooling anomaly. Moreno-Chamarro, Zanchettin, Lohmann, and Jungclaus (2017) expand on the specific ocean mechanisms that could be at play and further invoke a prolonged reduction in the SPG strength and northward heat transport favoring sea ice expansion and reduced ocean heat losses in the Nordic Seas. These results have been supported by a PMIP4 transient simulation for the past 2,000 years with the CESM model (Zhong et al., 2018). A similar mechanism is also described in Lehner et al. (2013), who also suggest that sea ice increases in the Arctic can be exported to the subpolar

North Atlantic, weakening deep convection, and subsequently, the AMOC, and thus further reducing the transport of heat into the Arctic. In these simulations with the CCSM3 model, the onset of the LIA follows mainly a large reduction in the total solar irradiance, with a marginal contribution from the strong volcanic eruptions in the fourteenth and fifteenth centuries. Other studies have also related colder and extended sea ice conditions in the North Atlantic and the Arctic to solar minima in simulations of the past millennium (Ammann et al., 2007; Landrum et al., 2012; Moffa-Sanchez et al., 2014) reported that the amplitude of the solar variability used to force the model increases the magnitude of the associated climate changes, while suppressing the effects of other natural forcings like volcanism on climate. However, the potential role of the solar forcing in driving the LIA cooling is still highly debated, since latest evidence suggests that the amplitude in the first reconstructions of the solar forcing was overestimated (e.g., Foukal et al., 2006). Furthermore, detection-attribution studies highlight a more important role of volcanic eruptions on large-scale climate variability than solar variations (Atwood et al., 2015; Schurer et al., 2014), whose effect is hardly detected on the past Northern Hemisphere temperature changes (Schurer et al., 2014). Unforced climate simulations can also show spontaneous cold events affecting the entire subpolar North Atlantic from decades to a century, related to feedback mechanisms between sea ice growth and changes in both the oceanic and atmospheric circulation (Drijfhout et al., 2013; Moreno-Chamarro et al., 2015).

In summary, this section highlights the current discrepancies between models and their limitations to disentangle the role of internally versus externally generated variability in dynamical variables such as the overturning and the barotropic ocean circulations in the North Atlantic. Further advances in our current understanding will rely on the success of new coordinated experiments like the *past1000* within PMIP4 (Jungclaus et al., 2017). In particular, the proposed Tier-1 experiments will use for the first time a common set of forcings, and all modeling groups have been encouraged to produce a relatively large ensemble (i.e., up to 10 members if possible).

5.2. Associated Climate Fingerprints and Stationarity Through Time

In addition to helping investigate drivers (e.g., the large-scale ocean circulation) of multidecadal climate variability in the North Atlantic, climate models can inform about their dynamically plausible links with upper ocean variables such as SST, which can be reconstructed directly by proxies. This information can be illustrated by the regression coefficients (also known in this context as fingerprints) between the indices described in section 3.2 (the strength of the AMOC, the SPG, and the DSO) and the North Atlantic SST fields. Figure 9 shows the corresponding results for the multimodel mean regression, with stippling highlighting areas of model agreement (in terms of the coefficient's sign). Regression coefficients are first calculated individually in each ensemble member and subsequently averaged to obtain the ensemble mean coefficient; results shown are the mean of the ensemble means, so that the contributions from each model are weighted equally. Regression coefficients thus account for both internal and externally forced variability, in contrast to the ensemble mean indices in section 5.1.

To evaluate the possibility of differences in these relationships that could emerge from different contributions from naturally and anthropogenically forced variability, fingerprints for the preindustrial and industrial eras are considered separately and compared. It is worth noting that last millennium climate reconstructions are typically calibrated and tested in the historical period against recent observations; thus, this test can help to identify whether links derived in present day's climate can be extrapolated to past millennia. Additional comparisons were made between the LIA and MCA (not shown), but the lack of major differences in regression patterns during these intervals suggests a weak sensitivity of SST fingerprints to the associated regional and global climate changes simulated in the models.

Substantial differences between preindustrial and industrial fingerprints may point to an anthropogenic origin of nonstationarities in relationships between SSTs and ocean circulation during the last several centuries, although they can also obey to the different period lengths (and timescales) covered in each case. Fingerprints can further be influenced by model resolution, as shown for the northwestern Atlantic warming due to CO_2 doubling (Saba et al., 2016). Since our aim here is to review different applications of climate model simulations and not to perform a thorough analysis of the ocean impacts related to each circulation variability, the regression coefficients are computed in phase, that is, without considering a lag between the variables. Also, for simplicity, no trends are removed in the industrial period associated with the global warming.

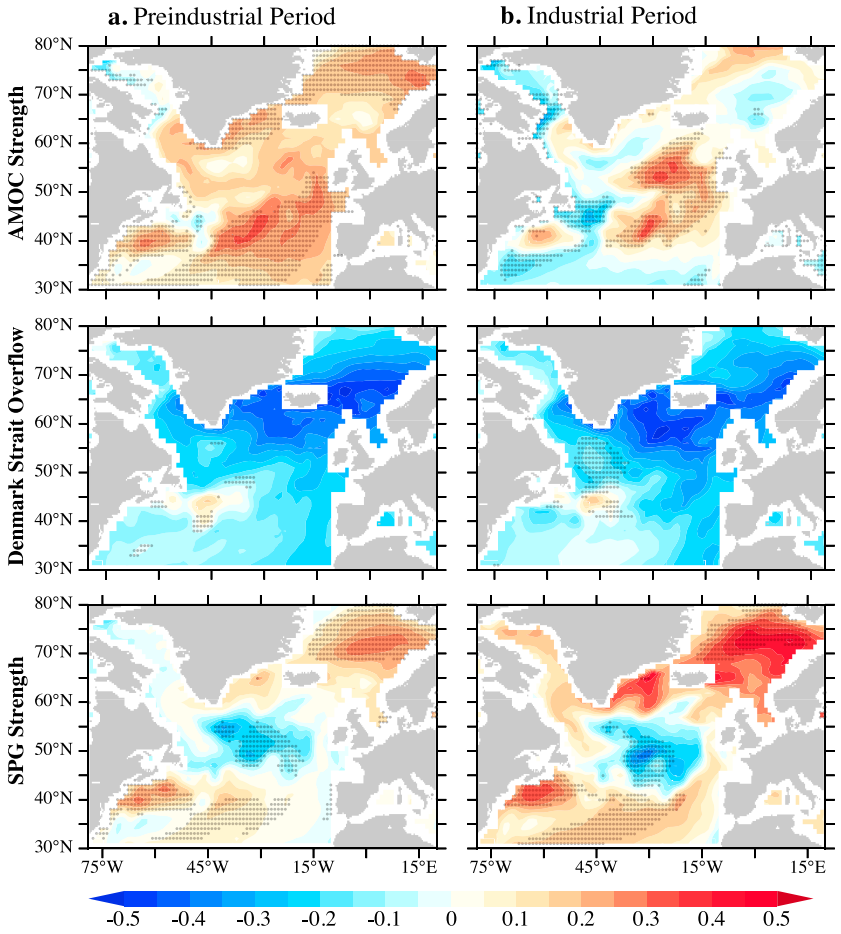

Figure 9. Model SST fingerprints for the ocean circulation and current indices. Regression coefficients (in standard deviation units) between the selected ocean circulation indices (AMOC, DSO, and SPG strength) and the SST fields for the preindustrial (850–1849 CE) and industrial periods (1850–2005 CE). Before regression coefficients are calculated in each individual model simulation, both the SST and the indices are first smoothed with a 10-year running mean and then standardized with respect to each period. The multimodel mean is based on the average of the individual ensemble means of the CESM, the MPI-ESL, and the IPSL-CM5A-LR. Stippling highlights regions of agreement between the three models regarding the sign of the regression coefficient. The ensemble mean of each model is shown in supporting information Figures S1–S3.

The three models agree on warmer SSTs over much of the North Atlantic for a stronger AMOC in the preindustrial period (Figure 9a). By contrast, the pattern and degree of agreement between models substantially change in the industrial period when the only common feature among the three models is positive regression coefficients over the eastern subpolar gyre. This result is consistent with previous studies from observations and models (Jungclaus et al., 2014; Robson et al., 2016) linking a weakened AMOC with a colder eastern subpolar North Atlantic. Zhang (2008) reported a similar link between the AMOC and eastern SPG subsurface temperatures (~400 m) in a 1,000-year control simulation with GFDL CM2.1. A multimodel analysis of 10 different CMIP preindustrial control simulations corroborates the sensitivity of the eastern subpolar gyre SSTs to the AMOC (Roberts et al., 2013). More recently, the study of Ortega et al. (2017), using control simulations from two state-of-the-art climate models, showed that this AMOC fingerprint also emerges in finer (eddy-permitting) resolutions. Moreover, in those simulations, the SST signals in the eastern SPG are strongest when the AMOC is leading by 6 years. Figure 9 also exhibits a cooling related with AMOC increase along the north coast of America, which had also been previously identified as a fingerprint of the AMOC (Caesar et al., 2018; Zhang, 2008). This signal is mainly coherent among the different model simulations over the preindustrial time frame and may be related to a northward shift of the Gulf Stream system (Caesar et al., 2018; Zhang & Vallis, 2007). Finally, the different fingerprints for AMOC indices under preindustrial and

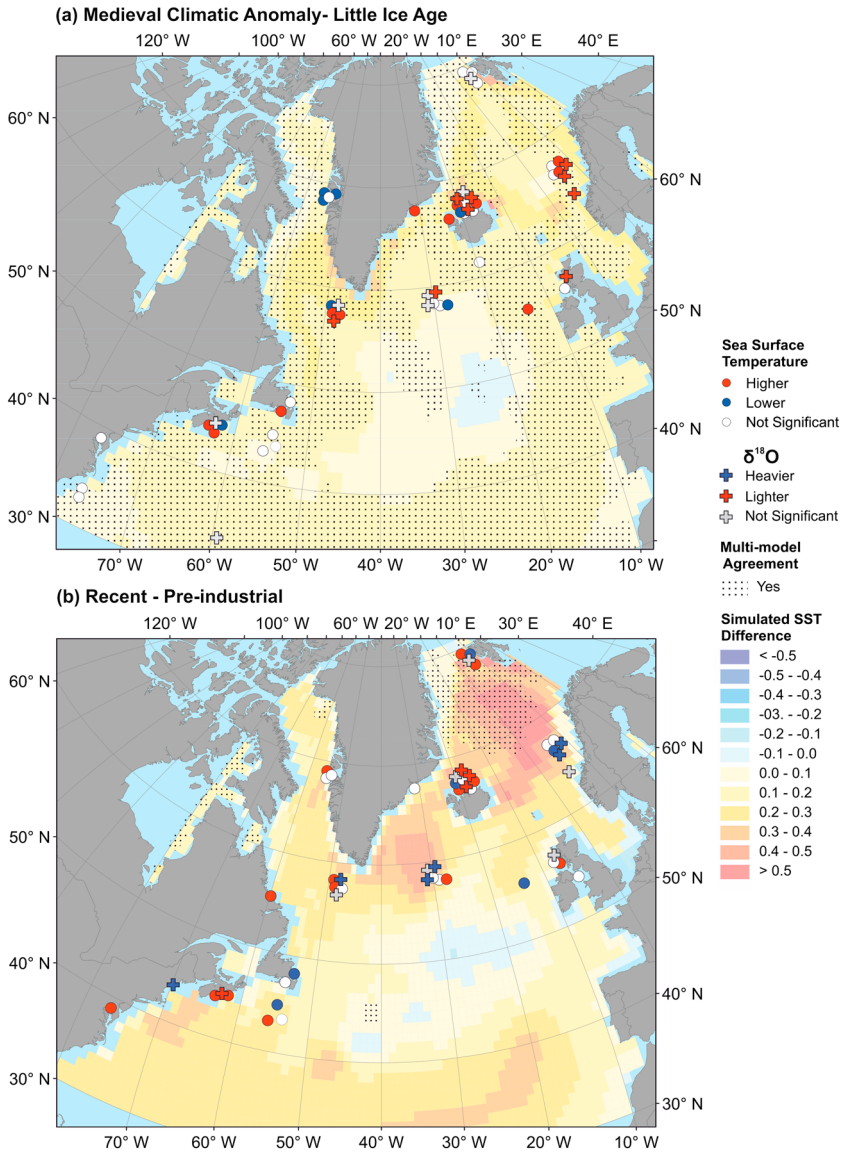

Figure 10. Proxy-model comparison of surface ocean temperature changes in the last millennium. SST (0 m) change simulated by the multimodel ensemble (shaded contours) or reconstructed SST (approximately 0–150 m) by the proxies (filled symbols). Stippling indicates regions in which all models show the same sign of change. In the proxies, colored circles indicate qualitative SST changes between the two periods: red for a warming, blue for a cooling, and white if the change is not significantly different from zero. Colored crosses are equivalent to the circles but represent $\delta^{18}O$-based proxies, which are a combination of temperature and salinity. (a) SST differences between the MCA (850–1250 years CE) and the LIA (1450–1850 years CE) (b) SST differences between the industrial (1851–2000 years CE) and the preindustrial (850–1850 years CE) periods (note that for the proxy data 1000-1850 years CE was used for the preindustrial period). See supporting information Table S2 for the details of the data used.

industrial conditions may reflect distinct roles of gyre and overturning ocean heat transport under internal variability and external forcing (Oldenburg et al., 2018).

In contrast to results for the AMOC index, there is much less agreement across models and time periods in fingerprints of DSO on the SSTs. We can still highlight a model tendency to show colder subpolar North Atlantic and Arctic conditions and warmer waters in the North Atlantic Current Extension when the DSO is stronger. Accounting for some leads and lags between the DSO and the SST might indeed enhance the SST response and improve the intermodel agreement. This may be especially true since overflow

waters propagating downstream can later influence the strength of the AMOC and SPG (Langehaug et al., 2012; Lohmann et al., 2014) and through their associated heat transports the SST field eventually. Although different from the DSO shown here, connections between SSTs across the Iceland-Scotland Ridge and its deep overflow were explored in three climate models (Lohmann et al., 2015; including one of the MPI-ESM simulations shown here), but as opposed than for the DSO, the authors found stronger overflows to be linked with warmer SSTs (and vice versa).

The model-mean fingerprint of the SPG strength on the SST is similar between the industrial and preindustrial periods, with larger amplitudes in the latter. The pattern features a distinct tripole with warming in the Labrador, Irminger, and Nordic Seas, cooling in the central and eastern subpolar North Atlantic, and warming in the Gulf Stream Extension, with all the three regions showing intermodel agreement. These regions show similar sensitivity to the SPG strength in the two higher-resolution simulations explored in Ortega et al. (2017), although with some regional differences, like a strong cooling in the Gulf of Saint Lawrence, which does not seem to be well resolved in the coarser-resolution models.

It has become relatively common to reconstruct large-scale modes of variability such as the NAO (Cook et al., 2002) and the Atlantic Multidecadal Variability (Wang et al., 2017) from a relatively large collection of proxy records, an exercise toward which the model SST fingerprints in Figure 9 can also contribute to validate proxies that could be used to reconstruct each of the indices herein considered. Previous reconstruction studies have used similar statistical relationships derived from models to test and refine their final proxy selection (Zanchettin et al., 2015). Model-based fingerprints can also be exploited for similar purposes with the gridded reconstructions of surface temperature already available, as used by Rahmstorf et al. (2015) to reconstruct the past AMOC evolution. However, this approach can introduce an additional source of uncertainty, inherent to the methodology applied to interpolate the surface temperature fields (Luterbacher et al., 2016; Wang et al., 2015). These uncertainties add to the key assumption that statistical relationships used for calibrating the reconstructions are stationary in time, which does not necessarily hold. Indeed, Figure 9 suggests that fingerprints can be both model and time dependent and therefore need a very detailed analysis to guarantee temporal and spatial consistency. Furthermore, given that SST fingerprints related to AMOC and SPG share some similarities, a high density of proxies extending over their regions of disagreement will be essential to disentangle their separate signals.

6. A Qualitative Proxy-Model Comparison

Proxy-model comparisons have been historically hampered by the distinct nature of both data sources, each subject to its own limitations. In the context of this study, we highlight potential limitations due to the relatively low model spatial resolution (typically of 100 km or larger, depending on the region), which can hinder the realistic representation of some regions where many proxy records are found, particularly on the shelves and slopes or under strongly eddy systems such as the NAC. Proxy reconstructions are generally unequally distributed in time and associated with temporal uncertainty. Also, proxy data include different climatic and nonclimatic signals that are not always easy to disentangle (Table 1). Temperature-sensitive proxies can also include sensing biases and represent specific seasons (at high latitudes generally toward the summer) and depths (Jonkers & Kučera, 2017; Leduc et al., 2010). These incompatibilities thus caution against the direct comparison of proxy records with model outputs at their closest grid points (Pages Hydro2k Consortium, 2017).

To circumvent some of these problems, we have performed a simple qualitative sea surface temperature model-proxy comparison in Figure 10. For this, from the screened records (section 3.1) we selected SST-sensitive proxies (~0–150 m depth; Table S2) and performed two sample *t* tests assuming unequal variance to assess if there was a significant shift (positive or negative) between the Medieval Climate Anomaly and the Little Ice Age (respectively defined as 900–1200 AD and 1450–1850 AD; Figure 10a) and between the recent period (since 1850 AD) and preindustrial times (1000–1850 years AD) periods (Figure 10b). A significance value of 0.05 was used without adjustment for multiple comparisons, and only those proxies guaranteeing a minimum of two temporal samples for each of the time periods were considered. In Figure 10 we always refer the SST change from the periods generally considered warmer (MCA, industrial) to the colder period (LIA, preindustrial).

Both proxies and models broadly agree on showing a widespread warming in the North Atlantic and the Nordic Seas when comparing the MCA with the LIA (Figure 10). There is a cluster of proxy records in Disko Bugt (West Greenland) distinctly showing a cooling. However, as discussed in section 4.2.3, the coastal setting of these records makes their SST interpretation difficult. Among the models, the largest differences are in the eastern SPG, a region that is not sampled by the proxies. A similar cooling in this region has been previously associated in climate models with an AMOC decline (Drijfhout et al., 2012), although out of our three models, only the IPSL-CM5A-LR simulation shows a weaker AMOC for the MCA than for the LIA, with the ensemble means of the two other models showing no significant changes. Results from other proxy reconstructions are inconclusive, with some suggesting a slowdown during the LIA of a key component of the AMOC such as the Florida Current during the LIA (Lund et al., 2006), and others supporting a strengthening (Rahmstorf et al., 2015; Thornalley et al., 2018). The warming in the Labrador and Nordic Seas and cooling in the eastern SPG region in the models could be otherwise related to a stronger SPG during the MCA than during the LIA, as described in Moreno-Chamarro, Zanchettin, Lohmann, Luterbacher, and Jungclaus (2017) for the MPI-ESM ensemble. In that study, the three members consistently show a SPG weakening during the LIA, also supported by proxies (Copard et al., 2012; Moffa-Sánchez & Hall, 2017), and they exhibit anomalous climate conditions in the North Atlantic and Arctic (Moreno-Chamarro, Zanchettin, Lohmann, & Jungclaus, 2017; Moreno-Chamarro, Zanchettin, Lohmann, Luterbacher, & Jungclaus, 2017) that resemble the SST pattern in Figure 10.

The transition from the preindustrial to the industrial period unveils larger discrepancies, both between and within the proxies and the models. On average, models support an overall warming, with a minor cooling over the warming hole region and the warmest anomalies in the Nordic Seas, possibly due to the effect of polar amplification. However, intermodel agreement is constrained to the polar latitudes. This is because the CESM simulations experience a major cooling in the North Atlantic during the industrial era, probably related to a strong effect of anthropogenic aerosols that overwhelms the greenhouse gas-related warming over the midlatitudes of the Northern Hemisphere (see Figure 8 in Otto-Bliesner et al., 2016). In the other two models, the North Atlantic experiences a major warming. Concerning the proxy records, a coherent pattern of change is hard to distinguish. Many closely located records show opposing anomalies as, for instance, in the Western North Atlantic, Svalbard. This lack of coherence between the proxy results could reflect some limitations in our approach. For example, some proxy time series might not have enough sampling points or suffer from a chronological error that is too large to constrain robustly the industrial period, which is only 170 years long (Abram et al., 2016). Indeed, the availability of fewer points makes the proxy mean more sensitive to extreme values. The length of the proxies is also rather variable and those with a shorter preindustrial period overemphasize the recent warming, in particular if part or all of the MCA is missing. In addition to this, some of the proxies, particularly those at coastal sites, may further reflect a local signal that is unlikely to be resolved in models of such a relatively coarse spatial resolution. The model-data discrepancy seen in Figure 10 over the industrial period might thus result from the multiple uncertainties and difficulties present in both sources of information.

Due to all these complications, it becomes essential to explore new ways to compare and exploit models and proxies together. Models can be used to explain phenomena registered by proxies, both at large spatial scales (as the MCA-LIA transition) and at the regional scale. Likewise, models can provide a test bed to investigate proxy biases by assessing if inferred recording biases in proxies are physically plausible, which could lead to a further understanding of proxy recording behavior.

Future efforts to make more meaningful proxy-model comparisons should be directed at bringing both communities closer and developing new methodologies. Using our refined knowledge to subsample the models to only target those regions and periods covered by the proxies, while taking their sensing bias into account, would be one of the ways forward. Improved model resolution can also help proxy-model comparison in those regions where, for example, local currents are poorly resolved (Saba et al., 2016). Other major advances could come with a more extensive use of proxy system forward models (Dee et al., 2016; Dolman & Laepple, 2018; Evans et al., 2013; Kretschmer et al., 2018), in particular in the context of the last millennium. For example, one of the avenues currently explored is the explicit modeling of other parts of the climate system, such as water isotopes (Sjolte et al., 2011; Stevenson et al., 2013; Werner, Langebroek, et al., 2011). This would allow model-data comparison in a more direct way and in multiple dimensions. Further

developments in proxy data assimilation with models, especially tailored to reconstruct the changes in the ocean circulation, will help to produce last millennium reanalyses that are more physically consistent with the proxy data (Hakim et al., 2016). For these efforts, having proxy information over the regions where models tend to present strong biases (e.g., the Gulf Stream) is essential.

7. Summary and Conclusions

In this review we have presented and discussed a state-of-the-art compilation of high-resolution paleoceanographic records north of 35°N spanning the North Atlantic and Nordic Seas (Figure 1). The number of data sets identified and discussed clearly highlights the increase in the number of proxy records in this region over the last 20 years and, hence, the need to bring them together to advance and review our up-to-date understanding of the decadal to multicentennial ocean variability across the last 2,000 years in this key region. The main findings from the compilation and discussion in this review are summarized below:

1. Surface ocean reconstructions of the relatively warm Atlantic waters show variable patterns in the three regions studied. The most southern region (30–45°N) shows large variability in the surface temperature conditions, with the most common signal being the anomalous conditions (either cooling or warming) starting in ~1850 CE (Figure 2). This diverging pattern perhaps arises from the complex regional interactions between the Gulf Stream and the Labrador Current (including changes in the Gulf Stream detachment) and/or larger basin scale circulation changes. Farther north in the subpolar North Atlantic, reconstructions from the NAC waters reveal diverging millennial trends likely resulting from seasonal or preferred habitat depth proxy biases (Figure 3). The records from the slope waters across the Scottish shelf are shorter and mostly reveal a common warming trend from 1800 CE to present not clearly recorded in the sediment cores of the subpolar North Atlantic (Figure 3). This geographical difference could be explained by differential warming of coastal/shelf environments versus central subpolar gyre. Surface reconstructions of the Atlantic inflow in the Nordic Seas largely reveal a millennial-scale cooling and increase drift ice with higher-resolution records showing a shift around 1300–1450 CE to colder conditions with more drift ice (Figure 4).
2. Surface conditions around East and South Greenland, largely influenced by polar EGC waters, consistently show a millennial-scale cooling accompanied by a gradual increase in sea/drift ice and a southward shift of the polar front (Figure 5). Records from the WGC are also consistent with these findings and show an increase in the influence of polar waters (EGC) versus Atlantic warm waters reaching West Greenland over the last 2,000 years (Figure 6b). Even if most records present the coldest and most ice-laden conditions during the LIA, some records around Greenland show a more step-like cooling close to the MCA-LIA transition (~1100–1500 CE; Figure 5). Contrastingly, the coastal setting of the reconstructions and the limited records in the northern northwest Atlantic with opposing interpretations ultimately limit the interpretation of past ocean conditions in this region and of the Labrador Current.
3. Deep subpolar North Atlantic high-resolution records spanning the last 2,000 years are sparse and mostly comprise near-bottom flow speed indicators particularly lying in the pathway of the Nordic Seas overflows and the Deep Western Boundary Current. The different depths, sedimentary setting, and the downstream position of the records in the pathway of the ISOW can perhaps explain the differences between some of them (Figures 7a–7d). The other deep sea records are found in the pathway of the DSOW and the DWBC/lower Labrador Sea Water. Although they present some similarities, further work is required in order to gain a more comprehensive picture of the deep circulation in the North Atlantic across the last 2,000 years.

This review paper has likewise discussed our current knowledge of last millennium North Atlantic variability from climate models. Results from three different sets of experiments performed with the IPSL-CM5A-LR, CESM, and MPI-ESM models have been used to illustrate the current uncertainties and aspects of intermodel agreement. The key conclusions and findings are described as follows:

1. While model simulations do not present a consensus picture of the climate variations in the last millennium, some studies share perspectives on the sensitivity of the AMOC to volcanic forcing and the role of volcanism in forcing overall colder conditions during the LIA. Disagreements among models arise in part from internal variability, and ensemble approaches have proved useful for analyzing the statistics of this

variability and isolating externally forced components. However, not having model ensembles of the same size hampers rigorous interpretation of model discrepancies.

2. Indices of AMOC, SPG, and DSO strengths computed in three of the models participating in PMIP3 reveal different responses to external forcing, even after accounting for different numbers of ensemble members. These differences could be due in part to the use of different forcing data sets, pointing to the need for increased standardization of model forcings and experimental protocols.
3. Model *fingerprints* (i.e., regressions) of ocean circulation indices onto SSTs show varying degrees of agreement among models in different time periods. For example, while DSO fingerprints show limited small-scale regional agreements across models, SPG fingerprints show a tripolar structure that is consistent in both the preindustrial and industrial periods. Moreover, while the models agree on some regional-scale features of preindustrial AMOC fingerprints, there is no consensus on industrial-era AMOC fingerprints outside of the eastern SPG. Based on our limited set of simulations, we conclude that linear relationships at zero time lag between SSTs and ocean circulation may be model dependent and nonstationary in time. These effects may bias results from studies that use fingerprints to relate proxy observations of upper ocean temperature to ocean circulation.

A comparison of model and data representations of MCA-LIA SST differences reveals agreement in most regions, with both models and proxies suggesting that the MCA was comparatively warmer over most of the North Atlantic and the Nordic Seas (Figure 10a). There is, however, no intermodel agreement on the sign of the temperature changes in the eastern SPG, with some simulations showing a weak surface warming and others a cooling in the MCA relative to the LIA (Figure 10a); this feature has been associated either with a weaker AMOC or a stronger SPG circulation during the MCA in previous studies. The changes experienced from the preindustrial to the industrial periods were also investigated and yielded even greater discrepancies: Whereas models agree on a polar-amplified SST warming especially in the Nordic Seas, the proxies show opposing cooling and warming signals over the whole region, even at closely located sites (Figure 10b).

Disagreements discussed in this review (1) among models, (2) among data types, and (3) between models and data stem from a combination of proxy analytical and representational errors and model physics and initial and boundary conditions. How can we make progress in reconciling these disparate constraints? One promising way forward is using ocean state estimation and/or data assimilation, which use model dynamics to interpolate in space and time between noisy, sparse observations. Such approaches have been used extensively in modern oceanography (e.g., Forget et al., 2015), and recent efforts relying principally on terrestrial, annually resolved data have shown promise for reconstructing regional variations in multiple climate variables over the Common Era (Hakim et al., 2016; Tardif et al., 2018). However, while these approaches provide a common framework for combining models and data, they are not a panacea, and their success ultimately depends on having a network of highly resolved observations with accurate uncertainty quantification and a robust representation of the dominant dynamics in models. Continuing to prioritize these efforts will expedite future progress in understanding North Atlantic variability over the past 2,000 years.

Author contribution

This article was co-led by P. Moffa-Sanchez and D. Reynolds on the proxy component and by E. Moreno-Chamarro and P. Ortega on the modeling component. P. M.-S., D. R., J. H., L. J., K. P., A. W., and L. C. all contributed toward the search selection of available proxy records and the regional discussions. E. M. C., P. O., D. S., D. A., J. J., and S. Y. all contributed to the discussion of the modeling section.

Acknowledgments
We would like to thank the reviewers and the Editor for their useful comments that helped improve this manuscript. We would also like to thank the numerous authors who made their published proxy reconstructions publicly available in order for us to review them and present them in this study. This paper is a contribution from the AMOC2K project of Oceans2K program as part of the PAGES 2K network. Work by P. M-S. was possible thanks to COFUND-MSCA Fellowship (663830-CU-125). Work by E. M. C. has been possible thanks to APPLICATE (European Union's Horizon 2020 research program, Grant GA727862). Work by D.J.R. was possible thanks to NERC funded Climate of the Last Millennium Project (NE/N001176/1). D. S. thanks Myriam Khodri for allowing using the IPSL-CM5A-LR last millennium simulation. The work was supported by the French national program LEFE/INSU with VADEMECUM project and the Blue-Action project (European Union's Horizon 2020 research and innovation program, Grant 727852). D.E.A. acknowledges support from an NSF postdoctoral fellowship. L.J. acknowledges support from the German climate modeling initiative PALMOD, funded by the Federal Ministry of Science and Education. S. Y. thanks the NCAR team responsible for creating and disseminating the CESM Last Millennium Ensemble (Bette Otto-Bliesner, Esther Brady, John Fasullo, Alexandra Jahn, Laura Landrum, Samantha Stevenson, Nan Rosenbloom, Andrew Mai, and Gary Strand), using computing resources provided by the National Science Foundation (NSF) and the Computational and Information Systems Lab at NCAR. S. Y. further acknowledges support provided by NSF EaSM2 Grant OCE-1243015. Primary data and code that is used in the analyses of the model runs and that may be useful in reproducing the authors work can be obtained at https://vesg.ipsl.upmc.fr/thredds/catalog/store/swingedi/ReviewPaper2018/catalog.html.

References

Abram, N. J., McGregor, H. V., Tierney, J. E., Evans, M. N., McKay, N. P., Kaufman, D. S., et al. (2016). Early onset of industrial-era warming across the oceans and continents. *Nature*, *536*(7617), 411–418. https://doi.org/10.1038/nature19082

Adey, W. H., Halfar, J., & Williams, B. (2013). Biological, physiological and ecological factors controlling high magnesium carbonate formation and producing a precision Arctic/Subarctic marine climate archive: the coralline genus Clathromorphum Foslie emend Adey., in *Smithsonian Institute Contributions to Marine Science*, pp. 1-48.

Ahmed, M., Anchukaitis, K. J., Asrat, A., Borgaonkar, H. P., Braida, M., Buckley, B. M., et al. (2013). Continental-scale temperature variability during the past two millennia. *Nature Geoscience*, *6*(5).

Allan, E., de Vernal, A., Knudsen, M. F., Hillaire-Marcel, C., Moros, M., Ribeiro, S., et al. (2018). Late Holocene Sea Surface Instabilities in the Disko Bugt Area, West Greenland, in Phase With δ18O Oscillations at Camp Century. *Paleoceanography and Paleoclimatology*, *33*, 227–243. https://doi.org/10.1002/2017PA003289

Alonso-García, M., Andrews, J. T., Belt, S. T., Cabedo-Sanz, P., Darby, D., & Jaeger, J. (2013). A comparison between multiproxy and historical data (ad 1990–1840) of drift ice conditions on the East Greenland Shelf (~66°N). *The Holocene*, *23*(12), 1672–1683. https://doi.org/10.1177/0959683613505343

Alonso-Garcia, M., Kleiven, H., McManus, J. F., Moffa-Sanchez, P., Broecker, W. S., & Flower, B. P. (2017). Freshening of the Labrador Sea as a trigger for Little Ice Age development. *Climate of the Past*, *13*(4), 317–331. https://doi.org/10.5194/cp-13-317-2017

Ammann, C., Joos, F., Schimel, D., Otto-Bliesner, B., & Tomas, R. (2007). Solar influence on climate during the past millennium: Results from transient simulations with the NCAR Climate System Model. *Proceedings of the National Academy of Sciences*, *104*(29241024116493676 33related:UT45naZ_lCgJ(10), 3713–3718. https://doi.org/10.1073/pnas.0605064103

Andersson, C., Risebrobakken, B., Jansen, E., & Dahl, S. O. (2003). Late Holocene surface ocean conditions of the Norwegian Sea (Vøring Plateau). *Paleoceanography*, *18*(2), 1044. https://doi.org/10.1029/2001PA000654

Andresen, C. S., McCarthy, D. J., Valdemar Dylmer, C., Seidenkrantz, M.-S., Kuijpers, A., & Lloyd, J. M. (2011). Interaction between subsurface ocean waters and calving of the Jakobshavn Isbræ during the late Holocene. *The Holocene*, *21*(2), 211–224. https://doi.org/10.1177/0959683610378877

Andrews, J. T., Bigg, G. R., & Wilton, D. J. (2014). Holocene ice-rafting and sediment transport from the glaciated margin of East Greenland (67–70°N) to the N Iceland shelves: detecting and modelling changing sediment sources. *Quaternary Science Reviews*, *91*, 204–217. https://doi.org/10.1016/j.quascirev.2013.08.019

Andrews, J. T., & Jennings, A. E. (2014). Multidecadal to millennial marine climate oscillations across the Denmark Strait (~ 66° N) over the last 2000 cal yr BP. *Climate of the Past*, *10*(1), 325–343. https://doi.org/10.5194/cp-10-325-2014

Andrews, J. T., Stein, R., Moros, M., & Perner, K. (2016). Late Quaternary changes in sediment composition on the NE Greenland margin (~73° N) with a focus on the fjords and shelf. *Boreas*, *45*(3), 381–397. https://doi.org/10.1111/bor.12169

Appleby, P. G., & Oldfield, F. (1978). The calculation of lead-210 dates assuming a constant rate of supply of unsupported 210Pb to the sediment. *CATENA*, *5*(1), 1–8. https://doi.org/10.1016/S0341-8162(78)80002-2

Atwood, A. R., Wu, E., Frierson, D. M. W., Battisti, D. S., & Sachs, J. P. (2015). Quantifying Climate Forcings and Feedbacks over the Last Millennium in the CMIP5–PMIP3 Models. *Journal of Climate*, *29*(3), 1161–1178.

Bakker, P., Govin, A., Thornalley, D. J. R., Roche, D. M., & Renssen, H. (2015). The evolution of deep-ocean flow speeds and δ13C under large changes in the Atlantic overturning circulation: Toward a more direct model-data comparison. *Paleoceanography*, *30*, 95–117. https://doi.org/10.1002/2015PA002776

Barrientos, N., Lear, C. H., Jakobsson, M., Stranne, C., O'Regan, M., Cronin, T. M., et al. (2018). Arctic Ocean benthic foraminifera Mg/Ca ratios and global Mg/Ca-temperature calibrations: New constraints at low temperatures. *Geochimica et Cosmochimica Acta*, *236*, 240–259. https://doi.org/10.1016/j.gca.2018.02.036

Belt, S. T., Massé, G., Rowland, S. J., Poulin, M., Michel, C., & LeBlanc, B. (2007). A novel chemical fossil of palaeo sea ice: IP25. *Organic Geochemistry*, *38*(1), 16–27. https://doi.org/10.1016/j.orggeochem.2006.09.013

Berner, K. S., Koç, N., Divine, D., Godtliebsen, F., & Moros, M. (2008). A decadal-scale Holocene sea surface temperature record from the subpolar North Atlantic constructed using diatoms and statistics and its relation to other climate parameters. *Paleoceanography*, *23*, PA2210. https://doi.org/10.1029/2006PA001339

Berner, K. S., Koç, N., Godtliebsen, F., & Divine, D. (2011). Holocene climate variability of the Norwegian Atlantic Current during high and low solar insolation forcing. *Paleoceanography*, *26*, PA2220. https://doi.org/10.1029/2010PA002002

Bianchi, G. G., & McCave, I. N. (1999). Holocene periodicity in North Atlantic climate and deep-ocean flow south of Iceland. *Nature*, *397*(6719), 515–517. https://doi.org/10.1038/17362

Biastoch, A., Kase, R. H., & Stammer, D. B. (2003). The sensitivity of the Greenland-Scotland Ridge overflow to forcing changes. *Journal of Physical Oceanography*, *33*(11), 2307–2319. https://doi.org/10.1175/1520-0485(2003)033<2307:TSOTGR>2.0.CO;2

Boessenkool, K. P., Hall, I. R., Elderfield, H., & Yashayaev, I. (2007). North Atlantic climate and deep-ocean flow speed changes during the last 230 years. *Geophysical Research Letters*, *34*, L13614. https://doi.org/10.1029/2007GL030285

Bond, G., Kromer, B., Beer, J., Muscheler, R., Evans, M. N., Showers, W., et al. (2001). Persistent Solar Influence on North Atlantic Climate During the Holocene. *Science*, *294*(5549), 2130–2136. https://doi.org/10.1126/science.1065680

Bond, G., Showers, W., Cheseby, M., Lotti, R., Almasi, P., DeMenocal, P., et al. (1997). A Pervasive Millennial-Scale Cycle in North Atlantic Holocene and Glacial Climates. *Science*, *278*(5341), 1257–1266. https://doi.org/10.1126/science.278.5341.1257

Bond, G. C., Showers, W., Elliot, M., Evans, M., Lotti, R., Hajdas, I., et al. (1999). The North Atlantic's 1-2 Kyr Climate Rhythm: Relation to Heinrich Events, Dansgaard/Oeschger Cycles and the Little Ice Age,. In P. U. Clark, R. S. Webb, & L. D. Keigwin (Eds.), *Mechanisms of Global Climate Change at Millennial Time Scales*. 35–58, Washington, DC: American Geophysical Union. https://doi.org/10.1029/GM112p0035

Bonnet, S., de Vernal, A., Hillaire-Marcel, C., Radi, T., & Husum, K. (2010). Variability of sea-surface temperature and sea-ice cover in the Fram Strait over the last two millennia. *Marine Micropaleontology*, *74*(3-4), 59–74. https://doi.org/10.1016/j.marmicro.2009.12.001

Bosse, A., Fer, I., Søiland, H., & Rossby, T. (2018). Atlantic Water transformation along its poleward pathway across the Nordic Seas. *Journal of Geophysical Research: Oceans*, *123*, 6428–6448. https://doi.org/10.1029/2018JC014147

Bower, A. S., Lozier, M. S., Gary, S. F., & Böning, C. W. (2009). Interior pathways of the North Atlantic meridional overturning circulation. *Nature*, *459*(7244), 243–247. https://doi.org/10.1038/nature07979

Butler, P. G., Wanamaker Jr., A. D., Scourse, J. D., Richardson, C. A., & Reynolds, D. J. (2013). Variability of marine climate on the North Icelandic Shelf in a 1357-year proxy archive based on growth increments in the bivalve Arctica islandica. *Palaeogeography, Palaeoclimatology, Palaeoecology 373*, 141–151. https://doi.org/10.1016/j.palaeo.2012.01.016

Braconnot, P., Harrison, S. P., Kageyama, M., Bartlein, P. J., Masson-Delmotte, V., Abe-Ouchi, A., et al. (2012). Evaluation of climate models using palaeoclimatic data. *Nature Climate Change*, *2*(6), 417–424. https://doi.org/10.1038/nclimate1456

Broecker, W. S. (2000). Was a change in thermohaline circulation responsible for the Little Ice Age? *Proceedings of the National Academy of Sciences*, *97*(4), 1339–1342. https://doi.org/10.1073/pnas.97.4.1339

Broecker, W. S. (2005). *The Role of the Ocean in Climate Yesterday, Today, and Tomorrow*. NY, USA: Eldigio Press, Lamont-Doherty Earth Observatory of Columbia University.

Buch, E. (1981). A review of the oceanographic conditions in subarea O and 1 in the decade 1970–79 NAFO Symposium on Environmental Conditions in the Northwest Atlantic during 1970–79. NAFO Scientific Council Studies 5.

Buckley, M. W., & Marshall, J. (2015). Observations, inferences, and mechanisms of the Atlantic Meridional Overturning Circulation: A review. *Reviews of Geophysics*, *54*, 5–63. https://doi.org/10.1002/2015RG000493

Butler, P. G., Richardson, C. A., Scourse, J. D., Wanamaker, A. D., Shammon, T. M., & Bennell, J. D. (2010). Marine climate in the Irish Sea: analysis of a 489-year marine master chronology derived from growth increments in the shell of the clam Arctica islandica. *Quaternary Science Reviews*, *29*(13-14), 1614–1632. https://doi.org/10.1016/j.quascirev.2009.07.010

Cabedo-Sanz, P., Belt, S. T., Jennings, A. E., Andrews, J. T., & Geirsdóttir, Á. (2016). Variability in drift ice export from the Arctic Ocean to the North Icelandic Shelf over the last 8000 years: A multi-proxy evaluation. *Quaternary Science Reviews*, *146*, 99–115. https://doi.org/10.1016/j.quascirev.2016.06.012

Caesar, L., Rahmstorf, S., Robinson, A., Feulner, G., & Saba, V. (2018). Observed fingerprint of a weakening Atlantic Ocean overturning circulation. *Nature*, *556*(7700), 191–196. https://doi.org/10.1038/s41586-018-0006-5

Cage, A. G., & Austin, W. E. N. (2010). Marine climate variability during the last millennium: The Loch Sunart record, Scotland, UK. *Quaternary Science Reviews*, *29*(13-14), 1633–1647. https://doi.org/10.1016/j.quascirev.2010.01.014

Calvo, E., Grimalt, J. O., & Jansen, E. (2002). High resolution U K37 sea surface temperature reconstruction in the Norwegian Sea during the Holocene. *Quaternary Science Reviews*, *21*(12-13), 1385–1394. https://doi.org/10.1016/S0277-3791(01)00096-8

Chan, P., Halfar, J., Adey, W., Hetzinger, S., Zack, T., Moore, G. W. K., et al. (2017). Multicentennial record of Labrador Sea primary productivity and sea-ice variability archived in coralline algal barium. *Nature Communications*, *8*(1), 15543. https://doi.org/10.1038/ncomms15543

Chapman, M. R., & Shackleton, N. J. (2000). Evidence of 550-year and 1000-year cyclicities in North Atlantic circulation patterns during the Holocene. *The Holocene*, *10*(3), 287–291. https://doi.org/10.1191/095968300671253196

Cheng, W., Chiang, J. C. H., & Zhang, D. (2013). Atlantic Meridional Overturning Circulation (AMOC) in CMIP5 Models: RCP and Historical Simulations. *Journal of Climate*, *26*(18), 7187–7197. https://doi.org/10.1175/JCLI-D-12-00496.1

Cléroux, C., Debret, M., Cortijo, E., Duplessy, J.-C., Dewilde, F., Reijmer, J., & Massei, N. (2012). High-resolution sea surface reconstructions off Cape Hatteras over the last 10 ka. *Paleoceanography*, *27*, PA1205. https://doi.org/10.1029/2011PA002184

Coats, S., Smerdon, J. E., Cook, B. I., & Seager, R. (2014). Are Simulated Megadroughts in the North American Southwest Forced? *Journal of Climate*, *28*(1), 124–142.

Coats, S., Smerdon, J. E., Cook, B. I., Seager, R., Cook, E. R., & Anchukaitis, K. J. (2016). Internal ocean-atmosphere variability drives megadroughts in Western North America. *Geophysical Research Letters*, *43*, 9886–9894. https://doi.org/10.1002/2016GL070105

Cook, E. R., Briffa, K. R., Meko, D. M., Graybill, D. A., & Funkhouser, G. (1995). The 'segment length curse' in long tree-ring chronology development for palaeoclimatic studies. *The Holocene*, *5*(2), 229–237. https://doi.org/10.1177/095968369500500211

Cook, E. R., D'Arrigo, R. D., & Mann, M. E. (2002). A well-verified, multiproxy reconstruction of the winter North Atlantic Oscillation index since AD 1400. *Journal of Climate*, *15*(13), 1754–1764. https://doi.org/10.1175/1520-0442(2002)015<1754:AWVMRO>2.0.CO;2

Copard, K., Colin, C., Henderson, G., Scholten, J., Douville, E., Sicre, M.-A., & Frank, N. (2012). Late Holocene intermediate water variability in the northeastern Atlantic as recorded by deep-sea corals. *Earth and Planetary Science Letters*, *313*, 34–44.

Cronin, T. M., Hayo, K., Thunell, R. C., Dwyer, G. S., Saenger, C., & Willard, D. A. (2010). The Medieval Climate Anomaly and Little Ice Age in Chesapeake Bay and the North Atlantic Ocean. *Palaeogeography, Palaeoclimatology, Palaeoecology*, *297*(2), 299–310. https://doi.org/10.1016/j.palaeo.2010.08.009

Cunningham, L. K., Austin, W. E. N., Knudsen, K. L., Eiríksson, J., Scourse, J. D., Wanamaker, A. D. Jr., et al. (2013). Reconstructions of surface ocean conditions from the northeast Atlantic and Nordic seas during the last millennium. *The Holocene*, *23*(7), 921–935. https://doi.org/10.1177/0959683613479677

Dahl-Jensen, D., Mosegaard, K., Gundestrup, N., Clow, G. D., Johnsen, S. J., Hansen, A. W., & Balling, N. (1998). Past Temperatures Directly from the Greenland Ice Sheet. *Science*, *282*(5387), 268–271. https://doi.org/10.1126/science.282.5387.268

Danabasoglu, G., Yeager, S. G., Kwon, Y.-O., Tribbia, J. J., Phillips, A. S., & Hurrell, J. W. (2012). Variability of the Atlantic Meridional Overturning Circulation in CCSM4. *Journal of Climate*, *25*(15), 5153–5172. https://doi.org/10.1175/JCLI-D-11-00463.1

Daniault, N., Mercier, H., Lherminier, P., Sarafanov, A., Falina, A., Zunino, P., et al. (2016). The northern North Atlantic Ocean mean circulation in the early 21st century. *Progress in Oceanography*, *146*, 142–158. https://doi.org/10.1016/j.pocean.2016.06.007

Dee, S. G., Steiger, N. J., Emile-Geay, J., & Hakim, G. J. (2016). On the utility of proxy system models for estimating climate states over the common era. *Journal of Advances in Modeling Earth Systems*, *8*, 1164–1179. https://doi.org/10.1002/2016MS000677

Denton, G. H., & Karlen, W. (1973). Holocene Climatic Variations--Their Pattern and Possible Cause. *Quaternary Research*, *3*(2), 155–205. https://doi.org/10.1016/0033-5894(73)90040-9

Deser, C., Phillips, A., Bourdette, V., & Teng, H. (2012). Uncertainty in climate change projections: the role of internal variability. *Climate Dynamics*, *38*(3-4), 527–546. https://doi.org/10.1007/s00382-010-0977-x

Dickson, B., Meincke, J., & Rhines, P. (Eds) (2008). *Arctic–Subarctic Ocean Fluxes Defining the Role of the Northern Seas in Climate*, (pp. 15–43). Netherlands: Springer.

Dickson, R. R., & Brown, J. (1994). The production of North Atlantic Deep Water: Sources, rates, and pathways. *Journal of Geophysical Research*, *99*(C6), 12,319–12,341. https://doi.org/10.1029/94JC00530

Dolman, A. M., & Laepple, T. (2018). Sedproxy: a forward model for sediment archived climate proxies. *Climate of the Past Discussions*, *14*(12), 1851–1868. https://doi.org/10.5194/cp-14-1851-2018

Drews, A., & Greatbatch, R. J. (2016). Atlantic Multidecadal Variability in a model with an improved North Atlantic Current. *Geophysical Research Letters*, *43*, 8199–8206. https://doi.org/10.1002/2016GL069815

Drijfhout, S., Gleeson, E., Dijkstra, H. A., & Livina, V. (2013). Spontaneous abrupt climate change due to an atmospheric blocking–sea-ice–ocean feedback in an unforced climate model simulation. *Proceedings of the National Academy of Sciences*, *110*(49), 19,713–19,718. https://doi.org/10.1073/pnas.1304912110

Drijfhout, S., van Oldenborgh, G. J., & Cimatoribus, A. (2012). Is a Decline of AMOC Causing the Warming Hole above the North Atlantic in Observed and Modeled Warming Patterns? *Journal of Climate*, *25*(24), 8373–8379. https://doi.org/10.1175/JCLI-D-12-00490.1

Eden, C., Greatbatch, R. J., & Böning, C. W. (2004). Adiabatically Correcting an Eddy-Permitting Model Using Large-Scale Hydrographic Data: Application to the Gulf Stream and the North Atlantic Current. *Journal of Physical Oceanography*, *34*(4), 701–719. https://doi.org/10.1175/1520-0485(2004)034<0701:ACAEMU>2.0.CO;2

Eiríksson, J., Knudsen, K. L., Larsen, G., Olsen, J., Heinemeier, J., Bartels-Jónsdóttir, H. B., et al. (2011). Coupling of palaeoceanographic shifts and changes in marine reservoir ages off North Iceland through the last millennium. *Palaeogeography, Palaeoclimatology, Palaeoecology*, *302*(1-2), 95–108. https://doi.org/10.1016/j.palaeo.2010.06.002

Eiríksson, J., Larsen, G., Knudsen, K. L., Heinemeier, J., & Símonarson, L. A. (2004). Marine reservoir age variability and water mass distribution in the Iceland Sea. *Quaternary Science Reviews*, *23*(20-22), 2247–2268. https://doi.org/10.1016/j.quascirev.2004.08.002

Elderfield, H., & Ganssen, G. J. N. (2000). Past temperature and δ 18 O of surface ocean waters inferred from foraminiferal Mg/Ca ratios. *Nature*, *405*(6785), 442–445. https://doi.org/10.1038/35013033

Erbs-Hansen, D. R., Knudsen, K. L., Olsen, J., Lykke-Andersen, H., Underbjerg, J. A., & Sha, L. (2013). Paleoceanographical development off Sisimiut, West Greenland, during the mid- and late Holocene: A multiproxy study. *Marine Micropaleontology*, *102*, 79–97. https://doi.org/10.1016/j.marmicro.2013.06.003

Esper, J., Cook, E. R., & Schweingruber, F. H. (2002). Low-Frequency Signals in Long Tree-Ring Chronologies for Reconstructing Past Temperature Variability. *Science*, *295*(5563), 2250–2253. https://doi.org/10.1126/science.1066208

Evans, D., Müller, W., Oron, S., & Renema, W. (2013). Eocene seasonality and seawater alkaline earth reconstruction using shallow-dwelling large benthic foraminifera. *Earth and Planetary Science Letters*, *381*, 104–115. https://doi.org/10.1016/j.epsl.2013.08.035

Featherstone, A. M., Butler, P. G., Peharda, M., Chauvaud, L., & Thébault, J. (2017). Influence of riverine input on the growth of Glycymeris glycymeris in the Bay of Brest, North-West France. *PLOS ONE*, *12*(12), e0189782. https://doi.org/10.1371/journal.pone.0189782

Forget, G., Campin, J. M., Heimbach, P., Hill, C. N., Ponte, R. M., & Wunsch, C. (2015). ECCO version 4: an integrated framework for non-linear inverse modeling and global ocean state estimation. *Geoscientific Model Development*, *8*(10), 3071–3104. https://doi.org/10.5194/gmd-8-3071-2015

Foukal, P., Fröhlich, C., Spruit, H., & Wigley, T. M. L. (2006). Variations in solar luminosity and their effect on the Earth's climate. *Nature*, *443*(7108), 161–166. https://doi.org/10.1038/nature05072

Freitas, F. S., Pancost, R. D., & Arndt, S. (2017). The impact of alkenone degradation on paleothermometry: A model-derived assessment. *Paleoceanography*, *32*, 648–672. https://doi.org/10.1002/2016PA003043

Gagen, M. H., Zorita, E., McCarroll, D., Zahn, M., Young, G. H. F., & Robertson, I. (2016). North Atlantic summer storm tracks over Europe dominated by internal variability over the past millennium. *Nature Geoscience*, *9*(8), 630–635. https://doi.org/10.1038/ngeo2752

Goodkin, N. F., Hughen, K. A., Doney, S. C., & Curry, W. B. (2008). Increased multidecadal variability of the North Atlantic Oscillation since 1781. *Nature Geosci*, *1*(12), 844–848. https://doi.org/10.1038/ngeo352

Goosse, H., Renssen, H., Timmermann, A., & Bradley, R. S. (2005). Internal and forced climate variability during the last millennium: a model-data comparison using ensemble simulations. *Quaternary Science Reviews*, *24*(12-13), 1345–1360. https://doi.org/10.1016/j.quascirev.2004.12.009

Gray, S. T., Graumlich, L. J., Betancourt, J. L., & Pederson, G. T. (2004). A tree-ring based reconstruction of the Atlantic Multidecadal Oscillation since 1567 AD. *Geophysical Research Letters*, *31*, L12205. https://doi.org/10.1029/2004GL019932

Gray, W. R., Weldeab, S., Lea, D. W., Rosenthal, Y., Gruber, N., Donner, B., & Fischer, G. (2018). The effects of temperature, salinity, and the carbonate system on Mg/Ca in Globigerinoides ruber (white): A global sediment trap calibration. *Earth and Planetary Science Letters*, *482*, 607–620. https://doi.org/10.1016/j.epsl.2017.11.026

Hakim, G. J., Emile-Geay, J., Steig, E. J., Noone, D., Anderson, D. M., Tardif, R., et al. (2016). The last millennium climate reanalysis project: Framework and first results. *Journal of Geophysical Research: Atmospheres*, *121*, 6745–6764. https://doi.org/10.1002/2016JD024751

Halfar, J., Adey, W. H., Kronz, A., Hetzinger, S., Edinger, E., & Fitzhugh, W. W. (2013). Arctic sea-ice decline archived by multicentury annual-resolution record from crustose coralline algal proxy. *Proceedings of the National Academy of Sciences*, *110*(49), 19,737–19,741. https://doi.org/10.1073/pnas.1313775110

Hall, I. R., Boessenkool, K. P., Barker, S., McCave, I. N., & Elderfield, H. (2010). Surface and deep ocean coupling in the subpolar North Atlantic during the last 230 years. *Paleoceanography*, *25*, PA2101. https://doi.org/10.1029/2009PA001886

Hansen, B., & Østerhus, S. (2000). North Atlantic–Nordic Seas exchanges. *Progress In Oceanography*, *45*(2), 109–208. https://doi.org/10.1016/S0079-6611(99)00052-X

Hawkins, E., & Sutton, R. (2009). The Potential to Narrow Uncertainty in Regional Climate Predictions. *Bulletin of the American Meteorological Society*, *90*(8), 1095–1108. https://doi.org/10.1175/2009BAMS2607.1

Hillaire-Marcel, C., & De Vernal, A. (2007). *Proxies in Late Cenozoic Paleoceanography*. Amsterdam, The Netherlands: Elsevier.

Hofer, D., Raible, C. C., & Stocker, T. F. (2011). Variations of the Atlantic meridional overturning circulation in control and transient simulations of the last millennium. *Climate of the Past*, *7*(1), 133–150. https://doi.org/10.5194/cp-7-133-2011

Holland, D. M., Thomas, R. H., de Young, B., Ribergaard, M. H., & Lyberth, B. (2008). Acceleration of Jakobshavn Isbræ triggered by warm subsurface ocean waters. *Nature Geoscience*, *1*(10), 659–664. https://doi.org/10.1038/ngeo316

Hughen, K. A. (2007). Chapter Five Radiocarbon Dating of Deep-Sea Sediments. In H. M. Claude, & V. A. De (Eds.), *Developments in Marine Geology* (pp. 185–210). Amsterdam, The Netherlands: Elsevier.

Inall, M., Gillibrand, P., Griffiths, C., MacDougal, N., & Blackwell, K. (2009). On the oceanographic variability of the North-West European Shelf to the West of Scotland. *Journal of Marine Systems*, *77*(3), 210–226. https://doi.org/10.1016/j.jmarsys.2007.12.012

Jansen, E., Overpeck, J., Briffa, K. R., Duplessy, J. C., Joos, F., Masson-Delmotte, V., et al. (2007). *Paleoclimate. Chapter 6*. Cambridge Université Press.

Jennings, A., Andrews, J., & Wilson, L. (2011). Holocene environmental evolution of the SE Greenland Shelf North and South of the Denmark Strait: Irminger and East Greenland current interactions. *Quaternary Science Reviews*, *30*(7-8), 980–998. https://doi.org/10.1016/j.quascirev.2011.01.016

Jennings, A. E., & Weiner, N. J. (1996). Environmental change in eastern Greenland during the last 1300 years: evidence from foraminifera and lithofacies in Nansen Fjord, 68°N. *The Holocene*, *6*(2), 179–191. https://doi.org/10.1177/095968369600600205

Jensen, K. G., Kuijpers, A., Koç, N., & Heinemeier, J. (2004). Diatom evidence of hydrographic changes and ice conditions in Igaliku Fjord, South Greenland, during the past 1500 years. *The Holocene*, *14*(2), 152–164. https://doi.org/10.1191/0959683604hl698rp

Jiang, H., Eiríksson, J., Schulz, M., Knudsen, K. L., & Seidenkrantz, M. S. (2005). Evidence for solar forcing of sea-surface temperature on the North Icelandic Shelf during the late Holocene. *Geology*, *33*(1), 73–76. https://doi.org/10.1130/G21130.1

Jiang, H., Muscheler, R., Björck, S., Seidenkrantz, M. S., Olsen, J., Sha, L., et al. (2015). Solar forcing of Holocene summer sea-surface temperatures in the northern North Atlantic. *Geology*, *43*(3), 203–206. https://doi.org/10.1130/G36377.1

Jiang, H., Seidenkrantz, M. S., Knudsen, K. L., & Eiríksson, J. (2001). Diatom surface sediment assemblages around Iceland and their relationships to oceanic environmental variables. *Marine Micropaleontology*, *41*(1-2), 73–96. https://doi.org/10.1016/S0377-8398(00)00053-0

Jonkers, L., Jiménez-Amat, P., Mortyn, P. G., & Brummer, G.-J. A. (2013). Seasonal Mg/Ca variability of N. pachyderma (s) and G. bulloides: Implications for seawater temperature reconstruction. *Earth and Planetary Science Letters*, *376*, 137–144. https://doi.org/10.1016/j.epsl.2013.06.019

Jonkers, L., & Kučera, M. (2015). Global analysis of seasonality in the shell flux of extant planktonic Foraminifera. *Biogeosciences*, *12*(7), 2207–2226. https://doi.org/10.5194/bg-12-2207-2015

Jonkers, L., & Kučera, M. (2017). Quantifying the effect of seasonal and vertical habitat tracking on planktonic foraminifera proxies. *Climate of the Past*, *13*(6), 573–586. https://doi.org/10.5194/cp-13-573-2017

Juggins, S. (2013). Quantitative reconstructions in palaeolimnology: new paradigm or sick science? *Quaternary Science Reviews*, *64*, 20–32. https://doi.org/10.1016/j.quascirev.2012.12.014

Jungclaus, J. H., Bard, E., Baroni, M., Braconnot, P., Cao, J., Chini, L. P., et al. (2017). The PMIP4 contribution to CMIP6 – Part 3: The last millennium, scientific objective, and experimental design for the PMIP4 past1000 simulations. *Geoscientific Model Development*, *10*(11), 4005–4033. https://doi.org/10.5194/gmd-10-4005-2017

Jungclaus, J. H., Lohmann, K., & Zanchettin, D. (2014). Enhanced 20th-century heat transfer to the Arctic simulated in the context of climate variations over the last millennium. *Climate of the Past*, *10*(6), 2201–2213. https://doi.org/10.5194/cp-10-2201-2014

Justwan, A., Koç, N., & Jennings, A. E. (2008). Evolution of the Irminger and East Icelandic Current systems through the Holocene, revealed by diatom-based sea surface temperature reconstructions. *Quaternary Science Reviews*, *27*(15-16), 1571–1582. https://doi.org/10.1016/j.quascirev.2008.05.006

Kageyama, M., Braconnot, P., Harrison, S. P., Haywood, A. M., Jungclaus, J. H., Otto-Bliesner, B. L., et al. (2018). The PMIP4 contribution to CMIP6 – Part 1: Overview and over-arching analysis plan. *Geoscientific Model Development*, *11*(3), 1033–1057. https://doi.org/10.5194/gmd-11-1033-2018

Kamenos, N. A. (2010). North Atlantic summers have warmed more than winters since 1353, and the response of marine zooplankton. *Proceedings of the National Academy of Sciences*, *107*(52), 22,442–22,447. https://doi.org/10.1073/pnas.1006141107

Katsman, C. A., Drijfhout, S. S., Dijkstra, H. A., & Spall, M. A. (2018). Sinking of Dense North Atlantic Waters in a Global Ocean Model: Location and Controls. *Journal of Geophysical Research: Oceans*, *123*, 3563–3576. https://doi.org/10.1029/2017JC013329

Keeley, S. P. E., Sutton, R. T., & Shaffrey, L. C. (2012). The impact of North Atlantic sea surface temperature errors on the simulation of North Atlantic European region climate. *Quarterly Journal of the Royal Meteorological Society*, *138*(668), 1774–1783. https://doi.org/10.1002/qj.1912

Keigwin, L. D. (1996). The little ice age and medieval warm period in the Sargasso Sea. *Science*, *274*(5292), 1504–1508. https://doi.org/10.1126/science.274.5292.1504

Keigwin, L. D., & Boyle, E. A. (2000). Detecting Holocene changes in thermohaline circulation. *Proceedings of the National Academy of Sciences of the United States of America*, *97*(4), 1343–1346. https://doi.org/10.1073/pnas.97.4.1343

Keigwin, L. D., & Pickart, R. S. (1999). Slope water current over the Laurentian Fan on interannual to millennial time scares. *Science*, *286*(5439), 520–523. https://doi.org/10.1126/science.286.5439.520

Keigwin, L. D., Sachs, J. P., & Rosenthal, Y. (2003). A 1600-year history of the Labrador Current off Nova Scotia. *Climate Dynamics*, *21*(1), 53–62. https://doi.org/10.1007/s00382-003-0316-6

Kissel, C., Laj, C., Mulder, T., Wandres, C., & Cremer, M. (2009). The magnetic fraction: A tracer of deep water circulation in the North Atlantic. *Earth and Planetary Science Letters*, *288*(3-4), 444–454. https://doi.org/10.1016/j.epsl.2009.10.005

Kissel, C., Van Toer, A., Laj, C., Cortijo, E., & Michel, E. (2013). Variations in the strength of the North Atlantic bottom water during Holocene. *Earth and Planetary Science Letters*, *369-370*, 248–259. https://doi.org/10.1016/j.epsl.2013.03.042

Koc, N., & Schrader, H. (1990). Surface sediment diatom distribution and Holocene paleotemperature variations in the Greenland. *Iceland and Norwegian Sea*, *5*(4), 557–580.

Kohl, A. (2010). Variable source regions of Denmark Strait and Faroe Bank Channel overflow waters. *Tellus Series a-Dynamic Meteorology and Oceanography*, *62*(4), 551–568. https://doi.org/10.1111/j.1600-0870.2010.00454.x

Kolling, H. M., Stein, R., Fahl, K., Perner, K., & Moros, M. (2017). Short-term variability in late Holocene sea ice cover on the East Greenland Shelf and its driving mechanisms. *Palaeogeography, Palaeoclimatology, Palaeoecology*, *485*, 336–350. https://doi.org/10.1016/j.palaeo.2017.06.024

Kolling, H. M., Stein, R., Fahl, K., Perner, K., & Moros, M. (2018). New insights into sea ice changes over the past 2.2 kyr in Disko Bugt, West Greenland. *arktos*, *4*(1), 11. https://doi.org/10.1007/s41063-018-0045-z

Krawczyk, D. W., Witkowski, A., Lloyd, J., Moros, M., Harff, J., & Kuijpers, A. (2013). Late-Holocene diatom derived seasonal variability in hydrological conditions off Disko Bay, West Greenland. *Quaternary Science Reviews*, *67*, 93–104. https://doi.org/10.1016/j.quascirev.2013.01.025

Krawczyk, D. W., Witkowski, A., Moros, M., Lloyd, J. M., Høyer, J. L., Miettinen, A., & Kuijpers, A. (2017). Quantitative reconstruction of Holocene sea ice and sea surface temperature off West Greenland from the first regional diatom data set. *Paleoceanography*, *32*, 18–40. https://doi.org/10.1002/2016PA003003

Kretschmer, K., Jonkers, L., Kucera, M., & Schulz, M. (2018). Modeling seasonal and vertical habitats of planktonic foraminifera on a global scale. *Biogeosciences*, *15*(14), 4405–4429. https://doi.org/10.5194/bg-15-4405-2018

Kuhlbrodt, T., Griesel, A., Montoya, M., Levermann, A., Hofmann, M., & Rahmstorf, S. (2007). On the driving processes of the Atlantic meridional overturning circulation. *Reviews of Geophysics*, *45*, RG2001. https://doi.org/10.1029/2004RG000166

Lamb, H. (1977). Climate: Present, Past and Future. In *Climatic History and the Future*, 835 pp, (Vol. 2), chapter 13. London: Methuen & Co.

Lamb, H. H. (1965). The early medieval warm epoch and its sequel. *Palaeogeography, Palaeoclimatology, Palaeoecology*, *1*, 13–37. https://doi.org/10.1016/0031-0182(65)90004-0

Lamb, H. H. (1979). Climatic variation and changes in the wind and ocean circulation: The Little Ice Age in the northeast Atlantic. *Quaternary Research*, *11*(1), 1–20. https://doi.org/10.1016/0033-5894(79)90067-X

Landrum, L., Otto-Bliesner, B. L., Wahl, E. R., Conley, A., Lawrence, P. J., Rosenbloom, N., & Teng, H. (2012). Last Millennium Climate and Its Variability in CCSM4. *Journal of Climate*, *26*(4), 1085–1111.

Langehaug, H. R., Medhaug, I., Eldevik, T., & Otterå, O. H. (2012). Arctic/Atlantic Exchanges via the Subpolar Gyre*. *Journal of Climate*, *25*(7), 2421–2439. https://doi.org/10.1175/JCLI-D-11-00085.1

Langehaug, H. R., Mjell, T. L., Otterå, O. H., Eldevik, T., Ninnemann, U. S., & Kleiven, H. F. (2016). On the reconstruction of ocean circulation and climate based on the "Gardar Drift". *Paleoceanography*, *31*, 399–415. https://doi.org/10.1002/2015PA002920

Lassen, S. J., Kuijpers, A., Kunzendorf, H., Hoffmann-Wieck, G., Mikkelsen, N., & Konradi, P. (2004). Late-Holocene Atlantic bottom-water variability in Igaliku Fjord, South Greenland, reconstructed from foraminifera faunas. *The Holocene*, *14*(2), 165–171. https://doi.org/10.1191/0959683604hl699rp

Lear, C. H., Rosenthal, Y., & Slowey, N. (2002). Benthic foraminiferal Mg/Ca-paleothermometry: a revised core-top calibration. *Geochimica et Cosmochimica Acta*, *66*(19), 3375–3387. https://doi.org/10.1016/S0016-7037(02)00941-9

Leduc, G., Schneider, R., Kim, J. H., & Lohmann, G. (2010). Holocene and Eemian sea surface temperature trends as revealed by alkenone and Mg/Ca paleothermometry. *Quaternary Science Reviews*, *29*(7–8), 989–1004. https://doi.org/10.1016/j.quascirev.2010.01.004

Lehner, F., Born, A., Raible, C. C., & Stocker, T. F. (2013). Amplified Inception of European Little Ice Age by Sea Ice–Ocean–Atmosphere Feedbacks. *Journal of Climate*, *26*(19), 7586–7602. https://doi.org/10.1175/JCLI-D-12-00690.1

Lehner, F., Joos, F., Raible, C. C., Mignot, J., Born, A., Keller, K. M., & Stocker, T. F. (2015). Climate and carbon cycle dynamics in a CESM simulation from 850 to 2100 CE. *Earth System Dynamics*, *6*(2), 411–434. https://doi.org/10.5194/esd-6-411-2015

Lehner, F., Raible, C. C., & Stocker, T. F. (2012). Testing the robustness of a precipitation proxy-based North Atlantic Oscillation reconstruction. *Quaternary Science Reviews*, *45*(C), 85–94. https://doi.org/10.1016/j.quascirev.2012.04.025

Li, J., Rypel, A. L., Zhang, S. Y., Luo, Y. M., Hou, G., Murphy, B. R., & Xie, S. G. (2017). Growth, longevity, and climate–growth relationships of Corbicula fluminea (Müller, 1774) in Hongze Lake, China. *Freshwater Science*, *36*(3), 595–608. https://doi.org/10.1086/693463

Lloyd, J., Moros, M., Perner, K., Telford, R. J., Kuijpers, A., Jansen, E., & McCarthy, D. (2011). A 100 yr record of ocean temperature control on the stability of Jakobshavn Isbrae, West Greenland. *Geology*, *39*(9), 867–870. https://doi.org/10.1130/G32076.1

Logemann, K., Ólafsson, J., Snorrason, Á., Valdimarsson, H., & Marteinsdóttir, G. (2013). The circulation of Icelandic waters – a modelling study. *Ocean Science*, *9*(5), 931–955. https://doi.org/10.5194/os-9-931-2013

Lohmann, G., Pfeiffer, M., Laepple, T., Leduc, G., & Kim, J.-H. (2013). A model-data comparison of the Holocene global sea surface temperature evolution. *Climate of the Past*, *9*(4), 1807–1839. https://doi.org/10.5194/cp-9-1807-2013

Lohmann, K., Jungclaus, J. H., Matei, D., Mignot, J., Menary, M., Langehaug, H. R., et al. (2014). The role of subpolar deep water formation and Nordic Seas overflows in simulated multidecadal variability of the Atlantic meridional overturning circulation. *Ocean Science*, *10*(2), 227–241. https://doi.org/10.5194/os-10-227-2014

Lohmann, K., Mignot, J., Langehaug, H. R., Jungclaus, J. H., Matei, D., Otterå, O. H., et al. (2015). Using simulations of the last millennium to understand climate variability seen in palaeo-observations: similar variation of Iceland–Scotland overflow strength and Atlantic Multidecadal Oscillation. *Climate of the Past*, *11*(2), 203–216. https://doi.org/10.5194/cp-11-203-2015

Lowe, D. J. (2011). Tephrochronology and its application: A review. *Quaternary Geochronology*, *6*(2), 107–153. https://doi.org/10.1016/j.quageo.2010.08.003

Lozier, M. S. (2012). Overturning in the North Atlantic. *Annual Review of Marine Science*, *4*(1), 291–315. https://doi.org/10.1146/annurev-marine-120710-100740

Lund, D. C., & Curry, W. (2006). Florida Current surface temperature and salinity variability during the last millennium. *Paleoceanography*, *21*, PA2009. https://doi.org/10.1029/2005PA001218

Lund, D. C., Lynch-Stieglitz, J., & Curry, W. B. (2006). Gulf Stream density structure and transport during the past millennium. *Nature*, *444*(7119), 601–604. https://doi.org/10.1038/nature05277

Luterbacher, J., Werner, J. P., Smerdon, J. E., Fernández-Donado, L., González-Rouco, F. J., Barriopedro, D., et al. (2016). European summer temperatures since Roman times. *Environmental Research Letters*, *11*(2), 024001. https://doi.org/10.1088/1748-9326/11/2/024001

Mann, M. E., Zhang, Z., Hughes, M. K., Bradley, R. S., Miller, S. K., Rutherford, S., & Ni, F. (2008). Proxy-based reconstructions of hemispheric and global surface temperature variations over the past two millennia. *Proceedings of the National Academy of Sciences of the United States of America*, *105*(36), 13,252–13,257. https://doi.org/10.1073/pnas.0805721105

Mann, M. E., Zhang, Z., Rutherford, S., Bradley, R. S., Hughes, M. K., Shindell, D., et al. (2009). Global Signatures and Dynamical Origins of the Little Ice Age and Medieval Climate Anomaly. *Science*, *326*(5957), 1256–1260. https://doi.org/10.1126/science.1177303

Marchitto, T. M., & de Menocal, B. P. (2003). Late Holocene variability of upper North Atlantic Deep Water temperature and salinity. *Geochemistry, Geophysics, Geosystems*, *4*(12), 1100. https://doi.org/10.1029/2003GC000598

Marsh, R., Haigh, I. D., Cunningham, S. A., Inall, M. E., Porter, M., & Moat, B. I. (2017). Large-scale forcing of the European Slope Current and associated inflows to the North Sea. *Ocean Science*, *13*(2), 315–335. https://doi.org/10.5194/os-13-315-2017

Massé, G., Rowland, S. J., Sicre, M. A., Jacob, J., Jansen, E., & Belt, S. T. (2008). Abrupt climate changes for Iceland during the last millennium: Evidence from high resolution sea ice reconstructions. *Earth and Planetary Science Letters*, *269*(3-4), 564–568.

McCave, I. N., & Hall, I. R. (2006). Size sorting in marine muds: Processes, pitfalls, and prospects for paleoflow-speed proxies. *Geochemistry, Geophysics, Geosystems*, *7*, Q10N05. https://doi.org/10.1029/2006GC001284

McGregor, H. V., Evans, M. N., Goosse, H., Leduc, G., Martrat, B., Addison, J. A., et al. (2015). Robust global ocean cooling trend for the pre-industrial Common Era. *Nature Geoscience*, *8*(9), 671–677. https://doi.org/10.1038/ngeo2510

Menary, M. B., Hodson, D. L. R., Robson, J. I., Sutton, R. T., Wood, R. A., & Hunt, J. A. (2015). Exploring the impact of CMIP5 model biases on the simulation of North Atlantic decadal variability. *Geophysical Research Letters*, *42*, 5926–5934. https://doi.org/10.1002/2015GL064360

Miettinen, A., Divine, D., Koç, N., Godtliebsen, F., & Hall, I. R. (2012). Multicentennial Variability of the Sea Surface Temperature Gradient across the Subpolar North Atlantic over the Last 2.8 kyr. *Journal of Climate*, *25*(12), 4205–4219. https://doi.org/10.1175/JCLI-D-11-00581.1

Miettinen, A., Divine, D. V., Husum, K., Koç, N., & Jennings, A. (2015). Exceptional ocean surface conditions on the SE Greenland shelf during the Medieval Climate Anomaly. *Paleoceanography*, *30*, 1657–1674. https://doi.org/10.1002/2015PA002849

Mignot, J., Khodri, M., Frankignoul, C., & Servonnat, J. (2011). Volcanic impact on the Atlantic ocean over the last millennium. *Climate of the Past Discussions*, *7*(4), 2511–2554. https://doi.org/10.5194/cpd-7-2511-2011

Miller, G. H., Geirsdóttir, Á., Zhong, Y., Larsen, D. J., Otto-Bliesner, B. L., Holland, M. M., et al. (2012). Abrupt onset of the Little Ice Age triggered by volcanism and sustained by sea-ice/ocean feedbacks. *Geophysical Research Letters*, *39*, L02708. https://doi.org/10.1029/2011GL050168

Mjell, T. L., Ninnemann, U. S., Eldevik, T., & Kleiven, H. K. F. (2015). Holocene multidecadal- to millennial-scale variations in Iceland-Scotland overflow and their relationship to climate. *Paleoceanography*, *30*, 558–569. https://doi.org/10.1002/2014PA002737

Mjell, T. L., Ninnemann, U. S., Kleiven, H. F., & Hall, I. R. (2016). Multidecadal changes in Iceland Scotland Overflow Water vigor over the last 600 years and its relationship to climate. *Geophysical Research Letters*, *43*, 2111–2117. https://doi.org/10.1002/2016GL068227

Moffa-Sanchez, P., Born, A., Hall, I. R., Thornalley, D. J. R., & Barker, S. (2014). Solar forcing of North Atlantic surface temperature and salinity over the past millennium. *Nature Geoscience*, *7*(4), 275–278. https://doi.org/10.1038/ngeo2094

Moffa-Sánchez, P., & Hall, I. R. (2017). North Atlantic variability and its links to European climate over the last 3000 years. *Nature Communications*, *8*(1), 1726. https://doi.org/10.1038/s41467-017-01884-8

Moffa-Sánchez, P., Hall, I. R., Barker, S., Thornalley, D. J., & Yashayaev, I. (2014). Surface changes in the eastern Labrador Sea around the onset of the Little Ice Age. *Paleoceanography*, *29*, 160–175. https://doi.org/10.1002/2013PA002523

Moffa-Sanchez, P., Hall, I. R., Thornalley, D. J., Barker, S., & Stewart, C. (2015). Changes in the strength of the Nordic Seas Overflows over the past 3000 years. *Quaternary Science Reviews*, *123*, 134–143. https://doi.org/10.1016/j.quascirev.2015.06.007

Moore, G. W. K., Halfar, J., Majeed, H., Adey, W., & Kronz, A. (2017). Amplification of the Atlantic Multidecadal Oscillation associated with the onset of the industrial-era warming. *Scientific Reports*, *7*(1), 40861. https://doi.org/10.1038/srep40861

Moreno-Chamarro, E., Ortega, P., González-Rouco, F., & Montoya, M. (2017). Assessing reconstruction techniques of the Atlantic Ocean circulation variability during the last millennium. *Climate Dynamics*, *48*(3-4), 799–819. https://doi.org/10.1007/s00382-016-3111-x

Moreno-Chamarro, E., Zanchettin, D., Lohmann, K., & Jungclaus, J. H. (2015). Internally generated decadal cold events in the northern North Atlantic and their possible implications for the demise of the Norse settlements in Greenland. *Geophysical Research Letters*, *42*, 908–915. https://doi.org/10.1002/2014GL062741

Moreno-Chamarro, E., Zanchettin, D., Lohmann, K., & Jungclaus, J. H. (2017). An abrupt weakening of the subpolar gyre as trigger of Little Ice Age-type episodes. *Climate Dynamics*, *48*(3-4), 727–744. https://doi.org/10.1007/s00382-016-3106-7

Moreno-Chamarro, E., Zanchettin, D., Lohmann, K., Luterbacher, J., & Jungclaus, J. H. (2017). Winter amplification of the European Little Ice Age cooling by the subpolar gyre. *Scientific Reports*, *7*(1), 9981. https://doi.org/10.1038/s41598-017-07969-0

Morey, A. E., Mix, A. C., & Pisias, N. G. (2005). Planktonic foraminiferal assemblages preserved in surface sediments correspond to multiple environment variables. *Quaternary Science Reviews*, *24*(7-9), 925–950. https://doi.org/10.1016/j.quascirev.2003.09.011

Morley, A., Schulz, M., Rosenthal, Y., Mulitza, S., Paul, A., & Rühlemann, C. (2011). Solar modulation of North Atlantic central Water formation at multidecadal timescales during the late Holocene. *Earth and Planetary Science Letters*, *308*(1-2), 161–171. https://doi.org/10.1016/j.epsl.2011.05.043

Moros, M., Andrews, J. T., Eberl, D. D., & Jansen, E. (2006). Holocene history of drift ice in the northern North Atlantic: Evidence for different spatial and temporal modes. *Paleoceanography*, *21*, PA2017. https://doi.org/10.1029/2005PA001214

Moros, M., Lloyd, J. M., Perner, K., Krawczyk, D., Blanz, T., de Vernal, A., et al. (2016). Surface and sub-surface multi-proxy reconstruction of middle to late Holocene palaeoceanographic changes in Disko Bugt. *West Greenland, Quaternary Science Reviews*, *132*, 146–160. https://doi.org/10.1016/j.quascirev.2015.11.017

Müller, J., Werner, K., Stein, R., Fahl, K., Moros, M., & Jansen, E. (2012). Holocene cooling culminates in sea ice oscillations in Fram Strait. *Quaternary Science Reviews*, *47*, 1–14. https://doi.org/10.1016/j.quascirev.2012.04.024

Nyland, B. F., Jansen, E., Elderfield, H., & Andersson, C. (2006). Neogloboquadrina pachyderma (dex. and sin.) Mg/Ca and δ18O records from the Norwegian Sea. *Geochemistry, Geophysics, Geosystems*, *7*, Q10P17. https://doi.org/10.1029/2005GC001055

Ohkouchi, N., Eglinton, T. I., Keigwin, L. D., & Hayes, J. M. (2002). Spatial and Temporal Offsets Between Proxy Records in a Sediment Drift. *Science*, *298*(5596), 1224–1227. https://doi.org/10.1126/science.1075287

Ólafsdóttir, S., Jennings, A. E., Geirsdóttir, A., Andrews, J., & Miller, G. H. (2010). Holocene variability of the North Atlantic Irminger current on the south- and northwest shelf of Iceland. *Marine Micropaleontology*, *77*(3-4), 101–118. https://doi.org/10.1016/j.marmicro.2010.08.002

Oldenburg, D., Armour, K. C., Thompson, L., & Bitz, C. M. (2018). Distinct Mechanisms of Ocean Heat Transport Into the Arctic Under Internal Variability and Climate Change. *Geophysical Research Letters*, *45*, 7692–7700. https://doi.org/10.1029/2018GL078719

Oppo, D. W., McManus, J. F., & Cullen, J. L. (2003). Palaeo-oceanography: Deepwater variability in the Holocene epoch. *Nature*, *422*(6929), 277–277. https://doi.org/10.1038/422277b

Ortega, P., Mignot, J., Swingedouw, D., Sévellec, F., & Guilyardi, E. (2015). Reconciling two alternative mechanisms behind bi-decadal variability in the North Atlantic. *Progress in Oceanography*, *137*, 237–249. https://doi.org/10.1016/j.pocean.2015.06.009

Ortega, P., Montoya, M., González-Rouco, F., Mignot, J., & Legutke, S. (2012). Variability of the Atlantic meridional overturning circulation in the last millennium and two IPCC scenarios. *Climate Dynamics*, *38*(9-10), 1925–1947. https://doi.org/10.1007/s00382-011-1081-6

Ortega, P., Robson, J., Moffa-Sanchez, P., Thornalley, D., Swingedouw, D. (2017). A last millennium perspective on North Atlantic variability: exploiting synergies between models and proxy data. *PAGES Magazine*, vol. *25*(1), 61–67, 2017, https://doi.org/10.22498/pages.25.1.61

Orvik, K. A., & Niiler, P. (2002). Major pathways of Atlantic water in the northern North Atlantic and Nordic Seas toward Arctic. *Geophysical Research Letters*, *29*(19), 1896. https://doi.org/10.1029/2002GL015002

Ottera, O. H., Bentsen, M., Drange, H., & Suo, L. (2010). External forcing as a metronome for Atlantic multidecadal variability. *Nature Geoscience*, *3*(10), 688–694. https://doi.org/10.1038/ngeo955

Otto-Bliesner, B. L., Brady, E. C., Fasullo, J., Jahn, A., Landrum, L., Stevenson, S., et al. (2016). Climate Variability and Change since 850 CE: An Ensemble Approach with the Community Earth System Model. *Bulletin of the American Meteorological Society*, *97*(5), 735–754. https://doi.org/10.1175/BAMS-D-14-00233.1

Ouellet-Bernier, M.-M., de Vernal, A., Hillaire-Marcel, C., & Moros, M. (2014). Paleoceanographic changes in the Disko Bugt area, West Greenland, during the Holocene. *The Holocene*, *24*(11), 1573–1583. https://doi.org/10.1177/0959683614544060

Pages_Hydro2k_Consortium (2017). Comparing proxy and model estimates of hydroclimate variability and change over the Common Era. *Climate of the Past*, *13*(12), 1851–1900. https://doi.org/10.5194/cp-13-1851-2017

Perner, K., Jennings, A. E., Moros, M., Andrews, J. T., & Wacker, L. (2016). Interaction between warm Atlantic-sourced waters and the East Greenland Current in northern Denmark Strait (68°N) during the last 10 600 cal a BP. *Journal of Quaternary Science*, *31*(5), 472–483. https://doi.org/10.1002/jqs.2872

Perner, K., Moros, M., Jansen, E., Kuijpers, A., Troelstra, S. R., & Prins, M. A. (2018). Subarctic Front migration at the Reykjanes Ridge during the mid- to late Holocene: evidence from planktic foraminifera. *Boreas*, *47*(1), 175–188. https://doi.org/10.1111/bor.12263

Perner, K., Moros, M., Jennings, A., Lloyd, J., & Knudsen, K. (2013). Holocene palaeoceanographic evolution off West Greenland. *The Holocene*, *23*(3), 374–387. https://doi.org/10.1177/0959683612460785

Perner, K., Moros, M., Lloyd, J. M., Jansen, E., & Stein, R. (2015). Mid to late Holocene strengthening of the East Greenland Current linked to warm subsurface Atlantic water. *Quaternary Science Reviews*, *129*, 296–307. https://doi.org/10.1016/j.quascirev.2015.10.007

Perner, K., Moros, M., Lloyd, J. M., Kuijpers, A., Telford, R. J., & Harff, J. (2011). Centennial scale benthic foraminiferal record of late Holocene oceanographic variability in Disko Bugt, West Greenland. *Quaternary Science Reviews*, *30*(19-20), 2815–2826. https://doi.org/10.1016/j.quascirev.2011.06.018

Prahl, F. G., Muehlhausen, L. A., & Zahnle, D. L. (1988). Further evaluation of long-chain alkenones as indicators of paleoceanographic conditions. *Geochimica et Cosmochimica Acta*, *52*(9), 2303–2310. https://doi.org/10.1016/0016-7037(88)90132-9

Prahl, F. G., Popp, B. N., Karl, D. M., & Sparrow, M. A. (2005). Ecology and biogeochemistry of alkenone production at Station ALOHA. *Deep Sea Research Part I: Oceanographic Research Papers*, *52*(5), 699–719. https://doi.org/10.1016/j.dsr.2004.12.001

Rahmstorf, S., Box, J. E., Feulner, G., Mann, M. E., Robinson, A., Rutherford, S., & Schaffernicht, E. J. (2015). Exceptional twentieth-century slowdown in Atlantic Ocean overturning circulation. *Nature Climate Change*, *5*(5), 475–480. https://doi.org/10.1038/nclimate2554

Ran, L., Jiang, H., Knudsen, K. L., & Eiríksson, J. (2011). Diatom-based reconstruction of palaeoceanographic changes on the North Icelandic shelf during the last millennium. *Palaeogeography, Palaeoclimatology, Palaeoecology*, *302*(1-2), 109–119. https://doi.org/10.1016/j.palaeo.2010.02.001

Rashid, H., Piper, D. J. W., Lazar, K. B., McDonald, K., & Saint-Ange, F. (2017). The Holocene Labrador Current: Changing linkages to atmospheric and oceanographic forcing factors. *Paleoceanography*, *32*, 498–510. https://doi.org/10.1002/2016PA003051

Rebotim, A., Voelker, A. H. L., Jonkers, L., Waniek, J. J., Meggers, H., Schiebel, R., et al. (2017). Factors controlling the depth habitat of planktonic foraminifera in the subtropical eastern North Atlantic. *Biogeosciences*, *14*(4), 827–859. https://doi.org/10.5194/bg-14-827-2017

Reynolds, D. J., Butler, P. G., Williams, S. M., Scourse, J. D., Richardson, C.A. Wanamaker Jr., A.D., et al. (2013). A multiproxy reconstruction of Hebridean (NW Scotland) spring sea surface temperatures between AD 1805 and 2010. *Palaeogeography, Palaeoclimatology, Palaeoecology*, *386*, 275–285. https://doi.org/10.1016/j.palaeo.2013.05.029.

Reynolds, D. J., Hall, I. R., Slater, S. M., Mette, M. J., Wanamaker, A. D., Scourse, J. D., et al. (2018). Isolating and reconstructing key components of North Atlantic Ocean variability from a sclerochronological spatial network. *Paleoceanography and Paleoclimatology*, *33*, 1086–1098. https://doi.org/10.1029/2018PA003366

Reynolds, D. J., Richardson, C. A., Scourse, J. D., Butler, P. G., Hollyman, P., Román-González, A., & Hall, I. R. (2017). Reconstructing North Atlantic marine climate variability using an absolutely-dated sclerochronological network. *Palaeogeography, Palaeoclimatology, Palaeoecology*, *465*, 333–346. https://doi.org/10.1016/j.palaeo.2016.08.006

Reynolds, D. J., Scourse, J. D., Halloran, P. R., Nederbragt, A. J., Wanamaker, A. D., Butler, P. G., et al. (2016). Annually resolved North Atlantic marine climate over the last millennium. *Nature Communications*, *7*(1), 13502. https://doi.org/10.1038/ncomms13502

Ribeiro, S., Moros, M., Ellegaard, M., & Kuijpers, A. (2012). Climate variability in West Greenland during the past 1500 years: evidence from a high-resolution marine palynological record from Disko Bay. *Boreas*, *41*(1), 68–83. https://doi.org/10.1111/j.1502-3885.2011.00216.x

Richter, T. O., Peeters, F. J. C., & van Weering, T. C. E. (2009). Late Holocene (0-2.4 ka BP) surface water temperature and salinity variability, Feni Drift, NE Atlantic Ocean. *Quaternary Science Reviews*, *28*(19-20), 1941–1955. https://doi.org/10.1016/j.quascirev.2009.04.008

Rignot, E., Koppes, M., & Velicogna, I. (2010). Rapid submarine melting of the calving faces of West Greenland glaciers. *Nature Geoscience*, *3*(3), 187–191. https://doi.org/10.1038/ngeo765

Risebrobakken, B., Jansen, E., Andersson, C., Mjelde, E., & Hevrøy, K. (2003). A high-resolution study of Holocene paleoclimatic and paleoceanographic changes in the Nordic Seas. *Paleoceanography*, *18*(1), 1017. https://doi.org/10.1029/2002PA000764

Roberts, C. D., Garry, F. K., & Jackson, L. C. (2013). A Multimodel Study of Sea Surface Temperature and Subsurface Density Fingerprints of the Atlantic Meridional Overturning Circulation. *Journal of Climate*, *26*(22), 9155–9174. https://doi.org/10.1175/JCLI-D-12-00762.1

Robson, J., Ortega, P., & Sutton, R. (2016). A reversal of climatic trends in the North Atlantic since 2005. *Nature Geoscience*, *9*(7), 513–517. https://doi.org/10.1038/ngeo2727

Rose, N. L. (2015). Spheroidal Carbonaceous Fly Ash Particles Provide a Globally Synchronous Stratigraphic Marker for the Anthropocene. *Environmental Science & Technology*, *49*(7), 4155–4162. https://doi.org/10.1021/acs.est.5b00543

Rosell-Melé, A., & Prahl, F. G. (2013). Seasonality of UK′37 temperature estimates as inferred from sediment trap data. *Quaternary Science Reviews*, *72*, 128–136. https://doi.org/10.1016/j.quascirev.2013.04.017

Saba, V. S., Griffies, S. M., Anderson, W. G., Winton, M., Alexander, M. A., Delworth, T. L., et al. (2016). Enhanced warming of the Northwest Atlantic Ocean under climate change. *Journal of Geophysical Research: Oceans*, *121*, 118–132. https://doi.org/10.1002/2015JC011346

Sachs, J. P. (2007). Cooling of Northwest Atlantic slope waters during the Holocene. *Geophysical Research Letters*, *34*, L03609. https://doi.org/10.1029/2006GL028495

Saenger, C., Came, R. E., Oppo, D. W., Keigwin, L. D., & Cohen, A. L. (2011). Regional climate variability in the western subtropical North Atlantic during the past two millennia. *Paleoceanography*, *26*, PA2206. https://doi.org/10.1029/2010PA002038

Schmidt, G. A., Jungclaus, J. H., Ammann, C. M., Bard, E.,Braconnot, P., Crowley, T. J., et al. (2011). Climate forcing reconstructions for use in PMIP simulations of the last millennium (v1.0). *Geoscientific Model Development*, *4*, 33–45, https://doi.org/10.5194/gmd-4-33-2011

Schleussner, C. F., Divine, D. V., Donges, J. F., Miettinen, A., & Donner, R. V. (2015). Indications for a North Atlantic ocean circulation regime shift at the onset of the Little Ice Age. *Climate Dynamics*, *45*(11-12), 3623–3633. https://doi.org/10.1007/s00382-015-2561-x

Schleussner, C. F., & Feulner, G. (2013). A volcanically triggered regime shift in the subpolar North Atlantic Ocean as a possible origin of the Little Ice Age. *Climate of the Past*, *9*(3), 1321–1330. https://doi.org/10.5194/cp-9-1321-2013

Schlitzer, R. (2015). Data analysis and visualization with Ocean Data View. *CMOS Bulletin SCMO*, *43*(1), 9–13.

Schmiedl, G., Mackensen, A., & Müller, P. J. (1997). Recent benthic foraminifera from the eastern South Atlantic Ocean: Dependence on food supply and water masses. *Marine Micropaleontology*, *32*(3-4), 249–287. https://doi.org/10.1016/S0377-8398(97)00023-6

Schoonover, J., Dewar, W. K., Wienders, N., & Deremble, B. (2016). Local Sensitivities of the Gulf Stream Separation. *Journal of Physical Oceanography*, *47*(2), 353–373.

Schurer, A. P., Tett, S. F. B., & Hegerl, G. C. (2014). Small influence of solar variability on climate over the past millennium. *Nature Geoscience*, *7*(2), 104–108. https://doi.org/10.1038/ngeo2040

Seidenkrantz, M.-S., Roncaglia, L., Fischel, A., Heilmann-Clausen, C., Kuijpers, A., & Moros, M. (2008). Variable North Atlantic climate seesaw patterns documented by a late Holocene marine record from Disko Bugt, West Greenland. *Marine Micropaleontology*, *68*(1-2), 66–83. https://doi.org/10.1016/j.marmicro.2008.01.006

Sejrup, H. P., Haflidason, H., & Andrews, J. T. (2011). A Holocene North Atlantic SST record and regional climate variability. *Quaternary Science Reviews*, *30*(21-22), 3181–3195. https://doi.org/10.1016/j.quascirev.2011.07.025

Sgubin, G., Swingedouw, D., Drijfhout, S., Mary, Y., & Bennabi, A. (2017). Abrupt cooling over the North Atlantic in modern climate models. *Nature Communications*, *8*(1), 14375. https://doi.org/10.1038/ncomms14375

Sha, L., Jiang, H., Liu, Y., Zhao, M., Li, D., Chen, Z., & Zhao, Y. (2015). Palaeo-sea-ice changes on the North Icelandic shelf during the last millennium: Evidence from diatom records. *Science China Earth Sciences*, *58*(6), 962–970. https://doi.org/10.1007/s11430-015-5061-2

Sha, L., Jiang, H., Seidenkrantz, M.-S., Knudsen, K. L., Olsen, J., Kuijpers, A., & Liu, Y. (2014). A diatom-based sea-ice reconstruction for the Vaigat Strait (Disko Bugt, West Greenland) over the last 5000yr. *Palaeogeography, Palaeoclimatology, Palaeoecology*, *403*, 66–79. https://doi.org/10.1016/j.palaeo.2014.03.028

Sha, L., Jiang, H., Seidenkrantz, M. S., Li, D., Andresen, C. S., Knudsen, K. L., et al. (2017). A record of Holocene sea-ice variability off West Greenland and its potential forcing factors. *Palaeogeography, Palaeoclimatology, Palaeoecology*, *475*(Supplement C), 115–124. https://doi.org/10.1016/j.palaeo.2017.03.022

Sha, L., Jiang, H., Seidenkrantz, M. S., Muscheler, R., Zhang, X., Knudsen, M. F., et al. (2016). Solar forcing as an important trigger for West Greenland sea-ice variability over the last millennium. *Quaternary Science Reviews*, *131*(Part A), 148–156. https://doi.org/10.1016/j.quascirev.2015.11.002

Sheldon, C. M., Seidenkrantz, M. S., Frandsen, P., Jacobsen, H. V., van Nieuwenhove, N., Solignac, S., et al. (2015). Variable influx of West Greenland Current water into the Labrador Current through the last 7200 years: a multiproxy record from Trinity Bay (NE Newfoundland). *arktos*, *1*(1), 8. https://doi.org/10.1007/s41063-015-0010-z

Sicre, M. A., Hall, I. R., Mignot, J., Khodri, M., Ezat, U., Truong, M. X., et al. (2011). Sea surface temperature variability in the subpolar Atlantic over the last two millennia. *Paleoceanography*, *26*, PA4218. https://doi.org/10.1029/2011PA002169

Sicre, M. A., Jacob, J., Ezat, U., Rousse, S., Kissel, C., Yiou, P., et al. (2008). Decadal variability of sea surface temperatures off North Iceland over the last 2000 years. *Earth and Planetary Science Letters*, *268*(1-2), 137–142. https://doi.org/10.1016/j.epsl.2008.01.011

Sicre, M. A., Weckström, K., Seidenkrantz, M. S., Kuijpers, A., Benetti, M., Masse, G., et al. (2014). Labrador current variability over the last 2000 years. *Earth and Planetary Science Letters*, *400*, 26–32. https://doi.org/10.1016/j.epsl.2014.05.016

Sigl, M., Winstrup, M., McConnell, J. R., Welten, K. C., Plunkett, G., Ludlow, F., et al. (2015). Timing and climate forcing of volcanic eruptions for the past 2,500 years. *Nature*, *523*(7562), 543–549. https://doi.org/10.1038/nature14565

Singh, H. K. A., Hakim, G. J., Tardif, R., Emile-Geay, J., & Noone, D. C. (2018). Insights into Atlantic multidecadal variability using the Last Millennium Reanalysis framework. *Climate of the Past*, *14*(2), 157–174. https://doi.org/10.5194/cp-14-157-2018

Sjolte, J., Hoffmann, G., Johnsen, S. J., Vinther, B. M., Masson-Delmotte, V., & Sturm, C. (2011). Modeling the water isotopes in Greenland precipitation 1959–2001 with the meso-scale model REMO-iso. *Journal of Geophysical Research*, *116*, D18105. https://doi.org/10.1029/2010JD015287

Slawinska, J., & Robock, A. (2018). Impact of Volcanic Eruptions on Decadal to Centennial Fluctuations of Arctic Sea Ice Extent during the Last Millennium and on Initiation of the Little Ice Age. *Journal of Climate*, *31*(6), 2145–2167. https://doi.org/10.1175/JCLI-D-16-0498.1

Spero, H. J., Bijma, J., Lea, D. W., & Bemis, B. E. (1997). Effect of seawater carbonate concentration on foraminiferal carbon and oxygen isotopes. *Nature*, *390*(6659), 497–500. https://doi.org/10.1038/37333

Spielhagen, R. F., Werner, K., Sorensen, S. A., Zamelczyk, K., Kandiano, E., Budeus, G., et al. (2011). Enhanced Modern Heat Transfer to the Arctic by Warm Atlantic Water. *Science*, *331*(6016), 450–453. https://doi.org/10.1126/science.1197397

Srokosz, M. A., & Bryden, H. L. (2015). Observing the Atlantic Meridional Overturning Circulation yields a decade of inevitable surprises. *Science*, *348*(6241), 1255575. https://doi.org/10.1126/science.1255575

Steinhilber, F., Beer, J., & Fröhlich, C. (2009). Total solar irradiance during the Holocene. *Geophysical Research Letters*, *36*, L19704. https://doi.org/10.1029/2009GL040142

Stenchikov, G., Delworth, T. L., Ramaswamy, V., Stouffer, R. J., Wittenberg, A., & Zeng, F. (2009). Volcanic signals in oceans. *Journal of Geophysical Research*, *114*, D16104. https://doi.org/10.1029/2008JD011673

Stevenson, S., McGregor, H. V., Phipps, S. J., & Fox-Kemper, B. (2013). Quantifying errors in coral-based ENSO estimates: Toward improved forward modeling of δ18O. *Paleoceanography*, *28*, 633–649. https://doi.org/10.1002/palo.20059

Suess, H. E. (1955). Radiocarbon Concentration in Modern Wood. *Science*, *122*(3166), 415–417. https://doi.org/10.1126/science.122.3166.415-a

Swingedouw, D., Mignot, J., Ortega, P., Khodri, M., Menegoz, M., Cassou, C., & Hanquiez, V. (2017). Impact of explosive volcanic eruptions on the main climate variability modes. *Global and Planetary Change*, *150*, 24–45. https://doi.org/10.1016/j.gloplacha.2017.01.006

Swingedouw, D., Ortega, P., Mignot, J., Guilyardi, E., Masson-Delmotte, V., Butler, P. G., et al. (2015). Bidecadal North Atlantic ocean circulation variability controlled by timing of volcanic eruptions. *Nature Communications*, *6*(1), 6545. https://doi.org/10.1038/ncomms7545

Swingedouw, D., Terray, L., Cassou, C., Voldoire, A., Salas-Mélia, D., & Servonnat, J. (2011). Natural forcing of climate during the last millennium: fingerprint of solar variability. *Climate Dynamics*, *36*(7-8), 1349–1364. https://doi.org/10.1007/s00382-010-0803-5

Tang, C. C. L., Ross, C. K., Yao, T., Petrie, B., DeTracey, B. M., & Dunlap, E. (2004). The circulation, water masses and sea-ice of Baffin Bay. *Progress in Oceanography*, *63*(4), 183–228. https://doi.org/10.1016/j.pocean.2004.09.005

Tardif, R., Hakim, G. J., Perkins, W. A., Horlick, K. A., Erb, M. P., Emile-Geay, J., et al. (2018), Last Millennium Reanalysis with an expanded proxy database and seasonal proxy modeling, Climate of the Past Discussions, 2018, 1-37.

Telford, R. J., & Birks, H. J. B. (2011). A novel method for assessing the statistical significance of quantitative reconstructions inferred from biotic assemblages. *Quaternary Science Reviews*, *30*(9-10), 1272–1278. https://doi.org/10.1016/j.quascirev.2011.03.002

Thibodeau, B., Not, C., Zhu, J., Schmittner, A., Noone, D., Tabor, C., et al. (2018). Last Century Warming Over the Canadian Atlantic Shelves Linked to Weak Atlantic Meridional Overturning Circulation. *Geophysical Research Letters*, *45*, 12,376–12,385. https://doi.org/10.1029/2018GL080083

Thornalley, D. J., Elderfield, H., & McCave, I. N. (2009). Holocene oscillations in temperature and salinity of the surface subpolar North Atlantic. *Nature*, *457*(7230), 711–714. https://doi.org/10.1038/nature07717

Thornalley, D. J. R., Blaschek, M., Davies, F. J., Praetorius, S., Oppo, D. W., McManus, J. F., et al. (2013). Long-term variations in Iceland–Scotland overflow strength during the Holocene. *Climate of the Past*, *9*(5), 2073–2084. https://doi.org/10.5194/cp-9-2073-2013

Thornalley, D. J. R., Oppo, D. W., Ortega, P., Robson, J. I., Brierley, C. M., Davis, R., et al. (2018). Anomalously weak Labrador Sea convection and Atlantic overturning during the past 150 years. *Nature*, *556*(7700), 227–230. https://doi.org/10.1038/s41586-018-0007-4

Urey, H. C. (1948). Oxygen Isotopes in Nature and in the Laboratory. *Science*, *108*(2810), 489–496. https://doi.org/10.1126/science.108.2810.489

Vernal, A. d., Henry, M., Matthiessen, J., Mudie, P. J., Rochon, A., Boessenkool, K. P., et al. (2001). Dinoflagellate cyst assemblages as tracers of sea-surface conditions in the northern North Atlantic, Arctic and sub-Arctic seas: the new 'n = 677' data base and its application for quantitative palaeoceanographic reconstruction. *Journal of Quaternary Science: Published for the Quaternary Research Association*, *16*(7), 681–698. https://doi.org/10.1002/jqs.659

Wanamaker, A. D., Butler, P. G., Scourse, J. D., Heinemeier, J., Eiríksson, J., Knudsen, K. L., & Richardson, C. A. (2012). Surface changes in the North Atlantic meridional overturning circulation during the last millennium. *Nature Communications*, *3*(1), 899. https://doi.org/10.1038/ncomms1901

Wanamaker, A. D., Kreutz, K. J., Schöne, B. R., Pettigrew, N., Borns, H. W., Introne, D. S., et al. (2008). Coupled North Atlantic slope water forcing on Gulf of Maine temperatures over the past millennium. *Climate Dynamics*, *31*(2-3), 183–194. https://doi.org/10.1007/s00382-007-0344-8

Wang, J., Emile-Geay, J., Guillot, D., McKay, N. P., & Rajaratnam, B. (2015). Fragility of reconstructed temperature patterns over the Common Era: Implications for model evaluation. *Geophysical Research Letters*, *42*, 7162–7170. https://doi.org/10.1002/2015GL065265

Wang, J., Yang, B., Ljungqvist, F. C., Luterbacher, J., Osborn, T. . J., Briffa, K. R., & Zorita, E. (2017). Internal and external forcing of multidecadal Atlantic climate variability over the past 1,200 years. *Nature Geoscience*, *10*(7), 512–517. https://doi.org/10.1038/ngeo2962

Wekerle, C., Wang, Q., Danilov, S., Schourup-Kristensen, V., von Appen, W.-J., & Jung, T. (2017). Atlantic Water in the Nordic Seas: Locally eddy-permitting ocean simulation in a global setup. *Journal of Geophysical Research: Oceans*, *122*, 914–940. https://doi.org/10.1002/2016JC012121

Werner, K., Spielhagen, R. F., Bauch, D., Hass, H. C., Kandiano, E., & Zamelczyk, K. (2011). Atlantic Water advection to the eastern Fram Strait - Multiproxy evidence for late Holocene variability. *Palaeogeography, Palaeoclimatology, Palaeoecology*, *308*(3-4), 264–276. https://doi.org/10.1016/j.palaeo.2011.05.030

Werner, M., Langebroek, P. M., Carlsen, T., Herold, M., & Lohmann, G. (2011). Stable water isotopes in the ECHAM5 general circulation model: Toward high-resolution isotope modeling on a global scale. *Journal of Geophysical Research*, *116*, D15109. https://doi.org/10.1029/2011JD015681

Williams, S., Adey, W., Halfar, J., Kronz, A., Gagnon, P., Bélanger, D., & Nash, M. (2018). Effects of light and temperature on Mg uptake, growth, and calcification in the proxy climate archive Clathromorphum compactum. *Biogeosciences*, *15*(19), 5745–5759. https://doi.org/10.5194/bg-15-5745-2018

Williams, S., Halfar, J., Zack, T., Hetzinger, S., Blicher, M., & Juul-Pedersen, T. (2018). Reprint of Comparison of climate signals obtained from encrusting and free-living rhodolith coralline algae. *Chemical Geology*, *476*, 418–428. https://doi.org/10.1016/j.chemgeo.2017.11.038

Wilson, R., Cook, E., D'Arrigo, R., Riedwyl, N., Evans, M. N., Tudhope, A., & Allan, R. (2010). Reconstructing ENSO: the influence of method, proxy data, climate forcing and teleconnections. *Journal of Quaternary Science*, *25*(1), 62–78. https://doi.org/10.1002/jqs.1297

Yan, X., Zhang, R., & Knutson, T. R. (2018). Underestimated AMOC Variability and Implications for AMV and Predictability in CMIP Models. *Geophysical Research Letters*, *45*, 4319–4328. https://doi.org/10.1029/2018GL077378

Zamelczyk, K., Rasmussen, T. L., Husum, K., & Hald, M. (2013). Marine calcium carbonate preservation vs. climate change over the last two millennia in the Fram Strait: Implications for planktic foraminiferal paleostudies. *Marine Micropaleontology*, *98*, 14–27. https://doi.org/10.1016/j.marmicro.2012.10.001

Zanchettin, D., Bothe, O., Lehner, F., Ortega, P., Raible, C. C., & Swingedouw, D. (2015). Reconciling reconstructed and simulated features of the winter Pacific/North American pattern in the early 19th century. *Climate of the Past*, *11*(6), 939–958. https://doi.org/10.5194/cp-11-939-2015

Zanchettin, D., Khodri, M., Timmreck, C., Toohey, M., Schmidt, A., Gerber, E. P., et al. (2016). The Model Intercomparison Project on the climatic response to Volcanic forcing (VolMIP): experimental design and forcing input data for CMIP6. *Geoscientific Model Development*, *9*(8), 2701–2719. https://doi.org/10.5194/gmd-9-2701-2016

Zanchettin, D., Timmreck, C., Graf, H. F., Rubino, A., Lorenz, S., Lohmann, K., et al. (2012). Bi-decadal variability excited in the coupled ocean–atmosphere system by strong tropical volcanic eruptions. *Climate Dynamics*, *39*(1-2), 419–444. https://doi.org/10.1007/s00382-011-1167-1

Zhang, R. (2008). Coherent surface-subsurface fingerprint of the Atlantic meridional overturning circulation. *Geophysical Research Letters*, *35*, L20705. https://doi.org/10.1029/2008GL035463

Zhang, R., & Vallis, G. K. (2007). The Role of Bottom Vortex Stretching on the Path of the North Atlantic Western Boundary Current and on the Northern Recirculation Gyre. *Journal of Physical Oceanography*, *37*(8), 2053–2080. https://doi.org/10.1175/JPO3102.1

Zhong, Y., Jahn, A., Miller, G. H., & Geirsdottir, A. (2018). Asymmetric Cooling of the Atlantic and Pacific Arctic During the Past Two Millennia: A Dual Observation-Modeling Study. *Geophysical Research Letters*, *45*, 12,497–12,505. https://doi.org/10.1029/2018GL079447